

Last Compiled October 14, 2014

# The Soft-Collinear Effective Theory

Christian W. Bauer (LBL) and Iain W. Stewart (MIT)

TASI Lecture Notes 2013 and 2014

&

Iain W. Stewart (MIT)

EFT course 8.851 and edX course 8.EFTx  
SCET Lecture Notes  
2013

©2014 by Christian W. Bauer and Iain W. Stewart

(The original version of these notes were typeset by Mobolaji Williams.)

PDF version:

[http://courses.edx.org/c4x/MITx/8.EFTx/asset/notes\\_scetnotes.pdf](http://courses.edx.org/c4x/MITx/8.EFTx/asset/notes_scetnotes.pdf)

# Abstract

## Contents

<b>1</b>	<b>Lecture Notes Introduction</b>	<b>4</b>
<b>2</b>	<b>Introduction to SCET</b>	<b>5</b>
2.1	What is SCET? . . . . .	5
2.2	Light-Cone Coordinates . . . . .	6
2.3	Momentum Regions: SCET I and SCET II . . . . .	8
<b>3</b>	<b>Ingredients for SCET</b>	<b>14</b>
3.1	Collinear Spinors . . . . .	14
3.2	Collinear Fermion Propagator and $\xi_n$ Power Counting . . . . .	16
3.3	Power Counting for Collinear Gluons and Ultrasoft Fields . . . . .	17
3.4	Collinear Wilson Line, a first look . . . . .	18
<b>4</b>	<b>SCET<sub>I</sub> Lagrangian</b>	<b>21</b>
4.1	SCET Quark Lagrangian . . . . .	21
4.1.1	Step 1: Lagrangian for the larger spinor components . . . . .	22
4.1.2	Step 2: Separate collinear and ultrasoft gauge fields . . . . .	23
4.1.3	Step 3: The Multipole Expansion for Separating momenta . . . . .	24
4.1.4	Final Result: Expand and put pieces together . . . . .	29
4.2	Wilson Line Identities . . . . .	30
4.3	Collinear Gluon and Ultrasoft Lagrangians . . . . .	31
4.4	Feynman Rules for Collinear Quarks and Gluons . . . . .	33
4.5	Rules for Combining Label and Residual Momenta in Amplitudes . . . . .	33
<b>5</b>	<b>Symmetries of SCET</b>	<b>37</b>
5.1	Spin Symmetry . . . . .	38
5.2	Gauge Symmetry . . . . .	38
5.3	Reparamterization Invariance . . . . .	41
5.4	Discrete Symmetries . . . . .	44
5.5	Extension to Multiple Collinear Directions . . . . .	44
<b>6</b>	<b>Factorization from Mode Separation</b>	<b>45</b>
6.1	Ultrasoft-Collinear Factorization . . . . .	46
6.2	Wilson Coefficients and Hard Factorization . . . . .	49
6.3	Operator Building Blocks . . . . .	50
<b>7</b>	<b>Wilson Coefficients and Hard Dynamics</b>	<b>52</b>
7.1	$b \rightarrow s\gamma$ , SCET Loops and Divergences . . . . .	52
7.2	$e^+e^- \rightarrow 2$ -jets, SCET Loops . . . . .	58
7.3	Summing Sudakov Logarithms . . . . .	62
<b>8</b>	<b>Deep Inelastic Scattering</b>	<b>65</b>
8.1	Factorization of Amplitude . . . . .	65
8.2	Renormalization of PDF . . . . .	70
8.3	General Discussion on Appearance of Convolutions in SCET <sub>I</sub> and SCET <sub>II</sub> . . . . .	72

<b>9</b>	<b>Dijet Production, <math>e^+e^- \rightarrow 2</math> jets</b>	<b>72</b>
9.1	Kinematics, Expansions, and Regions . . . . .	72
9.2	Factorization . . . . .	73
9.3	Perturbative Results . . . . .	74
9.4	Results with Resummation . . . . .	74
<b>10</b>	<b>SCET II</b>	<b>74</b>
<b>11</b>	<b>SCET<sub>II</sub> Applications</b>	<b>75</b>
11.1	$\gamma^*\gamma \rightarrow \pi^0$ . . . . .	76
11.2	$B \rightarrow D\pi$ . . . . .	76
11.3	Massive Gauge Boson Form Factor & Rapidity Divergences . . . . .	77
11.4	$p_T$ Distribution for Higgs Production & Jet Broadening . . . . .	77
<b>12</b>	<b>More SCET<sub>I</sub> Applications</b>	<b>77</b>
12.1	$B \rightarrow X_s\gamma$ . . . . .	78
12.2	Drell-Yan: $pp \rightarrow Xl^+l^-$ . . . . .	80
<b>A</b>	<b>More on the Zero-Bin</b>	<b>82</b>
A.1	0-bin subtractions with a 0-bin field Redefinition . . . . .	82
A.2	0-bin subtractions for phase space integrations . . . . .	82
<b>B</b>	<b>Feynman Rules with a mass</b>	<b>82</b>
<b>C</b>	<b>Feynman Rules for the Wilson line <math>W</math></b>	<b>83</b>
<b>D</b>	<b>Feynman Rules for Subleading Lagrangians</b>	<b>83</b>
D.1	Feynman rules for $J_{hl}$ . . . . .	86
<b>E</b>	<b>Integral Tricks</b>	<b>89</b>
<b>F</b>	<b>QCD Summary</b>	<b>90</b>

# 1 Lecture Notes Introduction

These notes provide reading material on the Soft-Collinear Effective Theory (SCET). They are intended to cover the material studied in the second half of my effective field theory graduate course at MIT. A complete hand written version of the notes I used when teaching this course in 2013 can be found at:

[http://http://www2.lns.mit.edu/~iains/talks/SCET\\_Lectures\\_Stewart\\_2013.pdf](http://http://www2.lns.mit.edu/~iains/talks/SCET_Lectures_Stewart_2013.pdf)

These latex notes will also appear as part of TASI lecture notes and a review article with Christian Bauer.

Familiarity will be assumed with various basic effective field theory (EFT) concepts, including power counting with operator dimensions, the use of field redefinitions, and top-down effective theories. Also the use of dimensional regularization for scale separation, the equivalences and differences with Wilsonian effective field theory, and the steps required to carry out matching computations for Wilson coefficients. A basic familiarity with heavy quark effective theory (HQET), the theory of static sources, is also assumed. In particular, familiarity with HQET as an example of a top-down EFT where we simultaneously study perturbative corrections and power corrections, and for understanding reparameterization invariance. These topics were covered in the first half of the EFT course.

A basic familiarity with QCD as a gauge theory will also be assumed. Given that SCET is a top-down EFT, we can derive it directly from expanding QCD and integrating out offshell degrees of freedom. This familiarity should include concepts like the fact that energetic quarks and gluons form jets, renormalization and renormalization group evolution for nonabelian gauge theory, and color algebra. Also some basic familiarity with the role of infrared divergences is assumed, namely how they cancel between virtual and real emission diagrams, and how they otherwise signal the presence of nonperturbative physics and the scale  $\Lambda_{\text{QCD}}$  as they do for parton distribution functions.

Finally it should be remarked that later parts of the notes are still a work in progress (particularly sections marked at the start as ROUGH which being around chapter 8). This file will be updated as more parts become available. Please let me know if you spot typos in any of chapters 1-7. The notes also do not yet contain a complete set of references. Some of the most frequent references I used for preparing various topics include:

1. Degrees of freedom, scales, spinors and propagators, power counting: [1, 2, 3]
2. Construction of  $\mathcal{L}_{\text{SCET}}$ , currents, multipole expansion, label operators, zero-bin, infrared divergences: [2, 4, 5]
3. SCET<sub>I</sub>, Gauge symmetry, reparameterization invariance: [4, 6, 7]
4. Ultrasoft-Collinear factorization, Hard-Collinear factorization, matching & running for hard functions: [1, 2, 4, 6]
5. DIS, SCET power counting reduces to twist, renormalization with convolutions: [8, 9]
6. SCET<sub>II</sub>, Soft-Collinear interactions, use of auxillary Lagrangians, power counting formula, rapidity divergences: [6, 3, 10, 5, 11]
7. Power corrections, deriving SCET<sub>II</sub> from SCET<sub>I</sub>: [12, 13, 10]

## 2 Introduction to SCET

### 2.1 What is SCET?

The Soft-Collinear Effective Theory is an effective theory describing the interactions of soft and collinear degrees of freedom in the presence of a hard interaction. We will refer to the momentum scale of the hard interaction as  $Q$ . For QCD another important scale is  $\Lambda_{\text{QCD}}$ , the scale of hadronization and nonperturbative physics, and we will always take  $Q \gg \Lambda_{\text{QCD}}$ .

Soft degrees of freedom will have momenta  $p_{\text{soft}}$ , where  $Q \gg p_{\text{soft}}$ . They have no preferred direction, so each component of  $p_{\text{soft}}^\mu$  for  $\mu = 0, 1, 2, 3$  has an identical scaling. Sometimes we will have  $p_{\text{soft}} \sim \Lambda_{\text{QCD}}$  so that the soft modes are nonperturbative (as in HQET for  $B$  or  $D$  meson bound states) and sometimes we will have  $p_{\text{soft}} \gg \Lambda_{\text{QCD}}$  so that the soft modes have components that we can calculate perturbatively.

Collinear degrees of freedom describe energetic particles moving preferentially in some direction (here motion collinear to a direction means motion near to but not exactly along that direction). In various situations the collinear degrees of freedom may be the constituents for one or more of

- energetic hadrons with  $E_H \simeq Q \gg \Lambda_{\text{QCD}} \sim m_H$ ,
- energetic jets with  $E_J \simeq Q \gg m_J = \sqrt{p_J^2} \gg \Lambda_{\text{QCD}}$ .

Both the soft and collinear particles live in the infrared, and hence are modes that are described by fields in SCET. Here we characterize infrared physics in the standard way, by looking at the allowed values of invariant mass  $p^2$  and noting that all offshell fluctuations described by SCET degrees of freedom have  $p^2 \ll Q^2$ . Thus SCET is an EFT which describes QCD in the infrared, but allows for both soft homogeneous and collinear inhomogeneous momenta for the particles, which can have different dominant interactions. The main power of SCET comes from the simple language it gives for describing interactions between hard  $\leftrightarrow$  soft  $\leftrightarrow$  collinear particles.

Phenomenologically SCET is useful because our main probe of short distance physics at  $Q$  is hard collisions:  $e^+e^- \rightarrow \text{stuff}$ ,  $e^-p \rightarrow \text{stuff}$ , or  $pp \rightarrow \text{stuff}$ . To probe physics at  $Q$  we must disentangle the physics of QCD that occurs at other scales like  $\Lambda_{\text{QCD}}$ , as well as at the intermediate scales like  $m_J$  that are associated with jet production. This process is made simpler by a separation of scales, and the natural language for this purpose is effective field theory. Generically in QCD a separation of scales is important for determining what parts of a process are perturbative with  $\alpha_s \ll 1$ , and what parts are nonperturbative with  $\alpha_s \sim 1$ . For some examples this is fairly straightforward, there are only two relevant momentum regions, one which is perturbative and the other nonperturbative, and we can separate them with a fairly standard operator expansion. But many of the most interesting hard scattering processes are not so simple, they involve either multiple perturbative momentum regions, or multiple nonperturbative momentum regions, or both. In most cases where we apply SCET we will be interested in two or more modes in the effective theory, such as soft and collinear, and often even more modes, such as soft modes together with two distinct types of collinear modes.

Part of the power of SCET is the plethora of processes that it can be used to describe. Indeed, it is not really feasible to generate a complete list. New processes are continuously being analyzed on a regular basis. Some example processes where SCET simplifies the physics include

- inclusive hard scattering processes:  $e^-p \rightarrow e^-X$  (DIS),  $p\bar{p} \rightarrow Xl^+l^-$  (Drell-Yan),  $pp \rightarrow HX$ , ... (either for the full inclusive process or for threshold resummation in the same process)

- exclusive jet processes: dijet event shapes in  $e^+e^- \rightarrow$  jets,  $pp \rightarrow H + 0$ -jets,  $pp \rightarrow W + 1$ -jet,  $e^-p \rightarrow e^- + 1$ -jet,  $pp \rightarrow$ dijets, ...
- exclusive hard scattering processes:  $\gamma^*\gamma \rightarrow \pi^0$ ,  $\gamma^*p \rightarrow \gamma^{(*)}p'$  (Deeply Virtual Compton), ...
- inclusive B-decays:  $B \rightarrow X_s\gamma$ ,  $B \rightarrow X_u\ell\bar{\nu}$ ,  $B \rightarrow X_s\ell^+\ell^-$
- exclusive B-decays:  $B \rightarrow D\pi$ ,  $B \rightarrow \pi\ell\bar{\nu}_\ell$ ,  $B \rightarrow K^*\gamma$ ,  $B \rightarrow \pi\pi$ ,  $B \rightarrow K^*K$ ,  $B \rightarrow J/\psi K$ , ...
- Charmonium production:  $e^+e^- \rightarrow J/\psi X$ , ...
- Jets in a Medium in heavy-ion collisions

Some of these examples combine SCET with other effective theories, such as HQET for the  $B$ -meson, or NRQCD for the  $J/\psi$ .

Before we dig in, it is useful to stop and ask **What makes SCET different from other EFT's?** Put another way, what are some of the things that make it more complicated than more traditional EFTs? Or another way, for the field theory aficionado, what are some of the interesting new techniques I can learn by studying this EFT? A brief list includes:

- We will integrate off-shell modes, but not entire degrees of freedom. (This is analogous to HQET where low energy fluctuations of the heavy quark remain in the EFT.)
- Having multiple fields that are defined for the same particle

$$\xi_n = \text{collinear quark field}, \quad q_s = \text{soft quark field}$$

which are required by power counting and to cleanly separate momentum scales.

- In traditional EFT we sum over operators with the same power counting and quantum numbers. In SCET some of these sums are replaced by convolutions,  $\sum_i C_i \mathcal{O}_i \rightarrow \int d\omega C(\omega) \mathcal{O}(\omega)$ .
- $\lambda$ , the power counting parameter of SCET, is not related to the mass dimensions of fields
- Various Wilson Lines, which are path-ordered line integrals of gauge fields,  $P \exp[ig \int ds n \cdot A(ns)]$ , play an important role in SCET. Some appear from integrating out offshell modes, others from dynamics in the EFT, and all are related to the interesting gauge symmetry structure of the effective theory.
- There are  $1/\epsilon^2$  divergences at 1-loop which require UV counterterms. This leads to explicit  $\ln(\mu)$  dependence in anomalous dimensions related to the so-called cusp anomalous dimensions, and to renormalization group equations whose solutions sum up infinite series of Sudakov double logarithms,  $\sum_k a_k [\alpha_s \ln^2(p/Q)]^k$ .

## 2.2 Light-Cone Coordinates

Before we get into concepts, which should decide on convenient coordinates. To motivate our choice, consider the decay process  $B \rightarrow D\pi$  in the rest frame of the  $B$  meson. This decay occurs through the exchange of a  $W$  boson mediating  $b \rightarrow c\bar{u}d$ , along with a valence spectator quark that starts in the  $B$  and ends in the  $D$  meson. We are concerned here with the kinematics. Aligning the  $\pi$  with the  $-\hat{z}$  axis it is easy to work out the pion's four momentum for this two-body decay,

$$p_\pi^\mu = (2.310 \text{ GeV}, 0, 0, -2.306 \text{ GeV}) \simeq Qn^\mu, \quad (2.1)$$

where  $n^\mu = (1, 0, 0, -1)$  in a  $0, 1, 2, 3$  basis for the four vector. Here  $n^2 = 0$  is a light-like vector and  $Q \gg \Lambda_{\text{QCD}}$ . This pion has large energy and has a four-momentum that is close to the light-cone. With a slight abuse of language we will often say that the pion is moving in the direction  $n$  (even though we really mean the direction specified by the  $1, 2, 3$  components of  $n^\mu$ ). The natural coordinates for particles whose energy is much larger than their mass are light-cone coordinates.

We would like to be able to decompose any four vector  $p^\mu$  using  $n^\mu$  as a basis vector. But unlike cartesian coordinates the component along  $n$  will not be  $n \cdot p$ , since  $n^2 = 0$ . If we want to describe the components (we do) then we will need another auxillary light-like vector  $\bar{n}$ . The vector  $n$  has a physical interpretation, we want to describe particles moving in the  $n$  direction, whereas  $\bar{n}$  is simply a devise we introduce to have a simple notation for components.

Thus we start with light-cone basis vectors  $n$  and  $\bar{n}$  which satisfy the properties

$$n^2 = 0, \quad \bar{n}^2 = 0, \quad n \cdot \bar{n} = 2, \quad (2.2)$$

where the last equation is our normalization convention. A standard choice, and the one we will most often use, is to simply take  $\bar{n}$  in the opposite direction to  $n$ . So for example we might have

$$n^\mu = (1, 0, 0, 1), \quad \bar{n}^\mu = (1, 0, 0, -1) \quad (2.3)$$

Other choices for the auxillary vector work just as well, e.g.  $n^\mu = (1, 0, 0, 1)$  with  $\bar{n}^\mu = (3, 2, 2, 1)$ , and later on this freedom in defining  $\bar{n}$  will be codified in a reparameterization invariance symmetry. For now we stick with the choice in Eq. (2.3).

It is now simple to represent standard 4-vectors in the light-cone basis

$$p^\mu = \frac{n^\mu}{2} \bar{n} \cdot p + \frac{\bar{n}^\mu}{2} n \cdot p + p_\perp^\mu \quad (2.4)$$

where the  $\perp$  components are orthogonal to both  $n$  and  $\bar{n}$ . With the choice in Eq. (2.3),  $p_\perp^\mu = (0, p^1, p^2, 0)$ . It is customary to represent a momentum in these coordinates by

$$p^\mu = (p^+, p^-, \vec{p}_\perp) \quad (2.5)$$

where the last entry is two-dimensional, and the minkowski  $p_\perp^2$  is the negative of the euclidean  $\vec{p}_\perp^2$  (ie. in our notation  $p_\perp^2 = -\vec{p}_\perp^2$ ). Here we have also defined

$$p^+ = p_+ \equiv n \cdot p, \quad p^- = p_- \equiv \bar{n} \cdot p. \quad (2.6)$$

As indicated the upper or lower  $\pm$  indices mean the same thing.

Using the standard  $(+ - - -)$  metric, the four-momentum squared is

$$p^2 = p^+ p^- + p_\perp^2 = p^+ p^- - \vec{p}_\perp^2. \quad (2.7)$$

We can also decompose the metric in this basis

$$g^{\mu\nu} = \frac{n^\mu \bar{n}^\nu}{2} + \frac{\bar{n}^\mu n^\nu}{2} + g_\perp^{\mu\nu}. \quad (2.8)$$

Finally we can define an antisymmetric tensor in the  $\perp$  space by  $\epsilon_\perp^{\mu\nu} = \epsilon^{\mu\nu\alpha\beta} \bar{n}_\alpha n_\beta / 2$ .

### 2.3 Momentum Regions: SCET I and SCET II

Lets continue with our exploration of the  $B \rightarrow D\pi$  decay with the goal of identifying the relevant quark and gluon degrees of freedom (d.o.f.) for designing an EFT to describe this process. We'll then do the same for a process with jets.

There are different ways of finding the relevant infrared degrees of freedom. We could characterize all possible regions giving rise to infrared singularities at any order in perturbation theory using techniques like the Landau equations, and then determine the corresponding momentum regions. We could carry out QCD loop calculations using a technique known as the method of regions, where the full result is obtained by a sum of terms that enter from different momentum regions. Then by examining these regions we could hypothesize that there should be corresponding EFT degrees of freedom for those regions that appear to correspond to infrared modes that should be in the EFT. (Either of these approaches may be useful, but note that when using them we must be careful that the degrees of freedom are appropriate to our true physical situation, and do not contain artifacts related to our choice of perturbative infrared regulators that are not present in the true nonperturbative QCD situation.) Instead, our approach in this section will be based solely on physical insight of what the relevant d.o.f. are, from thinking through what is happening in the hard scattering process we want to study. More mathematical checks that one has the right d.o.f. are also desirable, and we will talk about some examples of how to do this later on. This falls under the rubric of not fully trusting a physics argument without the math that backs it up, and visa versa.

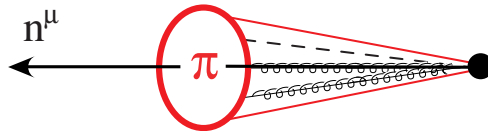
For  $B \rightarrow D\pi$  in the rest frame of the  $B$ , the constituents of the  $B$  meson are the nearly static heavy  $b$  quark, and the soft quarks and gluons with momenta  $\sim \Lambda_{\text{QCD}}$ , ie. just the standard degrees of freedom of HQET. Since  $|\vec{p}_D| = 2.31 \text{ GeV} \sim m_D = 1.87 \text{ GeV}$  the constituents of the  $D$  meson are also soft and described by HQET. The pion on the other hand is highly boosted. We can derive the momentum scaling of the pion constituents by starting with the  $(+, -, \perp)$  scaling of

$$p^\mu \sim (\Lambda_{\text{QCD}}, \Lambda_{\text{QCD}}, \Lambda_{\text{QCD}}) \quad \text{for constituents in the pion rest frame,}$$

and then by boosting along  $-\hat{z}$  by an amount  $\kappa = Q/\Lambda_{\text{QCD}}$ . The boost is very simple with light cone coordinates, taking  $p^- \rightarrow \kappa p^-$  and  $p^+ \rightarrow p^+/\kappa$ . Thus

$$p_c^\mu \sim \left( \frac{\Lambda_{\text{QCD}}^2}{Q}, Q, \Lambda_{\text{QCD}} \right) \quad (2.9)$$

for the energetic pions constituents in the  $B$  rest frame. This scaling describes the typical momenta of the quarks and gluons that bind into the pion moving with large momentum  $p_\pi^\mu = (0, Q, 0) + \mathcal{O}(m_\pi^2/Q)$ , as in



The important fact about Eq. (2.9) is that

$$p_c^- \gg p_c^\perp \gg p_c^+ . \quad (2.10)$$

Whenever the components of  $p_c^\mu$  obey this hierarchy we say it has a **collinear** scaling. Its convenient to describe this collinear scaling with a dimensionless parameter by writing

$$p_c^\mu \sim Q(\lambda^2, 1, \lambda) \quad (2.11)$$



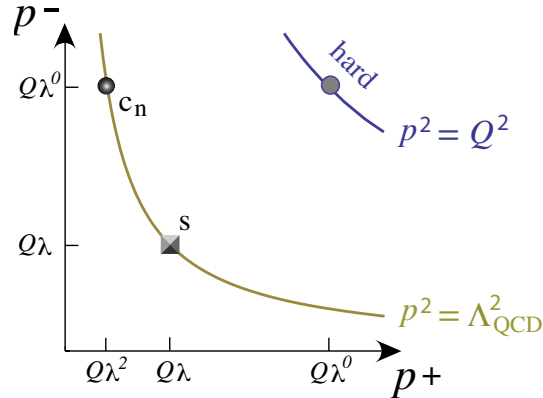


Figure 1: SCET<sub>II</sub> example. Relevant degrees of freedom for  $B \rightarrow D\pi$  with an energetic pion in the  $B$  rest frame.

where  $\lambda \ll 1$  is a small parameter. This result is generic. For our  $B \rightarrow D\pi$  example we have  $\lambda = \Lambda_{\text{QCD}}/Q$ .<sup>1</sup> This  $\lambda$  will be the power counting parameter of SCET. With this notation we can also say how the soft momenta of constituents in the  $B$  and  $D$  meson scale,

$$p_s^\mu \sim Q(\lambda, \lambda, \lambda). \quad (2.12)$$

Thus we see that we need both soft and collinear degrees of freedom for the  $B \rightarrow D\pi$  decay.

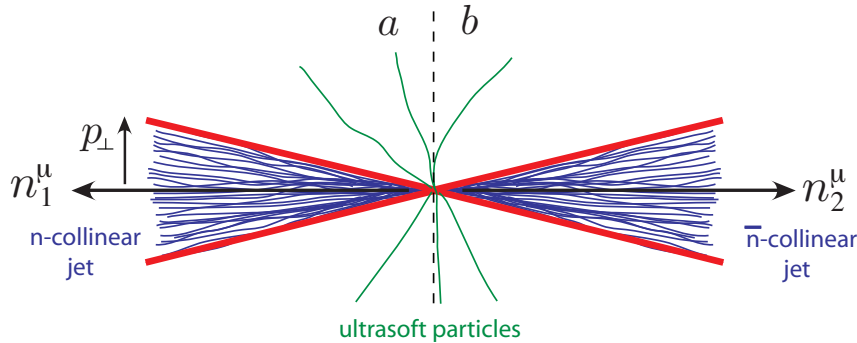
It is convenient to represent the degrees of freedom with a picture, as in Fig. 1. This picture has some interesting features. Unlike simpler effective theories SCET requires at least two variables to describe the d.o.f. The choice of  $p^-$  and  $p^+$  as the axis here suffices since the  $\perp$ -momentum satisfies  $p_\perp^2 \sim p^+p^-$  and hence does not provide additional information. The hyperbolas in the figures are lines of constant  $p^2 = p^+p^-$ . The labelled spots indicate the relevant momentum regions. We have included a hyperbola and a spot for the hard region where  $p^2 \sim Q^2$ , but these are the modes that are actually integrated out when constructing SCET. (For  $B \rightarrow D\pi$  they are fluctuations of order the heavy quark masses.) On the  $p^2 \sim \Lambda_{\text{QCD}}^2$  hyperbola in Fig. 1 we have two types of nonperturbative modes, collinear modes  $c_n$  for the pion constituents, and soft modes  $s$  for the  $B$  and  $D$  meson constituents. Since these modes live at the same typical invariant mass  $p^2$  we need another variable, namely  $p^-/p^+$ , to distinguish them. This variable is related to the rapidity,  $Y$ , since  $e^{2Y} = p^-/p^+$ . Put another way, we need both of the variables  $p^+$  and  $p^-$  to define the modes for the EFT.

The example in Fig. 1 is what is known as an SCET<sub>II</sub> type theory. Its defining characteristic is that the soft and collinear modes in the theory have the same scaling for  $p^2$ , they live on the same hyperbola. This type of theory turns out to be appropriate for a wide variety of different processes and hence we give it the generic name SCET<sub>II</sub>. Essentially this version of SCET is the appropriate one for hard processes which produce energetic identified hadrons, what we earlier called exclusive hard scattering and exclusive B-decays.

<sup>1</sup>Please do not be confused into thinking that you need to assign a precise definition to  $\lambda$ . It is only used as a scaling parameter to decide what operators we keep and what terms we drop in the effective field theory, so any definition which is equivalent by scaling is equally good. In the end any predictions we make for observables do not depend on the numerical value of  $\lambda$ . The only time we need a number for  $\lambda$  is when making a numerical estimate for the size of the terms that are higher order in the power expansion which we've dropped.

When looking at Fig. 1 we should interpret the collinear degrees of freedom as living mostly in a region about the  $c_n$  spot and the soft degrees of freedom as living mostly in a region about the  $s$  spot. An obvious question is what determines the boundary between these degrees of freedom. In a Wilsonian EFT the answer would be easy, there would be hard cutoffs that carve out the regions defined by these modes. But hard cutoffs break symmetries. For SCET the cutoffs must be “softer regulators” so as to not to break symmetries like Lorentz invariance and gauge invariance. Dimensional regularization is one regulator that can be used for this purpose. If we were only trying to distinguish modes with the invariant mass  $p^2$  then the dim.reg. scale parameter  $\mu$  would suffice for the cutoff between UV and IR modes, and we would be set to go. But in SCET we also need to distinguish modes in another dimension,  $\mu$  does not suffice to separate or distinguish the  $s$  and  $c_n$  modes of Fig. 1. We will see how to do this later on without spoiling any symmetries. In general it will require a combination of subtractions that localize the modes in the regions shown in the figure, as well as additional cutoff parameters. The bottom line is that the physical picture in Fig. 1 for where the modes live is the correct one to think about for the purpose of power counting. But when integrating over loop momenta in a virtual diagram involving one of these modes we integrate over all values with a soft regulator to avoid breaking symmetries.

Lets consider a second example involving QCD jets. Jets are collimated sprays of hadrons produced by the showering process of an energetic quark or gluon as it undergoes multiple splittings. The splitting is enhanced in the forward direction by the presence of collinear singularities. The simplest process is  $e^+e^- \rightarrow$  dijets, which at lowest order is the process  $e^+e^- \rightarrow \gamma^* \rightarrow q\bar{q}$  with each of the light quarks  $q$  and  $\bar{q}$  forming a jet. Let  $q^\mu$  be the momentum of the  $\gamma^*$ , then in the center-of-momentum frame (CM frame)  $q^\mu = (Q, 0, 0, 0)$  and sets the hard scale. If there are only two jets in the final state then by momentum conservation they will be back-to-back along the horizontal  $\hat{z}$  axis:



The  $x - y$  plane defines two hemispheres  $a$  and  $b$ , and we consider a process with one jet in each of them. The energy in each hemisphere is  $Q/2$  and is predominantly carried by the collimated particles in the jets. To describe the degrees of freedom we need two collinear directions. We align  $n_1^\mu$  with the direction of the first jet and  $n_2^\mu$  with the second. (These directions can be defined by using a jet algorithm to determine the particles inside a jet, or indirectly from the process of calculating a jet event shape like thrust.)

Lets first consider the energetic constituents of the  $n_1$ -jet. Since these constituents are collimated they have a  $\perp$ -momentum that is parametrically smaller than their large minus momentum,  $p_\perp \sim \Delta \ll p^- \sim Q$ . In order that we have a jet of hadrons and not a single hadron or small number of hadrons we must have  $\Delta \gg \Lambda_{\text{QCD}}$ . Thus the jets constituents have  $(+, -, \perp)$  momenta with respect to the axes  $n_1 = (1, -\hat{z})$  and  $\bar{n}_1 = (1, \hat{z})$  that have a collinear scaling

$$p_{n_1}^\mu \sim \left( \frac{\Delta^2}{Q}, Q, \Delta \right) = Q(\lambda^2, 1, \lambda). \quad (2.13)$$

As usual the scaling of the  $+$ -momentum is determined by noting that we are considering fluctuations about  $p^2 = 0$ , so  $p^+ \sim p_\perp^2/p^-$ . Here the power counting parameter is  $\lambda = \Delta/Q \ll 1$ . Note that the jet

constituents have the same scaling as the constituents of a collinear pion, but carry larger offshellness  $p^2$ . If we make  $\Delta$  so large that  $\Delta \sim Q$  then we no longer have a dijet configuration, and if we make  $\Delta$  so small that  $\Delta \sim \Lambda_{\text{QCD}}$  then the constituents will bind into one (or more) individual hadrons rather than the large collection of hadrons that make up the jet. Another way to characterize the presence of the jet is through the jet-mass  $m_J^2$ , since a jet will have  $Q^2 \gg m_J^2 \gg \Lambda_{\text{QCD}}^2$ . For our example here we can make use of the  $a$ -hemisphere jet-mass,

$$m_{J_a}^2 \equiv \left( \sum_{i \in a} p_i^\mu \right)^2 \sim p_{n_1}^+ p_{n_1}^- \sim \Delta^2 \ll Q^2. \quad (2.14)$$

For the constituents of the  $n_2$ -jet we simply repeat the discussion above, but with particles collimated about the direction,  $n_2 = \bar{n}_1 = (1, \hat{z})$ . A choice that makes this simple is  $\bar{n}_2 = n_1 = (1, -\hat{z})$ , since then we can simply take the  $n_1$ -jet analysis results with  $+ \leftrightarrow -$ . Using the same  $(+, -, \perp)$  components as for the  $n_1$ -jet we then have

$$p_{n_2}^\mu \sim \left( Q, \frac{\Delta^2}{Q}, \Delta \right) = Q(1, \lambda^2, \lambda). \quad (2.15)$$

Again a measurement of the  $b$ -hemisphere jet-mass can be used to ensure that there is only one jet in that region jet-mass,

$$m_{J_b}^2 \equiv \left( \sum_{i \in b} p_i^\mu \right)^2 \sim p_{n_2}^+ p_{n_2}^- \sim \Delta^2 \ll Q^2. \quad (2.16)$$

Finally in jet processes there are also soft homogeneous modes that account for soft hadrons that appear between the collimated jet radiation (as well as within it). The precise momentum of these degrees of freedom depends on the observable being studied, and the restrictions it imposes on this radiation. In our  $e^+e^- \rightarrow$  dijets example we can consider measuring that  $m_{J_a}^2$  and  $m_{J_b}^2$  are both  $\sim \Delta^2$ . In this case the homogeneous modes are ‘‘ultrasoft’’ with momentum scaling as

$$p_{us}^\mu \sim \left( \frac{\Delta^2}{Q}, \frac{\Delta^2}{Q}, \frac{\Delta^2}{Q} \right) = Q(\lambda^2, \lambda^2, \lambda^2). \quad (2.17)$$

To derive this we consider the restrictions that  $m_{J_a}^2 \sim \Delta^2$  imposes on the observed particles, noting in particular that with a collinear and ultrasoft particle in the  $a$ -hemisphere we have

$$(p_{n_1} + p_{us})^2 = p_{n_1}^2 + 2p_{n_1} \cdot p_{us} + p_{us}^2 \sim \Delta^2. \quad (2.18)$$

The term  $2p_{n_1}^- \cdot p_{us} = p_{n_1}^- p_{us}^+$  plus higher order terms, so  $p_{us}^+ \sim \Delta^2/p_{n_1}^- \sim \Delta^2/Q$ , which is the ultrasoft momentum scale given in Eq. (2.17). Any larger momentum for  $p_{us}^+$  is forbidden by the hemisphere mass measurement. The scaling of the other ultrasoft momentum components then follows from homogeneity.

If we draw the degrees of freedom, then for the double hemisphere mass distribution measurement of  $e^+e^- \rightarrow$  dijets in the  $p^+-p^-$  plane we find Fig. 2. Again we have labelled hard modes with momenta  $p^2 \sim Q^2$  that are integrated out in constructing the EFT (here they correspond to virtual corrections at the jet production scale). In the low energy effective theory we have two types of collinear modes  $c_n$  and  $c_{\bar{n}}$ , one for each jet, which live on the  $p^2 \sim \Delta^2$  hyperbola. Finally the ultrasoft modes live on a different hyperbola with  $p^2 \sim \Delta^4/Q^2$ . The collinear and ultrasoft modes all have  $p^2 \lesssim Q^2 \lambda^2$  and are degrees of freedom in SCET, while modes with  $p^2 \gg Q^2 \lambda^2$  are integrated out. When we are in a situation like this one, where the collinear and homogeneous modes live on hyperbolas with parametrically different scaling for  $p^2$ , then the resulting SCET is known as an SCET<sub>I</sub> type theory. Note that the  $c_n$  and  $us$  modes have

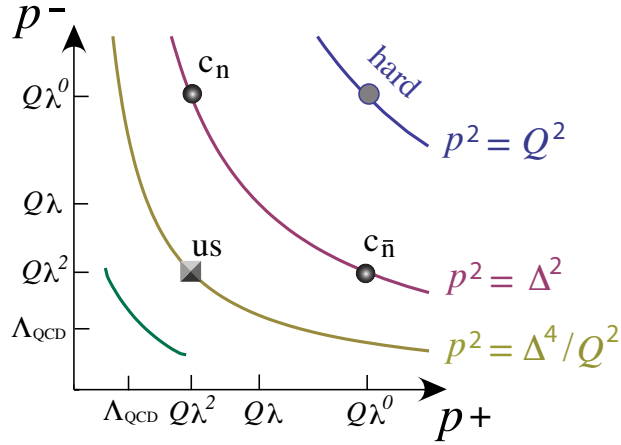


Figure 2: SCET<sub>I</sub> example. Relevant degrees of freedom for dijet production  $e^+e^- \rightarrow$  dijets with measured hemisphere invariant masses  $m_{J_a}^2$  and  $m_{J_b}^2$ .

$p^+$  momenta of the same size, whereas the  $c_{\bar{n}}$  and  $us$  modes have  $p^-$  momenta of the same size. The names collinear and ultrasoft denote the fact that these modes live on different hyperbolas.<sup>2</sup> Once again these degrees of freedom capture regions of momentum space, which are centered around the spots indicated and each of them extend into the infrared.

It is important to note in this dijet example that  $\Delta^4/Q^2 \gtrsim \Lambda_{\text{QCD}}^2$ , so in general the nonperturbative ultrasoft modes can live on an even smaller hyperbola  $p^2 \sim \Lambda_{\text{QCD}}^2$  than the perturbative contributions from ultrasoft modes that have  $p^2 \sim \Delta^4/Q^2$ . An additional  $p^2 \sim \Lambda_{\text{QCD}}^2$  hyperbola is shown in green in Fig. 2. If  $\Delta^4/Q^2 \sim \Lambda_{\text{QCD}}^2$  then the yellow and green hyperbolas are not distinguishable by power counting, and hence are equivalent. If on the other hand we are in a situation where  $\Delta^4/Q^2 \gg \Lambda_{\text{QCD}}^2$  then when we setup the SCET<sub>I</sub> theory both the perturbative ultrasoft modes with  $p^2 \sim \Delta^4/Q^2$  and the nonperturbative ultrasoft modes with  $p^2 \sim \Lambda_{\text{QCD}}^2$  will be part of our single ultrasoft degree of freedom. This is convenient because we can first formulate the  $\Delta/Q \ll 1$  expansion with the  $c_n$ ,  $c_{\bar{n}}$  and  $us$  d.o.f., and only later worry about making another expansion in  $Q\Lambda_{\text{QCD}}/\Delta^2 \ll 1$  to separate the two types of ultrasoft modes that would live on the yellow and green hyperbolas.

If we compare Fig. 1 and Fig. 2 we see that it is the relative behaviour of the collinear and soft/ultrasoft modes that determine whether we are in an SCET<sub>I</sub> or SCET<sub>II</sub> type situation. (There are also SCET<sub>II</sub> examples which involve jets with  $\perp$  measurements rather than jet masses, and we will meet these later on in Section 11.3 and 11.4.) Much of our discussion will be devoted to studying these two examples of SCET, since they are already quite rich and cover a wide variety of processes. In general however one should be aware that a more complicated process or set of measurements may well require a more sophisticated pattern of degrees of freedom. For example, we could have soft or collinear modes on more than one hyperbola, or might require modes with a new type of scaling. Indeed, this is not even uncommon, the collider physics example of  $pp \rightarrow$  dijets in the CM frame requires both SCET<sub>II</sub> type collinear modes for the incoming protons, and SCET<sub>I</sub> type collinear modes for the jets. Nevertheless, after having studied both SCET<sub>I</sub> and SCET<sub>II</sub> we will see that often these more complicated processes do not really require additional formalism, but rather simply require careful use of the tools we have already developed in studying SCET<sub>I</sub>

<sup>2</sup>In certain situations in the literature to use the names hard-collinear and soft to denote the same thing, and we will find occasion to explain why when discussing how SCET<sub>I</sub> can be used to construct SCET<sub>II</sub>.

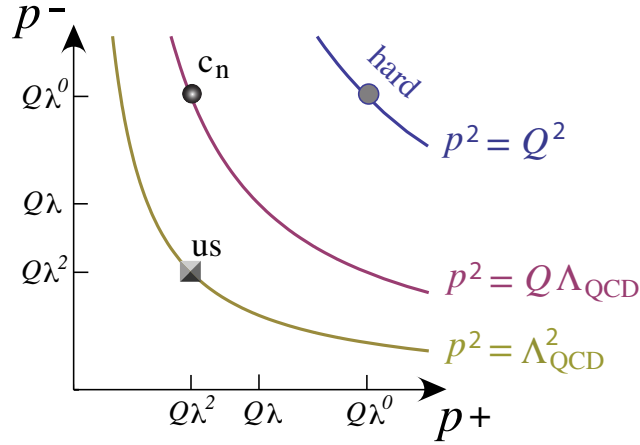


Figure 3: Another SCET<sub>I</sub> example. Relevant degrees of freedom for  $B \rightarrow X_s \gamma$  in the endpoint region.

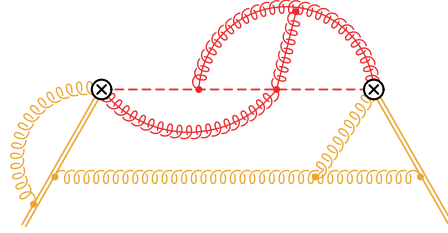
and SCET<sub>II</sub>.

A comment is also in order about the frame dependence of our degrees of freedom. In both of our examples we found it convenient to discuss the degrees of freedom in a particular frame (the  $B$  rest frame, or  $e^+e^-$  CM frame). Typically there is a natural reference frame to think about the analysis of a process, but of course the final result describing the dynamics of a process will actually not be frame dependent. Thus it is natural to ask what the d.o.f. and corresponding momentum regions would look like in a different frame. A simple example to discuss is a boost of the entire process along the  $\hat{z}$  axis. All the modes then slide along their hyperbolas (since  $p^2$  is unchanged). The important point is that the relative size of momenta of different d.o.f. is unchanged by this procedure: the  $p^+$  momenta of collinear and ultrasoft modes in SCET<sub>I</sub> will be the same size even after the boost, and the  $p^+$  momentum of a soft particle will always be larger than the  $p^+$  momentum of a collinear particle in SCET<sub>II</sub>. In  $B \rightarrow D\pi$  such a boost can take us to the pion rest frame, where its constituents are now soft, and the constituents of the  $B$  and  $D$  are now boosted. Some components of the SCET analysis may look a bit different if we use different frames, but the final EFT results for decay rates and cross sections will obey the expected overall boost relations. In general it is only the relative scaling of the momenta of various degrees of freedom that enter into expansions and the final physical result. The relative placement of the spots for our d.o.f. in SCET<sub>I</sub> and SCET<sub>II</sub> is not affected by the  $\hat{z}$  boost.

Before finishing our discussion of d.o.f. we consider one final example. For the purpose of studying SCET<sub>I</sub> it is useful to have an example with one jet rather than two, so the d.o.f. become simply  $c_n$  and  $us$ . This can occur for the process  $B \rightarrow X_s \gamma$  or for  $B \rightarrow X_u e \bar{\nu}$ . The underlying processes here are the flavor changing neutral current process  $b \rightarrow s \gamma$  or the semileptonic decay  $b \rightarrow u e \bar{\nu}$ . For these inclusive decays we sum over any collection of hadronic states  $X_s$  or  $X_u$  that can be produced from the  $s$  or  $u$  quark. In the  $B$  rest frame, the total energy of the  $\gamma$  or  $(e \bar{\nu})$  is  $E = (m_B^2 - m_X^2)/(2m_B)$  and ranges from 0 to  $(m_B^2 - m_{H_{\min}}^2)/(2m_B)$  where  $m_{H_{\min}}$  is the smallest appropriate hadron mass, either  $m_{H_{\min}} = m_{K^*}$  or  $m_\pi$  for  $X_s$  or  $X_u$  respectively. An interesting region to consider for the application of SCET is

$$\Lambda_{\text{QCD}}^2 \ll m_X^2 \ll Q^2 = m_B^2 \quad (2.19)$$

where the photon or  $(e \bar{\nu})$  recoils against a jet of hadrons which are the constituents of  $X$ . For  $B \rightarrow X_s \gamma$  the picture is (double line being the  $b$ -quark, yellow lines are soft particles, and red lines are collinear particles):



Here the jet mass is also the mass of the hadronic final state, and the situation which dominates the phenomenology has  $m_X^2 \sim Q\Lambda_{\text{QCD}}$ . We have collinear modes for the jet, and ultrasoft modes with  $p_{us}^2 \sim \Lambda_{\text{QCD}}^2$  which are the constituents of the  $B$  meson for this inclusive decay. Often the region where  $m_X^2 \ll Q^2$  is known as the endpoint region since  $E \sim m_B/2 - \Lambda_{\text{QCD}}$  and hence is close to the physical endpoint  $E = m_B/2$ . (The case  $m_X^2 \sim Q^2$  is then known as the local OPE region where the traditional HQET operator product expansion analysis suffices.) The picture of the modes for this case are shown in Fig. 3, and indeed yield an example of an SCET<sub>I</sub> theory with only one collinear mode.

### 3 Ingredients for SCET

Our objective in this section is to expand QCD and formulate collinear and ultrasoft degrees of freedom. In doing so, we will derive power counting expressions for operators and see what form the quark Lagrangian takes in a SCET theory.

#### 3.1 Collinear Spinors

We begin our exploration by considering the decomposition in the collinear limit of Dirac spinors  $u(p)$  for particles and  $v(p)$  for antiparticles. We will derive the collinear spinors by considering the expansion in momentum components, but then will convert this result into a decomposition into two types of terms rather than an infinite expansion.

For a collinear momentum  $p^\mu = (p^0, p^1, p^2, p^3)$  we have  $p^- = p^0 + p^3 \gg p_\perp^{1,2} \gg p^+ = p^0 - p^3$  so

$$\frac{\vec{\sigma} \cdot \vec{p}}{p^0} = \sigma_3 + \dots, \quad (3.1)$$

where the terms in the  $+\dots$  are smaller. Keeping only the leading term gives us the spinors

$$\begin{aligned} u(p) &= \frac{(2p^0)^{1/2}}{\sqrt{2}} \begin{pmatrix} \mathcal{U} \\ \frac{\vec{\sigma} \cdot \vec{p}}{p^0} \mathcal{U} \end{pmatrix} \implies u_n = \sqrt{\frac{p^-}{2}} \begin{pmatrix} \mathcal{U} \\ \sigma^3 \mathcal{U} \end{pmatrix} \\ v(p) &= \frac{(2p^0)^{1/2}}{\sqrt{2}} \begin{pmatrix} \frac{\vec{\sigma} \cdot \vec{p}}{p^0} \mathcal{V} \\ \mathcal{V} \end{pmatrix} \implies v_n = \sqrt{\frac{p^-}{2}} \begin{pmatrix} \sigma^3 \mathcal{V} \\ \mathcal{V} \end{pmatrix} \end{aligned} \quad (3.2)$$

where here  $\mathcal{U}$  and  $\mathcal{V}$  are each either  $\begin{pmatrix} 1 \\ 0 \end{pmatrix}$  or  $\begin{pmatrix} 0 \\ 1 \end{pmatrix}$ . From this analysis we see that in the collinear limit both quark and antiquarks remain as relevant degrees of freedom (and indeed, there is no suppression for pair creation from splitting). We also see that both spin components remain in each of the spinors. Recalling our default definitions of  $n^\mu$  and  $\bar{n}^\mu$ , we can calculate their contractions with the gamma matrix,

$$\not{n} = \gamma_0 - \gamma_3 = \begin{pmatrix} \mathbb{1} & -\sigma^3 \\ \sigma^3 & -\mathbb{1} \end{pmatrix}, \quad \not{\bar{n}} = \gamma_0 + \gamma_3 = \begin{pmatrix} \mathbb{1} & \sigma^3 \\ -\sigma^3 & -\mathbb{1} \end{pmatrix}. \quad (3.3)$$

Multiplying the first matrix by  $u_n$  or  $v_n$  from (3.2) gives the following relations

$$\not{n}u_n = 0, \quad \not{n}v_n = 0. \quad (3.4)$$

These can be recognized as the leading term in the equations of motion  $\not{p}u(p) = \not{p}v(p) = 0$  when expanded in the collinear limit. We can also define projection operators

$$P_n = \frac{\not{n}\not{\bar{n}}}{4} = \frac{1}{2} \begin{pmatrix} \mathbb{1} & \sigma^3 \\ \sigma^3 & \mathbb{1} \end{pmatrix}, \quad P_{\bar{n}} = \frac{\not{\bar{n}}\not{n}}{4} = \frac{1}{2} \begin{pmatrix} \mathbb{1} & -\sigma^3 \\ -\sigma^3 & \mathbb{1} \end{pmatrix}, \quad (3.5)$$

and then we have the relations

$$P_n u_n = \frac{\not{n}\not{\bar{n}}}{4} u_n = u_n, \quad P_{\bar{n}} v_n = \frac{\not{\bar{n}}\not{n}}{4} v_n = v_n. \quad (3.6)$$

The bottom line of this expansion is that when a hard interaction produces a collinear fermion or antifermion it will be the components obeying the spin relations in Eqs. (3.4) and (3.6) that appear at leading order.

For later purposes it will be useful to decompose the QCD Dirac field  $\psi$  into a field  $\xi_n$  that obeys these spin relations. From  $\{\gamma^\mu, \gamma^\nu\} = 2g^{\mu\nu}$  we note that

$$\frac{\not{n}\not{\bar{n}}}{4} + \frac{\not{\bar{n}}\not{n}}{4} = \mathbb{1}, \quad (3.7)$$

which allows us to write  $\psi$  in terms of two fields,

$$\psi = P_n \psi + P_{\bar{n}} \psi = \hat{\xi}_n + \varphi_{\bar{n}} \quad (3.8)$$

where we defined

$$\hat{\xi}_n = P_n \psi = \frac{\not{n}\not{\bar{n}}}{4} \psi, \quad \varphi_{\bar{n}} = P_{\bar{n}} \psi = \frac{\not{\bar{n}}\not{n}}{4} \psi. \quad (3.9)$$

These fields satisfy the desired spin relations

$$\not{n}\hat{\xi}_n = 0, \quad P_n \hat{\xi}_n = \hat{\xi}_n, \quad \not{n}\varphi_{\bar{n}} = 0, \quad P_{\bar{n}} \varphi_{\bar{n}} = \varphi_{\bar{n}}. \quad (3.10)$$

The label  $n$  on  $\hat{\xi}_n$  reminds us that it obeys these relations and that we will eventually be expanding about the  $n$ -collinear direction. Note that here we denote the collinear field components with a hat, as in  $\hat{\xi}_n(x)$ , since there are still further manipulations that are required before we arrive at our final SCET collinear field  $\xi_n(x)$ . Nevertheless both  $\hat{\xi}_n$  and  $\xi_n$  satisfy these spinor relations.

Having defined  $\hat{\xi}_n = P_n \psi$ , the corresponding result for the spinors is  $u_n = P_n u(p)$  and  $v_n = P_n v(p)$ , which do not precisely reproduce the lowest order expanded results in Eq. (3.2). Instead we find

$$\begin{aligned} u_n &= \frac{1}{2} \begin{pmatrix} \mathbb{1} & \sigma_3 \\ \sigma_3 & \mathbb{1} \end{pmatrix} \sqrt{p^0} \begin{pmatrix} \mathcal{U} \\ \frac{\vec{\sigma} \cdot \vec{p}}{p_0} \mathcal{U} \end{pmatrix} = \frac{\sqrt{p^0}}{2} \begin{pmatrix} \left(1 + \frac{p_3}{p_0} - \frac{(i\vec{\sigma} \times \vec{p}_\perp)_3}{p^0}\right) \mathcal{U} \\ \sigma_3 \left(1 + \frac{p_3}{p_0} - \frac{(i\vec{\sigma} \times \vec{p}_\perp)_3}{p^0}\right) \mathcal{U} \end{pmatrix} \\ &= \sqrt{\frac{p^-}{2}} \begin{pmatrix} \tilde{\mathcal{U}} \\ \sigma_3 \tilde{\mathcal{U}} \end{pmatrix} \end{aligned} \quad (3.11)$$

where the two component spinor is

$$\tilde{\mathcal{U}} = \sqrt{\frac{p^0}{2p^-}} \left(1 + \frac{p_3}{p_0} - \frac{(i\vec{\sigma} \times \vec{p}_\perp)_3}{p^0}\right) \mathcal{U}. \quad (3.12)$$

The same derivation gives

$$v_n = \sqrt{\frac{p^-}{2}} \begin{pmatrix} \sigma_3 \tilde{\mathcal{V}} \\ \tilde{\mathcal{V}} \end{pmatrix} \quad (3.13)$$

where  $\tilde{\mathcal{V}}$  is defined in terms of  $\mathcal{V}$  by a formula analogous to Eq. (3.12). Since the spin relations in Eqs. (3.4) and (3.6) do not depend on the form of the two component spinors ( $\tilde{\mathcal{U}}$  versus  $\mathcal{U}$  etc), they remain true. We will see later that the results for the  $u_n$  and  $v_n$  spinors involving  $\tilde{\mathcal{U}}$  and  $\tilde{\mathcal{V}}$  rather than  $\mathcal{U}$  and  $\mathcal{V}$  are required to avoid breaking a reparameterization symmetry in SCET. The extra terms appearing in the definition of  $\tilde{\mathcal{U}}$  ensure the proper structure under reparameterizations of the lightcone basis. Finally we note that

$$\sum_s \tilde{\mathcal{U}}^s \tilde{\mathcal{U}}^{\dagger s} = \mathbb{1}_{2 \times 2} \quad (3.14)$$

Thus if we take the product of  $u_n$  spinors

$$u_n \bar{u}_n = \frac{p^-}{2} \begin{pmatrix} \tilde{\mathcal{U}} \tilde{\mathcal{U}}^\dagger & -\tilde{\mathcal{U}} \tilde{\mathcal{U}}^\dagger \sigma_3 \\ \sigma_3 \tilde{\mathcal{U}} \tilde{\mathcal{U}}^\dagger & -\sigma_3 \tilde{\mathcal{U}} \tilde{\mathcal{U}}^\dagger \sigma_3 \end{pmatrix}, \quad (3.15)$$

and sum over spins, we have

$$\sum_s u_n^s \bar{u}_n^s = \frac{\not{n}}{2} \bar{n} \cdot p. \quad (3.16)$$

For later convenience we write down a set of projection operator identities easily derived from  $n^2 = 0$ ,  $\bar{n} \cdot n = 2$ , and/or hermitian conjugation  $\gamma^{\mu\dagger} = \gamma^0 \gamma^\mu \gamma^0$ :

$$P_n P_{\bar{n}} = 0, \quad P_n P_n = P_n, \quad P_n \not{n} = P_{\bar{n}} \not{n} = 0, \quad P_n \not{p} = \not{p}, \quad P_{\bar{n}} \not{n} = \not{n}, \quad P_n^\dagger = \gamma_0 P_{\bar{n}} \gamma_0. \quad (3.17)$$

None of these results depends on making the canonical back-to-back choice for  $\bar{n}$ . The last result is useful for the computation of  $\bar{\hat{\xi}}_n$  from  $\hat{\xi}_n = P_n \psi$ , i.e.

$$\bar{\hat{\xi}}_n = \hat{\xi}_n^\dagger \gamma^0 = \psi^\dagger P_n^\dagger \gamma^0 = \bar{\psi} P_{\bar{n}}. \quad (3.18)$$

Thus just like the relations for  $\hat{\xi}_n$  or  $\xi_n$  we have the following relations for  $\bar{\hat{\xi}}_n$  or  $\bar{\xi}_n$ :

$$\bar{\xi}_n \not{n} = 0, \quad \bar{\xi}_n P_n = 0, \quad \bar{\xi}_n P_{\bar{n}} = \bar{\xi}_n \frac{\not{n} \not{p}}{4} = \bar{\xi}_n. \quad (3.19)$$

In addition to our collinear decomposition of the Dirac spinors and field, we will also need spinors and quark fields for the ultrasoft degrees of freedom. However, since all ultrasoft momenta are homogeneous of order  $\lambda^2$  and the scaling of momenta does not affect the corresponding components of the ultrasoft spinors, which are the same as those in QCD.

### 3.2 Collinear Fermion Propagator and $\xi_n$ Power Counting

Having considered the decomposition of spinors in the collinear limit, we now turn to the fermion propagator in the collinear limit. Here  $p^2 + i0 = \bar{n} \cdot p n \cdot p + p_\perp^2$ , and since both of these terms are  $\sim \lambda^2$  there is no



expansion of the denominator of the propagator. We can however expand the numerator by keeping only the large  $\bar{n} \cdot p$  momentum, as

$$\frac{i\not{p}}{p^2 + i0} = \frac{i\not{p}}{2} \frac{\bar{n} \cdot p}{p^2 + i0} + \dots = \frac{i\not{p}}{2} \frac{1}{n \cdot p + \frac{p_\perp^2}{\bar{n} \cdot p} + i0 \text{sign}(\bar{n} \cdot p)} + \dots \quad (3.20)$$

The fermion-gluon coupling will be proportional to  $\not{p}/2$  and hence will form a projector  $P_n$  when combined with the  $\not{p}/2$  from the propagator. Therefore the displayed term in the propagator has overlap with our spinors  $u_n$  and  $v_n$ , just giving  $P_n u_n = u_n$  etc. The fact that both  $+i0$  and  $-i0$  occur in the expanded propagator is a reflection of the fact that the lowest order SCET Lagrangian will contain both propagating particles ( $\bar{n} \cdot p > 0$ ) and propagating antiparticles ( $\bar{n} \cdot p < 0$ ).

The leading collinear propagator displayed in Eq. (3.20) should be obtained from a time-ordered product of the effective theory field,  $\langle 0 | T \hat{\xi}_n(x) \hat{\xi}_n(0) | 0 \rangle$ . At this point we can already identify the  $\lambda$  power counting for the field  $\hat{\xi}_n$  by noting that if its propagator has the form in Eq. (3.20) then its action must be of the form

$$L_n^{(0)} = \int d^4x \mathcal{L}_n^{(0)} = \int \underbrace{d^4x}_{\mathcal{O}(\lambda^{-4})} \underbrace{\hat{\xi}_n}_{\mathcal{O}(\lambda^a)} \frac{\not{p}}{2} \underbrace{[in \cdot \partial + \dots]}_{\mathcal{O}(\lambda^2)} \underbrace{\hat{\xi}_n}_{\mathcal{O}(\lambda^a)} \sim \lambda^{2a-2}. \quad (3.21)$$

Here we used the fact that  $d^4x = \frac{1}{2}(dx^+)(dx^-)(d^2x_\perp) \sim (\lambda^0)(\lambda^{-2})(\lambda^{-1})^2 \sim \lambda^{-4}$  where the scaling for the coordinates  $x^\mu$  follows from those for the collinear momenta by writing  $x \cdot p_c = x^+ p_c^- + x^- p_c^+ + 2x_\perp \cdot p_c^\perp$  and demanding that the terms in this sum are all  $\mathcal{O}(1)$ . In (3.21) we assigned  $\hat{\xi}_n \sim \lambda^a$  with the goal of determining the value of  $a$ . To do this we take the standard approach of assigning a power counting to the leading order kinetic term in the action so that  $L_n^{(0)} \sim \lambda^0$ , which gives

$$\hat{\xi}_n \sim \xi_n \sim \lambda. \quad (3.22)$$

Even though we have not fully considered all the issues needed to define the SCET collinear field  $\xi_n$ , the further manipulations we will make in section 4 below will not effect its power counting, so we have also recorded here the fact that the SCET field  $\xi_n \sim \lambda$ . Note that this scaling dimension does not agree with the collinear quark fields mass dimension since  $[\hat{\xi}_n] = [\xi_n] = 3/2$ . This is simply a reflection of the fact that the SCET power counting for operators is not a power counting in mass dimensions. The observant reader will notice that the  $\lambda$  scaling of the collinear field is the same as its twist, and indeed the SCET power counting reduces to a (dynamic) twist expansion when the latter exists.

### 3.3 Power Counting for Collinear Gluons and Ultrasoft Fields

Similar to our procedure for the collinear fermion field, we can analyze the collinear gluon field  $A_n^\mu$  in our  $n$ -collinear basis to determine the  $\lambda$  scaling of its components. This information is necessary to formulate the importance of operators in SCET. We begin by writing the full theory covariant gauge gluon propagator, but we label the fields as  $A_n^\mu(x)$  to denote the fact that we will be considering a  $n$ -collinear momenta:

$$\int d^4x e^{ik \cdot x} \langle 0 | T A_n^\mu(x) A_n^\nu(0) | 0 \rangle = -\frac{i}{k^2} \left( g^{\mu\nu} - \tau \frac{k^\mu k^\nu}{k^2} \right) = -\frac{i}{k^4} (k^2 g^{\mu\nu} - \tau k^\mu k^\nu), \quad (3.23)$$

where  $\tau$  is our covariant gauge fixing parameter. From our standard power counting result from the light-cone coordinate section, we know that  $k^2 = k_+ k_- + k_\perp^2 = Q^2 \lambda^2$ . So the  $1/k^4$  on the RHS matches up with the scaling of the collinear integration measure

$$d^4x \sim \lambda^{-4} \sim \frac{1}{(k^2)^2} \quad (3.24)$$

Thus the quantity in the final parentheses in (3.23) must be the same order as the product of  $A_n^\mu(x)A_n^\nu(0)$  fields. If both of the  $\mu\nu$  indices are  $\perp$  then both of the terms in these parantheses are  $\sim \lambda^2$ , so therefore we must have  $A_{n\perp}^\mu \sim \lambda$ . If one index is  $+$  and the other  $-$  then again both terms are the same size and we find  $A_n^+ A_n^- \sim \lambda^2$ . To break the degeneracy we take both indices to be  $+$ , then  $g^{++} = 0$ ,  $(n \cdot k)^2 \sim \lambda^4$ , so  $A_n^+ \sim \lambda^2$  and  $A_n^- \sim \lambda^0$ . Other combinations also lead to this result, namely that the components of the collinear gluon field scales in the same way as the components of the collinear momentum

$$A_n^\mu \sim k^\mu \sim (\lambda^2, 1, \lambda). \quad (3.25)$$

This result is not so surprising considering that if we are going to formulate a collinear covariant derivative  $D^\mu = \partial^\mu + igA^\mu$  with collinear momenta  $\partial^\mu$  and gauge fields, then for each component both terms must have the same  $\lambda$  scaling. Indeed imposing this property of the covariant derivative is another way to derive Eq. (3.25).

The same logic can be used to derive the power counting for ultrasoft quark and gluon fields. Since the momentum  $k_{us}^\mu \sim (\lambda^2, \lambda^2, \lambda^2)$  the measure on ultrasoft fields scales as  $d^4x \sim \lambda^{-8}$ . Also the result is now uniform for the components of  $A_{us}^\mu$ . Once again we find that the gluon field scales like its momentum. For the ultrasoft quark we have the Lagrangian  $\mathcal{L} = \bar{\psi}_{us} i \not{D}_{us} \psi_{us}$  with  $iD_{us}^\mu = i\partial^\mu + gA_{us}^\mu \sim \lambda^2$ . Therefore  $\bar{\psi}_{us}\psi_{us} \sim \lambda^6$ . All together we have

$$A_{us}^\mu \sim (\lambda^2, \lambda^2, \lambda^2), \quad \psi_{us} \sim \lambda^3. \quad (3.26)$$

For a heavy quark field that is ultrasoft the Lagrangian is  $\mathcal{L}_{\text{HQET}} = \bar{h}_v^{us} i v \cdot D_{us} h_v^{us}$  which is again linear in the derivative, so  $h_v^{us} \sim \lambda^3$  as well.

For completeness we also remark that the power counting for momenta determines the power counting for states. For one-particle states of collinear particles (with a standard relativistic normalization):

$$\langle p' | p \rangle = 2p^0 \delta^3(\vec{p}' - \vec{p}) = p^- \delta(p^- - p'^-) \delta^2(\vec{p}'^\perp - \vec{p}^\perp) \sim \lambda^{-2} \quad (3.27)$$

Thus the single particle collinear state has  $|p\rangle \sim \lambda^{-1}$  for both quarks and gluons. Given the scaling of the collinear quark and gluon fields, this implies power counting results for the polarization objects. The collinear spinors  $u_n \sim \xi_n |p\rangle \sim \lambda^0$  which is consistent with our earlier Eq. (3.11). For the physical  $\perp$  components of polarization vectors for collinear gluons we also find  $\epsilon_\perp^\mu \sim \lambda^0$ .

Of particular importance in the result in Eq.(3.25) is the fact that  $\bar{n} \cdot A_n = A_n^- \sim \lambda^0$ , indicating that there is no  $\lambda$  suppression to adding  $A_n^-$  fields in SCET operators. To understand the relevance of this result we consider in the next section an example of matching for an external current from QCD onto SCET.

### 3.4 Collinear Wilson Line, a first look

To see what impact there is to having a set of gauge fields  $\bar{n} \cdot A_n \sim \lambda^0$  lets consider as an example the process  $b \rightarrow ue\bar{\nu}$ , where the  $b$  quark is heavy and decays to an energetic collinear  $u$  quark. This process has the advantage of only involving a single collinear direction. This decay has the following weak current with QCD fields

$$J_{QCD} = \bar{u} \Gamma b \quad (3.28)$$

where  $\Gamma = \gamma^\mu(1 - \gamma^5)$ . Without gluons we can match this QCD current onto a leading order current in SCET by considering the heavy  $b$  field to be the HQET field  $h_v$  and the lighter  $u$  field by the SCET field  $\xi_n$ . This is shown in Fig. 4 part (a), where we use a dashed line for collinear quarks. The resulting SCET operator is

$$\bar{\xi}_n \Gamma h_v. \quad (3.29)$$

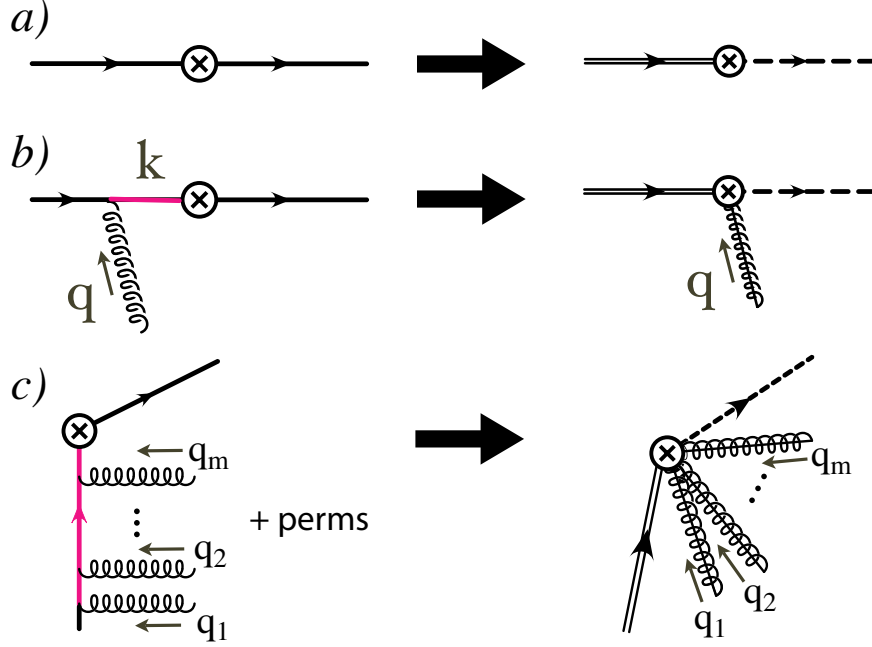


Figure 4: Tree level graphs for matching the heavy-to-light current.

Next we consider the case where an extra  $A_n^-$  gluon is attached to the heavy quark. This process is shown in Fig.4 part (b) and leads to an offshell propagator, shown by the pink line, that must be integrated out when constructing the EFT. The full theory amplitude for this process is (replacing external spinors and polarization vectors by SCET fields):

$$\begin{aligned}
A_n^\mu A^A \bar{\xi}_n \Gamma \frac{i(\not{k} + m_b)}{k^2 - m_b^2} ig T^A \gamma_\mu h_v &= -g \left( \frac{n^\mu}{2} \bar{n} \cdot A_n^A \right) \bar{\xi}_n \Gamma \frac{[m_b(1 + \psi) + \not{q}]}{2m_b v \cdot q + q^2} T^A \gamma_\mu h_v \\
&= -g \bar{n} \cdot A_n^A \bar{\xi}_n \Gamma \left[ \frac{m_b(1 + \psi) + \frac{\not{q}}{2} \bar{n} \cdot q}{m_b v \cdot n \bar{n} \cdot q} + \dots \right] T^A \frac{\not{q}}{2} h_v \\
&= -g \bar{n} \cdot A_n^A \bar{\xi}_n \Gamma \left[ \frac{\frac{\not{q}}{2} (1 - \psi) + v \cdot n}{v \cdot n \bar{n} \cdot q} + \dots \right] T^A h_v \\
&= \bar{\xi}_n \left( \frac{-g \bar{n} \cdot A_n}{\bar{n} \cdot q} \right) \Gamma h_v
\end{aligned} \tag{3.30}$$

In the first equality we have used the fact that the incoming  $b$  quark carries momentum  $m_b v^\mu$ , that  $k = m_b v + q$  so that  $k^2 - m_b^2 = 2m_b v \cdot q + q^2$ , and that

$$A_n^\mu = \underbrace{\frac{n^\mu}{2} \bar{n} \cdot A_n}_{O(\lambda^0)} + \underbrace{\frac{\bar{n}^\mu}{2} n \cdot A_n}_{O(\lambda^2)} + \underbrace{A_n^\perp}_{O(\lambda)} \tag{3.31}$$

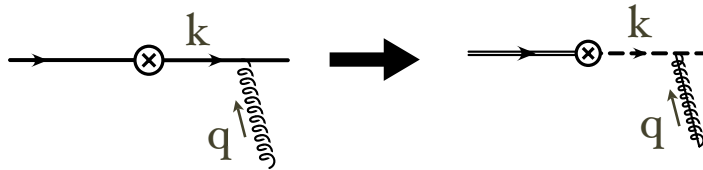
where we can keep only the  $\sim \lambda^0$  term. In the second equality in Eq. (3.30) we have expanded the numerator and denominator of the propagator in  $\lambda$  and kept only the lowest order terms. Since  $m_b v \cdot n \bar{n} \cdot q \sim Q^2 \lambda^0$  we see that the propagator is offshell by an amount of  $\sim Q^2$ , and hence is a hard propagator that we must

integrate out when constructing the corresponding SCET operator. In the third equality we use  $\not{n}^2 = 0$  and pushed the  $\not{n}$  through to the left. Noting that  $(1 - \not{\psi})h_v = 0$ , the fourth equality gives the final leading order result from this calculation. Thus we see that in SCET integrating out offshell hard propagators that are induced by  $\bar{n} \cdot A_n$  gluons leads to an operator for the leading order current with one collinear gluon coming out of the vertex, pictured on the RHS of Fig. 4 part (b).

Inspecting the final result in Eq. (3.30) we see that, in addition to being a great simplification of the original QCD amplitude for this gluon attachments, it is indeed of the same order in  $\lambda$  as the result in Eq. (3.29). Indeed it is straightforward to prove that the same  $(-g\bar{n} \cdot A_n/\bar{n} \cdot q)$  result will be obtained if we replace the heavy quark by a particle that is not  $n$ -collinear, such as a collinear quark in a different direction  $n'$  where  $n \cdot n' \gg \lambda^2$ . The sum of collinear momenta in the  $n$  and  $n'$  directions will also be offshell, for example when we add two back-to-back collinear momenta  $(p_n + p_{n'})^2 \sim \lambda^0$ . In all these situations we find operators with additional  $\bar{n} \cdot A_n \sim \lambda^0$  fields.

In summary, the off-shell quark has been integrated out and its effects have been parameterized by an effective operator. This was necessary because the virtual quark resulting from the interaction of a heavy quark or a  $n'$  collinear particle with a  $n$ -collinear gluon yields an off-shell momentum.

This result can be contrasted with what happens if we attach a single  $\bar{n} \cdot A_n$  collinear gluon field to the light collinear  $u$  quark, as shown below:



Calling the final  $u$  quark's momentum  $p$  we have  $k^\mu = p^\mu - q^\mu$ . However here since both  $p$  and  $q$  are  $n$ -collinear the propagator momentum  $k^\mu$  also has  $n$ -collinear scaling. In particular  $k^2 \sim \lambda^2$  and is not offshell, it instead represents a propagating mode within the effective theory. Thus this interaction is reproduced in SCET by a collinear propagator followed by a leading order Feynman rule that couples the  $\bar{n} \cdot A_n$  field to the collinear quark. Thus this diagram corresponds to a time ordered product of the leading order SCET current  $J^{(0)}$  with the leading order Lagrangian  $\mathcal{L}_n^{(0)}$ . If we attach more collinear gluons to the light  $u$  quark, the same remains true. We never get an offshell propagator that we have to integrate out when we have an interaction between  $n$ -collinear particles. Indeed we will also find that the components  $n \cdot A_n$  and  $A_n^\perp$  couple at leading order in T-products like the one shown above, so there is nothing special about the  $\bar{n} \cdot A_n$  components for these diagrams.

Lets now consider the situation of multiple gluon emission from the heavy quark. In this case we again have offshell propagators, which are represented by the pink line in Fig. 4 part (c). By inspection, it is clear that the generalization from one gluon emission to  $k$  gluon emissions with momenta  $q_1, \dots, q_k$  and propagators with momenta  $q_1, q_1 + q_2, \dots, \sum_{i=1}^k q_i$  yields

$$\bar{\xi}_n \sum_{\text{perm}} \frac{(-g)^k}{k!} \left( \frac{\bar{n} \cdot A_{q_1} \cdots \bar{n} \cdot A_{q_k}}{[\bar{n} \cdot q_1][\bar{n} \cdot (q_1 + q_2)] \cdots [\bar{n} \cdot \sum_{i=1}^k q_i]} \right) \Gamma h_v \quad (3.32)$$

Here the sum of permutations (perms) of the  $\{q_1, \dots, q_k\}$  momenta accounts for the fact that we must consider diagrams with crossed gluon lines on the LHS of Fig. 4 part (c). We also include the factor of  $k!$  as a symmetry factor to account for the fact that all  $k$  gluon fields are localized and identical and may be contracted with any external gluon state. Finally, by summing over the number of possible gluon emissions, we can write the complete tree level matching of the QCD current to the SCET current,

$$J_{\text{SCET}} = \bar{\xi}_n W_n \Gamma h_v, \quad (3.33)$$

where

$$W_n = \sum_k \sum_{\text{perm}} \frac{(-g)^k}{k!} \left( \frac{\bar{n} \cdot A_n(q_1) \cdots \bar{n} \cdot A_n(q_k)}{[\bar{n} \cdot q_1][\bar{n} \cdot (q_1 + q_2)] \cdots [\bar{n} \cdot \sum_{i=1}^k q_i]} \right). \quad (3.34)$$

Here  $W_n$  is the momentum space version of a Wilson line built from collinear  $A_n$  gluon fields. In position space the corresponding Wilson line is

$$W(0, -\infty) = \text{P exp} \left( ig \int_{-\infty}^0 ds \bar{n} \cdot A_n(\bar{n}s) \right) \quad (3.35)$$

Here P is the path ordering operator which is required for nonabelian fields and which puts fields with larger arguments to the left e.g.  $\bar{n} \cdot A_n(\bar{n}s) \bar{n} \cdot A_n(\bar{n}s')$  for  $s > s'$ .

In summary, we see that we have traded the field  $\bar{n} \cdot A_n$  for the Wilson line  $W_n[\bar{n} \cdot A_n]$ . Also, including this Wilson line in our current operator makes our current gauge invariant, as we will show below in the Gauge Symmetry section. For a situation with  $n$  and  $n'$  collinear fields the same type of Wilson lines  $W_n[\bar{n} \cdot A_n]$  are also generated in a manner that yields gauge invariant operators for each collinear sector.

## 4 SCET<sub>I</sub> Lagrangian

In this section, we derive the SCET quark Lagrangian by analyzing and separating the collinear and usoft gluons, and momentum degrees of freedom. On the way to our final result we introduce the label operator which provide a simple method to separate large (label) momenta from small (residual) momenta.

### 4.1 SCET Quark Lagrangian

Lets construct the leading order SCET collinear quark Lagrangian. This desired properties that this Lagrangian must satisfy include

- Yielding the proper spin structure of the collinear propagator
- Contain both collinear quarks and collinear antiquarks
- Have interactions with both collinear gluons and ultrasoft gluons
- Yield the correct LO propagator for different situations without requiring additional expansions
- Should be setup so we do not have to revisit the LO result when formulating power corrections

To explain what is meant by the fourth point consider the propagator obtained when a collinear quark interacts with a collinear gluon

$$\propto \frac{\bar{n} \cdot (p + q)}{n \cdot (p + q) \bar{n} \cdot (p + q) + (p_{\perp} + q_{\perp})^2 + i0}.$$

Here both the momentum  $p$  and  $q$  appear on equal footing, and no momenta are dropped in the denominator. This can be contrasted with the leading propagator obtained when a collinear quark interacts with an ultrasoft gluon

$$\propto \frac{\bar{n} \cdot p}{n \cdot (p+k) \bar{n} \cdot p + p_{\perp}^2 + i0}.$$

Here the ultrasoft  $k^\mu$  momentum is dropped for all components except  $n \cdot k$  where it is the same size as the collinear momentum  $n \cdot p$ . The dropping of  $k_{\perp} \ll p_{\perp}$  and  $\bar{n} \cdot k \ll \bar{n} \cdot p$  corresponds to carrying out a multipole expansion for the interaction of the ultrasoft gluon with the collinear quark. The LO collinear quark propagator must be smart enough to give the correct leading order result without further expansions, irrespective of whether it later emits a collinear gluon or ultrasoft gluon.

We will achieve the desired collinear Lagrangian in several steps.

#### 4.1.1 Step 1: Lagrangian for the larger spinor components

In this section we construct a Lagrangian for the field  $\hat{\xi}_n$ . It will satisfy the first two requirements in our bullet list.

We begin with the standard QCD lagrangian for massless quarks.

$$\mathcal{L}_{QCD} = \bar{\psi} i \not{D} \psi \quad (4.1)$$

Expanding  $\psi$  and  $D$  in our collinear basis gives us

$$\mathcal{L} = (\bar{\varphi}_{\bar{n}} + \bar{\xi}_n) \left( \frac{\not{n}}{2} in \cdot D + \frac{\not{n}}{2} i\bar{n} \cdot D + i\not{D}_{\perp} \right) (\varphi_{\bar{n}} + \hat{\xi}_n). \quad (4.2)$$

We can simplify this result by using the projection matrix identities for the collinear spinor found in section 3.1. In particular, various terms vanish such as

$$\frac{\not{n}}{2} i\bar{n} \cdot D \hat{\xi}_n = 0, \quad \bar{\varphi}_{\bar{n}} \frac{\not{n}}{2} in \cdot D = 0 \quad (4.3)$$

by virtue of the analog of (3.19) for  $\bar{\varphi}_{\bar{n}}$ . Lastly, terms like

$$\bar{\xi}_n i \not{D}_{\perp} \hat{\xi}_n = \bar{\xi}_n i \not{D}_{\perp} P_n \hat{\xi}_n = \bar{\xi}_n P_n i \not{D}_{\perp} \hat{\xi}_n = 0, \quad \bar{\varphi}_{\bar{n}} i \not{D}_{\perp} \varphi_{\bar{n}} = 0, \quad (4.4)$$

since  $\bar{\xi}_n P_n = 0$  and  $\bar{\varphi}_{\bar{n}} P_{\bar{n}} = 0$ . These simplifications leave us with the Lagrangian

$$\mathcal{L} = \bar{\xi}_n \frac{\not{n}}{2} in \cdot D \hat{\xi}_n + \bar{\varphi}_{\bar{n}} i \not{D}_{\perp} \hat{\xi}_n + \bar{\xi}_n i \not{D}_{\perp} \varphi_{\bar{n}} + \bar{\varphi}_{\bar{n}} \frac{\not{n}}{2} i\bar{n} \cdot D \varphi_{\bar{n}}. \quad (4.5)$$

So far this is just QCD written in terms of the  $\hat{\xi}_n$  and  $\varphi_{\bar{n}}$  fields. However, the field  $\varphi_{\bar{n}}$  corresponds to the spinor components which were subleading in the collinear limit. These spinor components will not show up in operators that mediate hard interactions at leading order. Therefore we will not need to consider a source term for  $\varphi_{\bar{n}}$  in the path integral.<sup>3</sup> This means that we can simply perform the quadratic fermionic

<sup>3</sup>At subleading order the coupling to the subleading components is introduced in operators via the combination involving  $\xi_n$  shown in the last line of Eq.(4.6), so there is still no reason to have a source term for  $\varphi_{\bar{n}}$ .

path integral over  $\varphi_{\bar{n}}$ . At tree level doing so is simply equivalent to imposing the full equation of motion for  $\varphi_{\bar{n}}$ . We find

$$\begin{aligned} 0 = \frac{\delta\mathcal{L}}{\delta\varphi_{\bar{n}}} : \quad & \frac{\not{n}}{2} i\bar{n} \cdot D\varphi_{\bar{n}} + i\not{D}_{\perp}\xi_n = 0 \\ & i\bar{n} \cdot D\varphi_{\bar{n}} + \frac{\not{n}}{2} i\not{D}_{\perp}\hat{\xi}_n = 0 \\ \varphi_{\bar{n}} = & \frac{1}{i\bar{n} \cdot D} i\not{D}_{\perp} \frac{\not{n}}{2} \hat{\xi}_n, \end{aligned} \quad (4.6)$$

where the second line is obtained by multiplying the first by  $\not{n}/2$  on the left, and the plus sign in the last line comes from using  $\not{n}i\not{D}_{\perp} = -i\not{D}_{\perp}\not{n}$ . Plugging this result back into our Lagrangian, two terms cancel, and the other two terms give the Lagrangian for the  $\hat{\xi}_n$  field

$$\mathcal{L} = \bar{\xi}_n \left( i\bar{n} \cdot D + i\not{D}_{\perp} \frac{1}{i\bar{n} \cdot D} i\not{D}_{\perp} \right) \frac{\not{n}}{2} \hat{\xi}_n. \quad (4.7)$$

The inverse derivative operator may look a little funny, but we can understand it in the same way we do for the operator  $1/\hat{r}$  in quantum mechanics, namely by defining it through its eigenvalues, which in this case are in momentum space. Say we have the operator  $\frac{1}{i\bar{n} \cdot \partial}$  acting on a field  $\phi(x)$ . Expressing this operation in momentum space gives

$$\frac{1}{i\bar{n} \cdot \partial} \phi(x) = \frac{1}{i\bar{n} \cdot \partial} \int d^4p e^{-ipx} \varphi(p) = \int d^4p e^{-ipx} \frac{1}{\bar{n} \cdot p} \varphi(p), \quad (4.8)$$

and the eigenvalues  $1/\bar{n} \cdot p$  define the inverse derivative operator.

Although we have a Lagrangian for  $\hat{\xi}_n$  we are not yet done. In particular we have not yet separated the collinear and ultrasoft gauge fields, nor the corresponding momentum components. These remaining steps will be to

2. Separate the collinear and ultrasoft gauge fields.
3. Separate the collinear and usoft momentum components with a multipole expansion.

We then can expand in the fields and momenta and keep the leading pieces.

#### 4.1.2 Step 2: Separate collinear and ultrasoft gauge fields

Recall that  $A_n^\mu \sim (\lambda^2, 1, \lambda) \sim p_n^\mu$  and  $A_n^\mu \sim (\lambda^2, \lambda^2, \lambda^2) \sim k_{us}^\mu$ . Since  $k_{us}^2 \ll p_n^2$  the ultrasoft gluons encode much longer wavelength fluctuations, so from the perspective of the collinear fields we can think of  $A_{us}^\mu$  like a classical background field. In background field gauge we would write  $A^\mu = Q^\mu + A_{cl}^\mu$  where  $Q^\mu$  is the quantum gauge field and  $A_{cl}^\mu$  is the classical background field that only appears on external lines. In general there is no need for a relationship between the full QCD gluon field  $A^\mu$  and the SCET fields  $A_{us}^\mu$  and  $A_n^\mu$ , but if one exists then it does make matching computations much simpler. Based on the analogy with a background gauge field you might not be too surprised to learn that a relation exists which encodes basic tree level matching

$$A^\mu = A_n^\mu + A_{us}^\mu + \dots \quad (4.9)$$

Here the ellipsis stand for additional terms involving Wilson lines which only will become relevant when we formulate power corrections, and hence will be ignored for our leading order analysis here (they are given below in Eq.(.)). The interpretation of  $A_{us}^\mu$  as a background field to  $\xi_n$  and  $A_n^\mu$  will also prove useful

when we derive the collinear gluon lagrangian and when we later consider gauge transformations in the theory.

Now, comparing the power counting between components of  $A_n^\mu$  and  $A_{us}^\mu$ , we find

$$\begin{aligned}\bar{n} \cdot A_n &\sim \lambda^0 \gg \bar{n} \cdot A_{us} \sim \lambda^2 \\ A_{\perp n}^\mu &\sim \lambda \gg A_{\perp us}^\mu \sim \lambda^2 \\ n \cdot A_n &\sim \lambda^2 \sim n \cdot A_{us}.\end{aligned}\tag{4.10}$$

So we see that  $A_{\perp us}^\mu$  and  $\bar{n} \cdot A_{us}$  can be dropped from our leading order analysis because in the combination  $A_n^\mu + A_{us}^\mu$  they are always dominated by the collinear gluon term. Conversely,  $n \cdot A_{us}$  cannot be dropped because it is of the same order as  $n \cdot A_n$ .

### 4.1.3 Step 3: The Multipole Expansion for Separating momenta

We want to find a way to isolate momenta that have different scaling with  $\lambda$ . Such a procedure is useful because it will allow us to formulate power corrections in a manner where operators give homogeneous contributions in  $\lambda$  order by order. For example, consider the denominator of the propagator of a quark with momentum  $p_n + k_{us}$  expanded to keep the leading and first subleading terms

$$\begin{aligned}\frac{1}{(p_n + k_{us})^2} &= \frac{1}{(p_n^- + k_{us}^-)(p_n^+ + k_{us}^-) + (p_n^\perp + k_{us}^\perp)^2} \\ &= \frac{1}{p_n^- (p_n^+ + k_{us}^+) + p_n^{\perp 2}} - \frac{2k_{us}^\perp \cdot p_n^\perp}{[p_n^- (p_n^+ + k_{us}^+) + p_n^{\perp 2}]^2} + \dots\end{aligned}\tag{4.11}$$

By power counting, we see that the first term scales as  $\lambda^{-2}$  and the second term scales as  $\lambda^{-1}$ . Although the first term dominates the second, we need to be able to reproduce the second term at the level of the Lagrangian when higher order corrections are needed. Expressed more formally, we would like a systematic multipole expansion. Our desired expansion is similar to the one found in *E&M* which gives corrections to the electrostatic potential for a given charge distribution.

In position space the multipole expansion corresponds to expanding the long wavelength field,  $A_{us}(x) = A_{us}(0) + x \cdot i\partial A_{us}(0) + \dots$ . To see what is going on here we can Fourier transform the operators (taking one-dimensional fields and ignoring indices for simplicity)

$$\begin{aligned}\int dx \bar{\psi}(x) A_{us}(0) \psi(x) &= \int dx \int dp_1 dp_2 dk e^{ip_1 x} e^{-ik(0)} e^{-ip_2 x} \bar{\psi}(p_1) A_{us}(k) \psi(p_2) \\ &= \int dp_1 dp_2 dk \delta(p_1 - p_2) \bar{\psi}(p_1) A_{us}(k) \psi(p_2).\end{aligned}\tag{4.12}$$

We see immediately that this corresponds to a 3-point Feynman rule where the small momentum  $k$  is ignored relative to the large momenta  $p_1$  and  $p_2$ , and that total momentum is not conserved at the vertex. For the next order term we get

$$\int dx \bar{\psi}(x) x (i\partial A_{us})(0) \psi(x) = \int dp_1 dp_2 dk \delta'(p_1 - p_2) k \bar{\psi}(p_1) A_{us}(k) \psi(p_2).\tag{4.13}$$

Here the Feynman rule involves a  $k\delta'(p_1 - p_2)$  and we must integrate by parts to obtain the multipole momentum conservation expressed by  $\delta(p_1 - p_2)$ . This integration by parts differentiates other parts of a diagram that carry this momentum, in particular the neighbouring propagators, which then would produce terms like the 2nd term in Eq. (4.11).



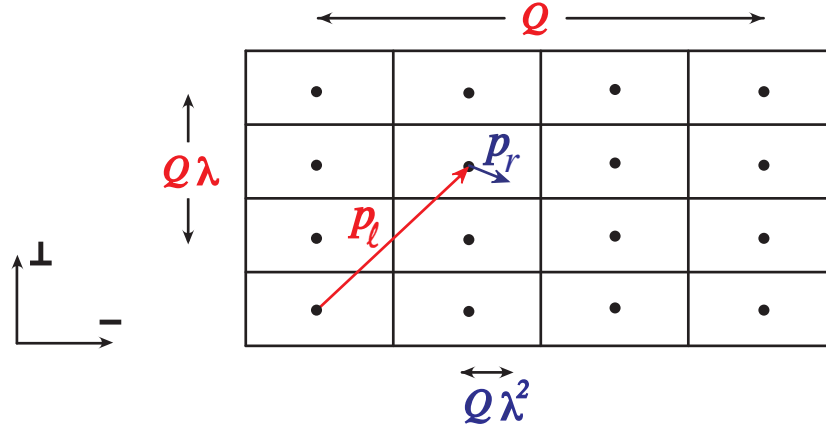


Figure 5: Grid to picture the separation of momenta into label and residual components.

Since Feynman diagrams are almost always evaluated in momentum space it would be more convenient to have a multipole expansion formalism that avoids the step of going through position space. In the remainder of this section we will set up a formalism to achieve this. It will allow us to 1) simply derive the corresponding momentum space Feynman rules, 2) simplify the formulation of gauge transformations in the effective theory, and 3) incorporate the multipole expansion into propagators rather than vertices.

For the moment we only consider the quark part of the field  $\hat{\xi}_n(x)$ . We will add the anti-quark part later on. Computing the Fourier transform  $\tilde{\xi}_n(p)$  of the quark part of our field we have

$$\tilde{\xi}_n(p) = \int d^4x e^{ip \cdot x} \hat{\xi}_n(x). \quad (4.14)$$

Now to separate momentum scales, we define our momentum  $p^\mu$  to be a sum of a large momentum components  $p_\ell^\mu$  called the *label* momentum and a small momentum  $p_r^\mu$  called the *residual* momentum.

$$\begin{aligned} p^\mu &= p_\ell^\mu + p_r^\mu \\ p_\ell^\mu &\sim Q(0, 1, \lambda) \\ p_r^\mu &\sim Q(\lambda^2, \lambda^2, \lambda^2) \end{aligned} \quad (4.15)$$

This decomposition is similar to the one found in HQET where the quark momentum is  $p^\mu = m v^\mu + k^\mu$ . Although at the end of the day all momenta will be continuous, it turns out that it is quite convenient for understanding the multipole expansion to interpret the  $p_\ell$  as defining a grid of points, and the  $p_r$  as defining locations in the surrounding boxes. This expansion is only necessary for the  $p^-$  and  $p^\perp$  momenta since there are no label  $p^+$  momenta, so we have a grid as shown in Fig. 5 (for convenience we show only one of the  $p_\perp^\mu$  components). Note that any momentum  $p^\mu$  has a unique decomposition in terms of label and residual components. Since  $p_\ell \gg p_r$  the spacing between grid points is always much larger than the spacing between points in a box. This setup has the advantage of allowing us to cleaning separate momentum scales in integrands, arranging things so every loop integrand is homogeneous in  $\lambda$ .

In practice the grid picture is a bit misleading, since actually the boxes are infinite and with momentum components  $(p_\ell, p_r)$  we are really dealing with a product of continuous spaces  $\mathbb{R}^3 \times \mathbb{R}^4/\mathcal{I}$  where  $\mathcal{I}$  are a group of relations that remove redundancy order by order in  $\lambda$ . ( $\mathcal{I}$  includes the set of RPI transformations that we will discuss later on.) Nevertheless it is very convenient to derive the rules for integrals on the

label-residual space by working with a more familiar discrete label and continuous residual momentum picture, and then taking the continuum limit.

Thus if we are integrating the collinear momentum  $p$  over a certain region, we will write

$$\int d^4p \rightarrow \sum_{p_\ell \neq 0} \int d^4p_r \quad (4.16)$$

where we do not include  $p_\ell = 0$  in the sum over all  $p_\ell$  values, because  $p_\ell = 0$  does not define a collinear momentum. Indeed the  $p_\ell = 0$  bin corresponds to the ultrasoft modes. For an ultrasoft momentum  $p$  we simply have

$$\int d^4p \rightarrow \int d^4p_r. \quad (4.17)$$

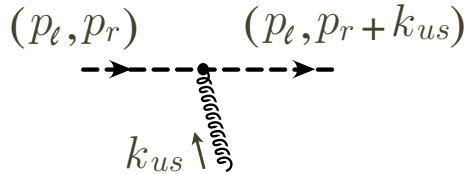
With this momentum separation we can also label our fields by both components

$$\tilde{\xi}_n(p) \rightarrow \tilde{\xi}_{n,p_\ell}(p_r). \quad (4.18)$$

We also have separate conservation laws for label and residual momenta

$$\int d^4x e^{i(p_\ell - q_\ell) \cdot x} e^{i(p_r - q_r) \cdot x} = \delta_{p_\ell, q_\ell} \delta^4(p_r - q_r) (2\pi)^4. \quad (4.19)$$

Every collinear field carries both label and residual momenta, they are both conserved at all vertices, but Feynman rules may depend on only one or the other of these components. For example, what was previously a nonconservation of momenta for an interaction between collinear and ultrasoft particles now becomes two separate conservations of momenta.



An example is shown in the figure above.

Finally, since all fields carry residual momenta the conservation law just corresponds to locality of the field theory with respect to the Fourier transformed variable  $p_r \rightarrow x$ . Therefore we transform the residual momenta back to position space to obtain our final collinear quark field

$$\xi_{n,p_\ell}(x) = \int \frac{d^4p_r}{(2\pi)^4} e^{-ip_r \cdot x} \tilde{\xi}_{n,p_\ell}(p_r). \quad (4.20)$$

We will build operators using these fields. Altogether, the above steps allow us to rewrite our hatted collinear field  $\hat{\xi}_n(x)$  as

$$\begin{aligned} \hat{\xi}_n(x) &= \int \frac{d^4p}{(2\pi)^4} e^{-ip \cdot x} \tilde{\xi}_n(p) = \sum_{p_\ell \neq 0} \int d^4p_r e^{-ip_\ell \cdot x} e^{-ip_r \cdot x} \tilde{\xi}_{n,p_\ell}(p_r) \\ &= \sum_{p_\ell \neq 0} e^{-ip_\ell \cdot x} \xi_{n,p_\ell}(x). \end{aligned} \quad (4.21)$$

We can identify several facts about label conservation for the field  $\xi_{n,p_\ell}(x)$

- Interactions with ultrasoft gluons or quarks leave the label momenta of collinear fields conserved.
- Interactions with collinear gluons or quarks will change label momenta.
- The label  $n$  for the collinear direction is preserved by both ultrasoft and collinear interactions. Only a hard (external) interaction can couple fields with different collinear directions.

Now that we have separated momentum scales in our fields we would like to do the same with derivatives that act on these fields. Since  $\xi_{n,p_\ell}(x)$  contains only residual momenta, we know that

$$i\partial_\mu \xi_{n,p_\ell}(x) \sim \lambda^2 \xi_{n,p_\ell}(x). \quad (4.22)$$

We also define a label momentum operator such that

$$\mathcal{P}^\mu \xi_{n,p_\ell}(x) \equiv p_\ell^\mu \xi_{n,p_\ell}(x). \quad (4.23)$$

Recall that  $\mathcal{P}^\mu$  and  $p_\ell^\mu$  only contains the components  $\bar{\mathcal{P}} \equiv \bar{n} \cdot \mathcal{P} \sim p_\ell^- \sim \lambda^0$  and  $\mathcal{P}_\perp^\mu \sim p_\ell^\perp \sim \lambda$ . Therefore we have  $n \cdot \mathcal{P} = 0$ . Also

$$i\bar{n} \cdot \partial \ll \bar{\mathcal{P}}, \quad i\partial_\perp^\mu \ll \mathcal{P}_\perp^\mu. \quad (4.24)$$

The main advantage of the label operator is that it provides a definite power counting for derivatives. It is also notationally friendly in that it removes the necessity of a label sum. We can see this by rewriting our field  $\hat{\xi}_n(x)$  in terms of label momenta

$$\begin{aligned} \hat{\xi}_n(x) &= \sum_{p_\ell \neq 0} e^{-ip_\ell \cdot x} \xi_{n,p_\ell}(x) \\ &= e^{-i\mathcal{P} \cdot x} \sum_{p_\ell \neq 0} \xi_{n,p_\ell}(x) \\ &\equiv e^{-i\mathcal{P} \cdot x} \xi_n(x). \end{aligned} \quad (4.25)$$

In the last line we defined  $\xi_n(x) = \sum_{p_\ell \neq 0} \xi_{n,p_\ell}$ . Since the label operator allows us to encode the phase factor involving label momenta as an operator, we can suppress the momentum labels on our collinear fields if there is no reason to make them explicit. For field products we have

$$\hat{\xi}_n(x) \hat{\xi}_n(x) = e^{-i\mathcal{P} \cdot x} \xi_n(x) \xi_n(x) \quad (4.26)$$

where the label operator acts on both fields. Consequently, conservation of label momenta is simply encoded by this phase factor and is manifest at the level of operators.

Lastly, we must deal with anti-particles and gluons. For the anti-particles, we expand our Dirac field into two parts

$$\begin{aligned} \psi(x) &= \int d^4p \delta(p^2) \theta(p^0) [u(p)a(p)e^{-ip \cdot x} + v(p)b^\dagger(p)e^{ip \cdot x}] \\ &= \psi^+(x) + \psi^-(x) \end{aligned} \quad (4.27)$$

we then associate each part with a collinear field and expand as a sum over label momenta.

$$\begin{aligned} \psi^+ &\longrightarrow \hat{\xi}_n^+(x) = \sum_{p_\ell \neq 0} e^{-ip_\ell \cdot x} \xi_{n,p_\ell}^+(x), \\ \psi^- &\longrightarrow \hat{\xi}_n^-(x) = \sum_{p_\ell \neq 0} e^{ip_\ell \cdot x} \xi_{n,p_\ell}^-(x), \end{aligned} \quad (4.28)$$

where both have a  $\theta(p_\ell^0) = \theta(\bar{n} \cdot p_\ell)$ . Because of charge conjugation symmetry it is convenient to combine the particle and anti-particle fields back into a single field. In order to do this we have to deal with the opposite signs for their phase. To do this we define

$$\xi_{n,p_\ell}(x) \equiv \xi_{n,p_\ell}^+(x) + \xi_{n,-p_\ell}^-(x) \quad (4.29)$$

where  $p_\ell$  has either sign, but one picks out particles and one picks out antiparticles. Thus the action of the fields  $\xi_{n,p_\ell}$  and  $\bar{\xi}_{n,p_\ell}$  is that for

$$\begin{aligned} \bar{n} \cdot p_\ell > 0 & : && \text{a particle is destroyed or created} \\ \bar{n} \cdot p_\ell < 0 & : && \text{an antiparticle is created or destroyed} \end{aligned}$$

The sign convention for the label momentum is easy to remember since it is in the same direction as the fermion number flow. With this definition, we may write

$$\hat{\xi}_n(x) = e^{-i\mathcal{P} \cdot x} \xi_{n,p_\ell}(x), \quad (4.30)$$

and all the manipulations we were making with particle fields carry through for the fields that have both particles and antiparticles. For collinear gluons, we proceed analogously to find

$$\hat{A}_n^\mu = \sum_{q_\ell \neq 0} e^{-iq_\ell \cdot x} A_{n,q_\ell}^\mu = e^{-i\mathcal{P} \cdot x} A_n^\mu(x) \quad (4.31)$$

where

$$A_n^\mu(x) = \sum_{q_\ell \neq 0} A_{n,q_\ell}^\mu. \quad (4.32)$$

Since the gluon field  $A_n^\mu = A_n^{\mu A} T^A$  where  $A_n^{\mu A}(x)$  is real we also have

$$[A_{n,q_\ell}^{\mu A}(x)]^* = A_{n,-q_\ell}^{\mu A}(x). \quad (4.33)$$

Once again for  $q_\ell^- > 0$  the field  $A_{n,q_\ell}$  destroys a gluon, while for  $q_\ell^- < 0$  it creates a gluon.

With our conventions the action of the label operator on a bunch of labelled fields is

$$\mathcal{P}^\mu(\phi_{q_1}^\dagger \phi_{q_2}^\dagger \cdots \phi_{p_1} \phi_{p_2} \cdots) = (p_1^\mu + p_2^\mu + \cdots - q_1^\mu - q_2^\mu - \cdots)(\phi_{q_1}^\dagger \phi_{q_2}^\dagger \cdots \phi_{p_1} \phi_{p_2} \cdots). \quad (4.34)$$

Thus it gives a minus sign when acting on daggered fields. It is also useful to note that if we differentiate an arbitrary collinear field  $\hat{\phi}_n(x)$  that it yields

$$\begin{aligned} i\partial^\mu \hat{\phi}_n(x) &= i\partial_\mu \sum_{p \neq 0} e^{-ip \cdot x} \phi_{n,p}(x) \\ &= \sum_{p \neq 0} e^{-ip \cdot x} (\mathcal{P}^\mu + i\partial^\mu) \phi_{n,p}(x) \\ &= e^{-i\mathcal{P} \cdot x} (\mathcal{P}^\mu + i\partial^\mu) \phi_n(x). \end{aligned} \quad (4.35)$$

In the last line, we can suppress the exponent if we assume that label momenta are always conserved. Effectively, by introducing the label operator we have replaced the ordinary derivative operation by

$$i\partial^\mu \hat{\phi}_n(x) \rightarrow (\mathcal{P}^\mu + i\partial^\mu) \phi_n(x). \quad (4.36)$$

#### 4.1.4 Final Result: Expand and put pieces together

At last, we may construct our final leading order Lagrangian. We begin with the previously derived result:

$$\mathcal{L} = \bar{\xi}_n \left( in \cdot D + i\not{D}_\perp \frac{1}{i\bar{n} \cdot D} i\not{D}_\perp \right) \frac{\not{n}}{2} \hat{\xi}_n. \quad (4.37)$$

Changing  $i\partial_\mu \rightarrow (\mathcal{P}_\mu + i\partial_\mu)$  and  $\hat{\xi}_n \rightarrow \xi_n$  and expanding our derivative operators, we have

$$\begin{aligned} in \cdot D &= in \cdot \partial + gn \cdot A_n + gn \cdot A_n \\ iD_\perp &= \underbrace{(\mathcal{P}_\perp^\mu + gA_{n\perp}^\mu)}_{\sim\lambda} + \underbrace{(i\partial_\perp^\mu + gA_{\perp,us}^\mu)}_{\sim\lambda^2} + \dots \\ i\bar{n} \cdot D &= \underbrace{(\bar{\mathcal{P}} + g\bar{n} \cdot A_n)}_{\sim\lambda^0} + \underbrace{(i\bar{n} \cdot \partial + g\bar{n} \cdot A_{us})}_{\sim\lambda^2} + \dots \end{aligned} \quad (4.38)$$

where the ellipses again denote additional  $\sim\lambda^2$  terms that can be dropped in our leading order analysis (but later on we will see are required by gauge symmetry when considering power suppressed operators). Keeping only the lowest order terms, we have the following quark lagrangian

$$\boxed{\mathcal{L}_{n\xi}^{(0)} = e^{-ix \cdot \mathcal{P}} \bar{\xi}_n \left( in \cdot D + i\not{D}_{n\perp} \frac{1}{i\bar{n} \cdot D_n} i\not{D}_{n\perp} \right) \frac{\not{n}}{2} \xi_n}, \quad (4.39)$$

where the collinear covariant derivatives are

$$\begin{aligned} iD_{n\perp}^\mu &= \mathcal{P}_\perp^\mu + gA_{n\perp}^\mu, \\ i\bar{n} \cdot D_n &= \bar{\mathcal{P}} + g\bar{n} \cdot A_n. \end{aligned} \quad (4.40)$$

It is also convenient to define for completeness  $in \cdot D_n = in \cdot \partial + gn \cdot A_n$ .

#### Remarks:

- Both terms with covariant derivatives in the  $(\dots)$  in  $\mathcal{L}_{n\xi}^{(0)}$  are of order  $\lambda^2$  so the leading order Lagrangian is order  $\lambda^4$  (recalling that the fields scale as  $\xi_n \sim \lambda$ ). Since for a Lagrangian with collinear fields  $\int d^4x \sim \lambda^{-4}$  this gives us an action that is  $\sim \lambda^0$  as desired. The superscript (0) on the Lagrangian denotes this power counting for the action.
- All fields are defined at  $x$ , and derivatives for this coordinate scale as  $i\partial^\mu \sim \lambda^2$  so the action is explicitly local at the scale  $Q\lambda^2$ .
- The action is also local at the scale of  $\mathcal{P}_\perp^\mu \sim Q\lambda$  since these derivatives occur in the numerator. It only has non-locality at the hard scale through the inverse  $\bar{\mathcal{P}} \sim \lambda^0$ . The fact that there is locality except at the hard scale is a key feature of SCET<sub>I</sub>. Some attempts to tweak the formalism described here, in order to simplify SCET, lead to actions that are non-local at the small scale  $\sim \lambda^2$  because they integrate out some onshell particles, while leaving other onshell particles to be described by an action. We will avoid doing this, taking the attitude that low energy locality is a desired property for the effective field theory.
- If we are considering a situation without ultrasoft particles, and without hard interactions that do not couple to a particular component, then the interaction of collinear fermions alone could equally

well be described by the QCD Lagrangian. Indeed, even in the presence of ultrasoft fields we can write a Dirac type Lagrangian that is equivalent to Eq. (4.39) by

$$\mathcal{L}_{n\xi}^{(0)} = e^{-ix \cdot \mathcal{P}} \bar{\Xi}_n i \mathcal{D} \Xi_n, \quad \Xi_n \equiv \begin{pmatrix} \xi_n \\ \varphi_{\bar{n}} \end{pmatrix}, \quad i \mathcal{D} = \frac{\not{n}}{2} i n \cdot D + \frac{\not{n}}{2} i \bar{n} \cdot D_n + i \mathcal{D}_{n\perp} = i \mathcal{D}_n + \frac{\not{n}}{2} g n \cdot A_{us}. \quad (4.41)$$

Integrating out  $\varphi_{\bar{n}}$  exactly reproduces Eq.(4.39). This Lagrangian is not equivalent to QCD due to the coupling to the ultrasoft gluon field, and the zero-bin subtractions related to  $p_\ell \neq 0$  that will be discussed later on. But this form does make it more clear why the collinear particles share many of the properties of the full QCD Lagrangian (for example, we have the same renormalization properties for the gauge coupling).

The computation of the propagator from  $\mathcal{L}_{n\xi}^{(0)}$  is also greatly simplified without the need for any additional power counting. Specifically, Eq. (4.39) gives the collinear quark propagator

$$\frac{i \not{n}}{2} \frac{\bar{n} \cdot p_\ell}{(\bar{n} \cdot p_\ell)(n \cdot p_r) + (p_{\ell\perp})^2 + i0}. \quad (4.42)$$

The leading order Lagrangian is smart enough that it gives the correct propagator in different situations without having to make further expansions. This is important to ensure that the leading order Lagrangian strictly give  $\mathcal{O}(\lambda^0)$  terms, while subleading Lagrangians (and operators) will be responsible for power corrections. For example, if we have an interaction with an ultrasoft gluon then

$$\begin{array}{c} (p_\ell, p_r) \quad (p_\ell, p_r + k_{us}) \\ \dashrightarrow \quad \dashrightarrow \\ \quad \quad \quad \uparrow k_{us} \\ \quad \quad \quad \text{gluon} \end{array} = \frac{i \not{n}}{2} \frac{\bar{n} \cdot p_\ell}{(\bar{n} \cdot p_\ell)(n \cdot p_r + n \cdot k_{us}) + (p_{\ell\perp})^2 + i0}, \quad (4.43)$$

while if we have an interaction with a collinear gluon then

$$\begin{array}{c} (p_\ell, p_r) \quad (p_\ell + q_\ell, p_r + q_r) \\ \dashrightarrow \quad \dashrightarrow \\ \quad \quad \quad \uparrow q_\ell \\ \quad \quad \quad \text{gluon} \\ (q_\ell, q_r) \end{array} = \frac{i \not{n}}{2} \frac{(\bar{n} \cdot p_\ell + \bar{n} \cdot q_\ell)}{(\bar{n} \cdot p_\ell + \bar{n} \cdot q_\ell)(n \cdot p_r + n \cdot q_r) + (p_{\ell\perp} + q_{\ell\perp})^2 + i0}. \quad (4.44)$$

## 4.2 Wilson Line Identities

With the label operator formalism there are several neat identities that we can derive for Wilson lines. In particular we can show that all occurrences of the field  $\bar{n} \cdot A_n$  can always be entirely replaced by the Wilson line  $W_n$ . As an example we will show how this is done for the Lagrangian  $\mathcal{L}_{n\xi}^{(0)}$ . In position space the defining equations for a Wilson line are  $W(x, x) = 1$  and its equation of motion, which we can transform to momentum space

$$\begin{aligned} i \bar{n} \cdot D_x W(x, -\infty) &= 0 \quad (\text{position space}) \\ &\Downarrow \text{Fourier Transform} \\ i \bar{n} \cdot D_n W_n &= (\bar{P} + g \bar{n} \cdot A_n) W_n = 0. \end{aligned} \quad (4.45)$$

With this definition, the action of  $i\bar{n} \cdot D_n$  on a product of  $W_n$  and some arbitrary operator is

$$\begin{aligned} i\bar{n} \cdot D_n(W_n \mathcal{O}) &= (\bar{\mathcal{P}} + g\bar{n} \cdot A_n)W_n \mathcal{O} \\ &= [(\bar{\mathcal{P}} + g\bar{n} \cdot A_n)W_n] \mathcal{O} + W_n \bar{\mathcal{P}} \mathcal{O} \\ &= W_n \mathcal{P} \mathcal{O} \end{aligned} \quad (4.46)$$

So we have the operator equation

$$i\bar{n} \cdot D_n W_n = W_n \bar{\mathcal{P}} \quad (4.47)$$

and with  $W_n^\dagger W_n = 1$  we have

$$i\bar{n} \cdot D_n = W_n \bar{\mathcal{P}} W_n^\dagger, \quad \bar{\mathcal{P}} = W_n^\dagger i\bar{n} \cdot D_n W_n, \quad (4.48)$$

as operator identities. Since by collinear gauge invariance we can always group  $\bar{n} \cdot A_n$  with  $\bar{\mathcal{P}}$  to give  $i\bar{n} \cdot D_n$ , the first identity implies that we can always swap  $\bar{n} \cdot A_n$  for the Wilson line  $W_n$ . Inverting these results also gives useful operator identities

$$\frac{1}{i\bar{n} \cdot D_n} = W_n^\dagger \frac{1}{\bar{\mathcal{P}}} W_n, \quad \frac{1}{\bar{\mathcal{P}}} = W_n \frac{1}{i\bar{n} \cdot D_n} W_n^\dagger. \quad (4.49)$$

The first relation allows us to rewrite  $\mathcal{L}_{n\xi}^{(0)}$  as

$$\mathcal{L}_{n\xi}^{(0)} = e^{-ix \cdot \bar{\mathcal{P}}} \bar{\xi}_n \left( i\bar{n} \cdot D + i\not{D}_{n\perp} W_n^\dagger \frac{1}{\bar{\mathcal{P}}} W_n i\not{D}_{n\perp} \right) \frac{\not{n}}{2} \xi_n. \quad (4.50)$$

It is also useful to note that we can use the label operator to write a tidy expression for the Wilson line which is built from fields that carry both label and residual momenta:

$$W_n(x) = \left[ \sum_{\text{perms}} \exp \left( \frac{-g}{\bar{\mathcal{P}}} \bar{n} \cdot A_n(x) \right) \right]. \quad (4.51)$$

### 4.3 Collinear Gluon and Ultrasoft Lagrangians

To derive the collinear gluon Lagrangian, we treat usoft and collinear degrees of freedom separately by letting  $A_{us}^\mu$  represent a background field with respect to  $A_n^\mu$ . We begin with the gluon Lagrangian from QCD:

$$\mathcal{L} = - \underbrace{\frac{1}{2} \text{Tr}\{G^{\mu\nu} G_{\mu\nu}\}}_{\text{Gauge Kinetic Term}} + \underbrace{\tau \text{Tr}\{(i\partial_\mu A^\mu)^2\}}_{\text{Gauge Fixing Term}} + 2 \underbrace{\text{Tr}\{\bar{c} i\partial_\mu [iD^\mu, c]\}}_{\text{Ghost Term}} \quad (4.52)$$

where  $G^{\mu\nu} = \frac{i}{g}[D^\mu, D^\nu]$ . Here we are using a notation with fundamental color matrices,  $G_{\mu\nu} = G_{\mu\nu}^A T^A$ ,  $c = c^A T^A$ , etc., and recall that  $\text{Tr}(T^A T^B) = T_F \delta^{AB} = \delta^{AB}/2$ . Expanding the covariant derivative as we did in the quark sector we keep only the leading order terms. For a covariant derivative acting on collinear fields the leading order terms are

$$iD^\mu \rightarrow i\mathcal{D}^\mu = \frac{n^\mu}{2} (\bar{\mathcal{P}} + g\bar{n} \cdot A_n) + (\mathcal{P}_\perp^\mu + gA_{\perp,n}^\mu) + \frac{\bar{n}}{2} (i\bar{n} \cdot \partial + g\bar{n} \cdot A_n + g\bar{n} \cdot A_{us}). \quad (4.53)$$

Recall that the field  $A_{us}^\mu$  varies much more slowly than  $A_n^\mu$ , so we can think of  $A_{us}^\mu$  as a background field from the perspective of the collinear fields (even though it is a quantum field in its own right). The gauge fixing and ghost terms for the collinear Lagrangian should break the collinear gauge symmetry, but we do





$$\begin{aligned}
& \text{Diagram 1: } \begin{array}{c} a, \mu \quad b, \nu \\ \text{Spring with line} \\ (q, k) \end{array} &= \frac{-i}{\bar{n} \cdot q \, n \cdot k + q_{\perp}^2 + i0} \left( g_{\mu\nu} - (1 - \tau) \frac{q_{\mu} q_{\nu}}{\bar{n} \cdot q \, n \cdot k + q_{\perp}^2} \right) \delta_{a,b} \\
& \text{Diagram 2: } \begin{array}{c} a, \mu \\ \text{Spring with line} \\ \text{Spring} \quad \text{Spring} \\ b, \nu \quad c, \lambda \\ q_1 \quad q_2 \end{array} &= g f^{abc} n_{\mu} \left\{ \bar{n} \cdot q_1 g_{\nu\lambda} - \frac{1}{2} \left( 1 - \frac{1}{\tau} \right) [\bar{n}_{\lambda} q_{1\nu} + \bar{n}_{\nu} q_{2\lambda}] \right\} \\
& \text{Diagram 3: } \begin{array}{c} a, \mu \quad b, \nu \\ \text{Spring with line} \quad \text{Spring} \\ \text{Spring} \quad \text{Spring} \\ d, \rho \quad c, \lambda \end{array} &= -\frac{1}{2} i g^2 n_{\mu} \left\{ f^{abe} f^{cde} (\bar{n}_{\lambda} g_{\nu\rho} - \bar{n}_{\rho} g_{\nu\lambda}) \right. \\
& \quad \left. + f^{ade} f^{bce} (\bar{n}_{\nu} g_{\lambda\rho} - \bar{n}_{\lambda} g_{\nu\rho}) + f^{ace} f^{bde} (\bar{n}_{\nu} g_{\lambda\rho} - \bar{n}_{\rho} g_{\nu\lambda}) \right\} \\
& \text{Diagram 4: } \begin{array}{c} a, \mu \quad b, \nu \\ \text{Spring with line} \quad \text{Spring} \\ \text{Spring} \quad \text{Spring} \\ c, \lambda \quad d, \rho \end{array} &= \frac{1}{4} i g^2 n_{\mu} n_{\nu} \bar{n}_{\rho} \bar{n}_{\lambda} \left( 1 - \frac{1}{\alpha} \right) \left\{ f^{ace} f^{bde} + f^{ade} f^{bce} \right\}
\end{aligned}$$

Figure 7: Collinear gluon propagator with label momentum  $q$  and residual momentum  $k$ , and the order  $\lambda^0$  interactions of collinear gluons with the usoft gluon field. Here usoft gluons are springs, collinear gluons are springs with a line, and  $\tau$  is the covariant gauge fixing parameter in Eq. (4.55).

#### 4.4 Feynman Rules for Collinear Quarks and Gluons

For convenience we summarize some of the Feynman rules that follow from the collinear quark and gluon Lagrangians. We do not show the purely ultrasoft interactions which are identical to those of QCD, nor do we show the purely collinear gluon interactions which are also identical to those of QCD.

The Feynman rules that follow from the leading order collinear quark Lagrangian are shown in Fig. 6 where each collinear line carries momenta  $(p, p_r)$  with label momenta  $p^{\mu} = \bar{n} \cdot p \, n^{\mu} / 2 + p_{\perp}^{\mu}$  and residual momentum  $p_r^{\mu}$ . Only one momentum  $p$  or  $p'$  is indicated for lines where the Feynman rule depends only on the label momentum. For the collinear quark propagator we have contributions from both quarks and antiquarks which give:

$$\frac{i\not{n}}{2} \frac{\theta(\bar{n} \cdot p)}{n \cdot p_r + \frac{p_{\perp}^2}{\bar{n} \cdot p} + i0} + \frac{i\not{n}}{2} \frac{\theta(-\bar{n} \cdot p)}{n \cdot p_r + \frac{p_{\perp}^2}{\bar{n} \cdot p} - i0} = \frac{i\not{n}}{2} \frac{\bar{n} \cdot p}{\bar{n} \cdot p \, n \cdot p_r + p_{\perp}^2 + i0} \quad (4.58)$$

The Feynman rules between collinear gluons and ultrasoft gluons are shown in Fig. 7 with a collinear gluon in background field gauge that is ultrasoft covariant and specified by the parameter  $\tau$ .

#### 4.5 Rules for Combining Label and Residual Momenta in Amplitudes

In practical calculations the grid picture in Fig. 5 is not to be taken literally. Doing so would correspond to using a Wilsonian EFT with finite cutoff's (edges for the grid boxes) that distinguish the size of momenta.

Instead of this, we need to use a Continuum EFT picture where the EFT modes have propagators that extend over all momenta, but integrands which obtain their key contribution from the momentum region these modes are built to describe. The terms needed to correct the (otherwise incorrect) ultraviolet contributions of the resulting Continuum EFT are included as perturbative Wilson coefficients for low energy operators. The Wilsonian and Continuum versions of EFT are really two different pictures of the same thing, in much the same way that two different renormalization schemes may represent the physics in different ways, but in the end still do encode the same physics. Nevertheless there are many practical advantages to the Continuum EFT framework, and it makes setting up SCET much easier. In particular it allows us to use regulators like dimensional regularization which naturally preserve spacetime and gauge symmetries. To setup up SCET in this continuum framework we need to understand how the redundancy  $\mathcal{I}$  in the label-residual momentum space  $\mathbb{R}^{d-1} \times \mathbb{R}^d/\mathcal{I}$  (for the case with  $d$ -dimensions) is resolved, given a pair of momenta components  $(p_\ell, p_r) \in \mathbb{R}^{d-1} \times \mathbb{R}^d$ . The upshot is that in the simplest cases the residual momentum can simply be dropped or absorbed into a label momentum in the same direction (making it continuous), while in the most complicated cases the formalism leads to so-called 0-bin subtractions for collinear integrands. These subtractions ensure that the collinear modes do not double count an IR region that is already properly included from an ultrasoft integrand. For future convenience we list the rules in this section, but caution the reader that some parts of this section are best understood when read together with one of the one-loop examples from section 7, and also after having read the discussion of the reparameterization invariance symmetry in section 5.3 that describes the redundancy  $(p_\ell^\mu) + (p_r^\mu) = (p_\ell^\mu + \beta^\mu) + (p_r^\mu - \beta^\mu)$  which specifies  $\mathcal{I}$ .

For an arbitrary tree level diagram in SCET we will have some set of external lines that are either ultrasoft or collinear (and either in the initial or final state), and also a set of collinear and ultrasoft propagators. For the external lines that are ultrasoft we have only residual momenta  $k_{us}^\mu$  and the onshell condition  $k_{us}^2 = 0$ . For the external lines that are collinear it suffices to take label momenta  $p_\ell^- = \bar{n} \cdot p_\ell$  and  $p_{\ell\perp}^\mu$ , and a single residual momentum  $p_r^+$ . This amounts to picking  $\beta^\mu$  above to contain the full  $p_r^-$  and  $p_{r\perp}^\mu$  components. The onshell condition for the collinear particles is then simply  $p_\ell^- p_r^+ - \vec{p}_{\ell\perp}^2 = 0$ . All propagators for intermediate collinear and ultrasoft lines are then simply determined by momentum conservation as usual. At leading order in  $\lambda$  this prescription for tree diagrams simply amounts to the same thing as dropping any ultrasoft momentum components  $k_{us}^-$  and  $k_{us}^\perp$  from collinear propagators, though of course these momenta can still appear within ultrasoft propagators. At higher orders in  $\lambda$  these ultrasoft momentum components can also appear from collinear propagators through Lagrangian insertions, which yield terms like the second one in Eq. (4.11).

For loop diagrams and loop integrations we need several rules for operations on the label-residual momentum space. Internal collinear lines should be considered as carrying loop momenta with two parts  $q = (q_\ell, q_r)$ , while ultrasoft propagators only carry loop momenta  $k_r$ . There is a separate momentum conservation for the label and residual momenta. After using momentum conservation we have label momenta from either external collinear particles or collinear loops, and residual momenta for external ultrasoft particle, external collinear particles from  $p_r^+$ , and from collinear and ultrasoft loops.

First we note that if we integrate over all label momenta  $q_\ell$  and residual momenta  $q_r$  that this will be equal to an integration over all of the  $q^\mu$  momentum space, since it does not depend on how we divide the momentum into the two components. For notational convenience we denote the label space integration as a sum rather than an integral. In  $d$ -dimensions we have

$$\sum_{q_\ell} \int d^d q_r = \int d^d q, \quad (4.59)$$

where we have recombined the label and residual momenta for the minus components, and the  $(d-2)$   $\perp$ -components. This is relevant for combining the two collinear loop integrations back into a single  $d$ -

dimensional integration. In particular at leading order in  $\lambda$  after having used momentum conservation there will always be one  $q_r^\mu$  for each collinear loop integration, where  $q_r^-$  and  $q_r^\perp$  do not appear in any collinear or ultrasoft propagator, and hence not in the integrand  $F(q_\ell^-, q_\ell^\perp, q_r^+)$ . We can therefore use this residual momentum integration in Eq. (4.59) to obtain a full integration

$$1)^{\text{naive}} : \quad \sum_{q_\ell} \int d^d q_r F(q_\ell^-, q_\ell^\perp, q_r^+) = \sum_{q_\ell} \int d^d q_r F(q_\ell^- + q_r^-, q_\ell^\perp + q_r^\perp, q_r^+) = \int d^d q F(q^-, q^\perp, q^+). \quad (4.60)$$

In the first step we use the fact that  $F$  is constant throughout each box in the grid picture of Fig. 5 so its the same with the first two arguments shifted by residual momenta. (In the continuum EFT picture its the same property,  $F$  does not depend on residual momenta in these components.) In the final equality we then combined the momenta back into a standard dimensional regularization integration as in Eq. (4.59). Essentially at leading order in  $\lambda$  Eq. (4.60) amounts to the same thing that would be achieved by never considering the split into label and residual momenta in the first place, and simply writing down the integrand without ultrasoft momenta appearing in the  $-$  or  $\perp$  components in collinear propagators, which corresponds to the lowest order term in the ultrasoft multipole expansion (and is an easy way to think about the outcome of the above formal procedure). We have called this rule 1)<sup>naive</sup> because there is one final complication that we will have to deal with, namely that the integration on  $q_\ell$  must avoid producing additional divergences when this collinear momentum enters the ultrasoft regime. We denote this fact by  $q_\ell \neq 0$  if  $q$  is the momentum of a collinear propagator. These are referred to as 0-bin restrictions.<sup>4</sup> We will discuss the change needed which handles this complication below. Often the results for collinear loop integrals are called “naive” if one uses Eq. (4.60). The result from this naive result will be correct if the added terms which properly handle this complication turn out to be zero, which happens in some cases.

At higher orders in  $\lambda$  there will be dependence on the residual momentum components from higher order terms in the multipole expansion of the collinear propagators. If these terms correspond to the momentum components  $q_r^-$  and  $q_r^\perp$  that do not appear inside any ultrasoft propagators then the resulting integration is zero

$$2) : \quad \sum_{q_\ell} \int d^d q_r (q_r)^j F(q_\ell^-, q_\ell^\perp, q_r^+) = 0, \quad (4.61)$$

where  $(q_r)^j$  denotes positive powers of the  $q_r^-$  and  $q_r^\perp$  momenta,  $j > 0$ . Here Eq. (4.61) is like the dimensional regularization rule,  $\int d^d q (q^2)^j = 0$  for  $j > 0$ , which is a consequence of retaining Lorentz invariance with this regulator. Eq. (4.61) is the analogous statement in the residual momentum space and ensures that we do not obtain nontrivial contributions from higher order terms in the multipole expansion, unless the residual loop momentum corresponds to a physical momentum for an ultrasoft loop integration. Both ultrasoft loop integrations and ultrasoft external particles introduce residual momenta into propagators that can not be absorbed by a rule like that in Eq. (4.59). If we consider a case with an ultrasoft loop integration, then there will be dependence on the residual momentum also in an ultrasoft propagator, so the integration will give

$$\sum_{q_\ell} \int d^d q_r \int d^d k_r F(q_\ell^-, q_\ell^\perp, q_r^+, k_r^\mu) = \int d^d q \int d^d k F(q^-, q^\perp, q^+, k^\mu), \quad (4.62)$$

which in general is nonzero. This integrand corresponds to a mixed two-loop diagram with one loop momentum with collinear scaling and one with ultrasoft scaling.

<sup>4</sup>After imposing momentum conservation we get a set of such restrictions, one for each collinear propagator. For example  $q_\ell \neq -p_\ell$  if there is a collinear propagator carrying momentum  $q + p$ .

Finally let us consider the implications of the zero-bin when combining label and residual momenta. Rather than Eq. (4.59) we can have

$$\sum_{q_\ell \neq 0} \int d^d q_r, \quad (4.63)$$

where  $q_\ell \neq 0$  is simply a label to denote the fact that the label momentum  $q_\ell$  must be large in order to correspond to a collinear particle carrying total momentum  $q$ . If  $q_\ell = 0$  then the particle would instead be ultrasoft, and we will often have included another diagram in SCET to account for the different integrand that accounts for the proper expansion in this special case. Thus these zero-bin restrictions avoid double counting between the SCET fields, which effectively means double counting from the resulting loop integrations. It is easy to determine what the set of restrictions are for any diagram, since we have one such condition for every collinear propagator. At leading order in  $\lambda$  only the zero-bin subtractions corresponding to collinear gluon propagators can give non-zero contributions since operators containing an ultrasoft quark together with collinear fields are power suppressed. In a continuum EFT these zero-bin restrictions are implemented by subtraction terms which can be determined as follows

$$\begin{aligned} 1): \quad \sum_{q_\ell \neq 0} \int d^d q_r F(q_\ell^-, q_\ell^\perp, q_r^+) &= \sum_{q_\ell \neq 0} \int d^d q_r F(q_\ell^- + q_r^-, q_\ell^\perp + q_r^\perp, q_r^+) \\ &= \sum_{q_\ell} \int d^d q_r F(q_\ell^- + q_r^-, q_\ell^\perp + q_r^\perp, q_r^+) - \int d^d q_r F^0(q_r^-, q_r^\perp, q_r^+) \\ &= \int d^d q F(q^-, q^\perp, q^+) - \int d^d q_r F^0(q_r^-, q_r^\perp, q_r^+) \\ &= \int d^d q [F(q^-, q^\perp, q^+) - F^0(q^-, q^\perp, q^+)]. \end{aligned} \quad (4.64)$$

Here the integrand  $F^0$  is derived from expanding the integrand for  $F$  by taking the label momenta that appear in its first two arguments to instead scale as ultrasoft momenta  $\sim \lambda^2$ , expanding, and keeping the dominant and any sub-dominant scaling terms up to those that are the same order in  $\lambda$  as the original loop integration. If the original integrand  $F \sim \lambda^{-4}$ , then this corresponds to keeping just the terms up to  $F^0 \sim \lambda^{-8}$ , which is often the leading term. (Together with the standard scaling for the collinear measure,  $d^d q \sim \lambda^4$  and for the residual measure  $d^d q_r \sim \lambda^8$  these two integrands give contributions that are both the same order in  $\lambda$ .) In the last line we combine the subtraction term back together with the original integrand, since the integration variables are after all just dummy variables. This set of steps makes it clear that zero-bin contributions are encoded by subtractions.<sup>5</sup> The scaling for the subtraction is shown pictorially in Fig. 8. The  $F^0$  term subtracts singularities from  $F$  that come from the region where the collinear momentum behaves like an ultrasoft momentum. In general when the subtraction integration is non-trivial there will always exist a corresponding ultrasoft diagram where the integration is ultrasoft from the start, which precisely corresponds with the contribution that the subtractions is allowing us to avoid double counting.

In general, when one has a continuum EFT with modes that live in a two dimensional space, such as those in Fig. 8, one has subtractions induced by the presence of modes at smaller (or equal)  $p^2$ . Therefore

<sup>5</sup>In fact, an alternate formulation of zero-bin subtractions that avoids the use of notation like  $q_\ell \neq 0$  is to note that in a theory with both collinear and ultrasoft modes, each collinear propagator is actually a distribution, like a generalized +-function, that induces these subtraction terms. The fact that we drop higher order terms in the  $\lambda$  expansion when determining  $F^0$  implies that we are making the minimal subtraction that avoids double counting IR singularities. Indeed there in principle could still be a double counting by a "constant" contribution, but such constants will be properly taken care of by the matching procedure. The minimal subtraction also ensures that the matching result remains independent of the IR regulator as desired.

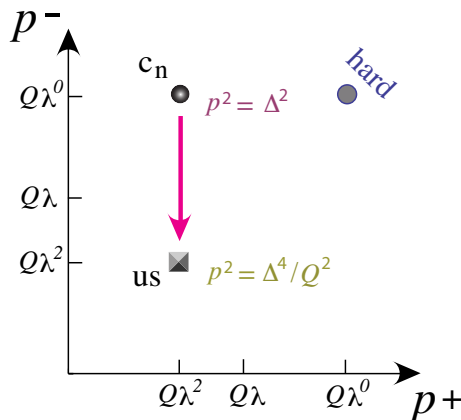


Figure 8: SCET<sub>I</sub> zero-bin from one collinear direction scaling into the ultrasoft region.

there are ultrasoft subtractions for the collinear modes, but no collinear subtractions for the ultrasoft modes.

It also should be remarked that depending on the choice of infrared regulators, the subtraction terms very often give scaleless integrations of combined dimension  $d - 4$  in dimensional regularization. These then just yield terms proportional to  $(1/\epsilon_{\text{UV}}^j - 1/\epsilon_{\text{IR}}^j)$ , which are only important to properly interpret whether factors of  $1/\epsilon$  from the naive collinear loop integration that used Eq. (4.60) are UV poles that require a counterterm, or are IR poles that correspond with physical IR singularities in QCD. In particular this is often the case for the simplest measurements with an offshellness IR regulator for collinear external lines. More complicated measurements (such as those depending on a jet algorithm) or other choices of IR regulators (like a gluon mass or a cutoff) will lead to zero-bin subtractions that are not scaleless.

We will return to this discussion when carrying out explicit examples of collinear loops in section 7.

## 5 Symmetries of SCET

In quantum field theory Lagrangians are often built up from symmetries and dimensional analysis. So far our leading order SCET Lagrangians were derived directly from QCD at tree level. To go further, and determine whether loops can change the form of the Lagrangians (through Wilson coefficients or additional operators) we need to exploit symmetries and power counting. In this section, we will introduce the SCET gauge symmetries and reparameterization invariance (RPI) as a way to constrain SCET operators. We will find that the gauge symmetry formalism is a simple restatement of the standard QCD picture except with two separate gauge fields. RPI is a manifestation of the Lorentz symmetry which was broken by the choice of light-cone coordinates, and which acts independently in each collinear sector. We will also examine the spin symmetries of the SCET Lagrangian, although here we will find that there are no surprises beyond what we know from QCD.

## 5.1 Spin Symmetry

To examine the spin symmetry of  $\mathcal{L}_{n\xi}^{(0)}$  it is convenient to write the Lagrangian in a two component form. From Eq. (3.11) we can write

$$\xi_n = \frac{1}{\sqrt{2}} \begin{pmatrix} \varphi_n \\ \sigma^3 \varphi_n \end{pmatrix}, \quad (5.1)$$

where  $\varphi_n$  is a two-component field,  $\dim \varphi_n = \dim \xi_n = 3/2$ , and  $\varphi_n \sim \lambda$ . With this two-component field the SCET Lagrangian is

$$\mathcal{L} = \varphi_n^\dagger \left[ in \cdot D + iD_{n\perp}^\mu \frac{1}{i\bar{n} \cdot D} iD_{n\perp}^\nu (g_{\mu\nu}^\perp + i\epsilon_{\mu\nu}^\perp \sigma_3) \right] \varphi_n. \quad (5.2)$$

Due to the  $\sigma_3$  the spin symmetry is not an  $SU(2)$ , but rather just the  $U(1)$  helicity symmetry corresponding to spin along the direction of motion  $n$  of the collinear fields. The relevant generator is

$$S_z = i\epsilon_{\perp}^{\mu\nu} [\gamma^\mu, \gamma^\nu] \rightarrow h = \sigma_3. \quad (5.3)$$

We can relate this symmetry to the chiral symmetry by noting that under chiral symmetry  $\xi_n$  transforms as

$$\xi_n \rightarrow \gamma^5 \xi_n = \begin{pmatrix} 0 & 1 \\ 1 & 0 \end{pmatrix} \frac{1}{\sqrt{2}} \begin{pmatrix} \sigma^3 \phi_n \\ \phi_n \end{pmatrix} \quad \text{so} \quad \varphi_n \rightarrow \sigma_3 \varphi_n. \quad (5.4)$$

This  $U(1)_A$  axial-symmetry is broken by fermion masses and non-perturbative instanton effects. Just like in QCD it is a useful symmetry for determining the structure of perturbation theory results. This implies that in SCET it is useful for determining the basis of operators we obtain when integrating out hard particles, and for relating Wilson coefficients.

## 5.2 Gauge Symmetry

The standard gauge transformation in QCD is

$$U(x) = \exp[i\alpha^A(x)T^A]. \quad (5.5)$$

When we go to SCET we need to have gauge transformations which do not inject large momenta into our EFT fields, that is, the transformations must leave us within our effective field theory. For example, if we used a gauge transformation where  $\alpha^A$  satisfied

$$i\partial_\mu \alpha^A \sim Q\alpha^A \quad (5.6)$$

then  $\xi'_n = U(x)\xi_n$  would no longer have  $p^2 \leq Q^2\lambda^2$  and would not be described by SCET. There are two acceptable SCET gauge transformations which are defined by their momentum scale. They are

$$\text{collinear } U_n(x) : i\partial^\mu U_n(x) \sim Q(\lambda^2, 1, \lambda)U_n(x) \quad (5.7)$$

$$\text{ultrasoft } U_u(x) : i\partial^\mu U_u(x) \sim Q(\lambda^2, \lambda^2, \lambda^2)U_u(x). \quad (5.8)$$

There is also a global color transformation which for convenience we group together with the  $U_u$ . To avoid double counting, in the collinear transformation we fix  $U_n(n \cdot x = -\infty) = 1$ . We can implement a collinear gauge transformation on the collinear fields  $\xi_{n, p_i}$  via a Fourier transform. Since  $\psi(x) \rightarrow U(x)\psi(x)$  is equivalent to  $\tilde{\psi}(p) \rightarrow \int dq \tilde{U}(p-q)\tilde{\psi}(q)$ , the transformation involves a convolution in label momenta. To understand how the collinear gauge field transforms under a collinear gauge transformation, we need to

recall that there is a background usoft gauge field  $A_{us}^\mu$ . Consequently we must take  $\partial_\mu \rightarrow \mathcal{D}_\mu^{us}$  so that  $A_n^\mu$  transforms as a quantum field in an  $A_{us}^\mu$  background. Therefore the collinear gauge transformations are

$$\begin{aligned}\xi_{n,p}(x) &\rightarrow (U_n)_{p-q}(x) \xi_{n,q}(x), \\ A_{n,p}^\mu(x) &\rightarrow U_{n,p-q}(x) \left( g A_{n,q-q'}^\mu(x) + \delta_{q,q'} i \mathcal{D}_{us}^\mu \right) U_{n,q'}^\dagger(x),\end{aligned}\tag{5.9}$$

where we sum over repeated momentum label indices. It is convenient to setup a matrix notation for these convolutions by defining

$$(\hat{U}_n)_{p_\ell, q_\ell} \equiv (U_n)_{p_\ell - q_\ell},\tag{5.10}$$

where the LHS is the  $(p_\ell, q_\ell)$  element of a matrix in momentum space, and the RHS is a number (both are of course also matrices in color). Then Eq. (5.9) with a sum over repeated indices becomes  $\xi_{n,p_\ell} \rightarrow (\hat{U}_n)_{p_\ell, q_\ell} \xi_{n, q_\ell}$ . And if we suppress indices then we have  $\xi_n \rightarrow (\hat{U}_n) \xi_n$ .

Finally the ultrasoft fields do not transform under a collinear gauge transformation, since the resulting field would have a large momentum and hence no longer be ultrasoft. Essentially this means that by definition our collinear gauge transformations do not turn ultrasoft gluons into collinear gluons.

### Collinear Gauge Transformations : $U_n(x)$

Therefore our set of Collinear Gauge Transformations with the matrix notation for momentum space labels are

- $\xi_n(x) \rightarrow \hat{U}_n(x) \xi_n(x)$
- $A_n^\mu(x) \rightarrow \hat{U}_n(x) (A_n^\mu(x) + \frac{i}{g} \mathcal{D}_{us}^\mu) \hat{U}_n^\dagger(x)$
- $q_{us}(x) \rightarrow q_{us}(x)$
- $A_{us}^\mu(x) \rightarrow A_{us}^\mu(x)$

When using the momentum label notation the condition  $U_n(n \cdot x = -\infty) = 1$  becomes  $(U_n)_{p_\ell \rightarrow 0} = \delta_{p_\ell, 0}$  for the zero-bin  $p_\ell = 0$  (the ultrasoft transformations do not modify large momenta, but the collinear transformations do).

For usoft gauge transformations, the field  $\xi_n$  and  $A_n^\mu$  transform as quantum fields under a background gauge transformation, which is to say they transform as matter fields with the appropriate representation. The usoft fields have their usual gauge transformations from QCD.

### Ussoft Gauge Transformations : $U_u(x)$

Therefore for the Ultrasoft Gauge Transformations we have

- $\xi_n(x) \rightarrow U_{us}(x) \xi_n(x)$
- $A_n^\mu(x) \rightarrow U_{us}(x) A_n^\mu(x) U_{us}^\dagger(x)$
- $q_{us}(x) \rightarrow U_{us}(x) q_{us}(x)$
- $A_{us}^\mu(x) \rightarrow U_{us}(x) (A_{us}^\mu(x) + \frac{i}{g} \partial^\mu) U_{us}^\dagger(x)$

Since all of the fields transform, these ultrasoft gauge transformations connect fields in operators that are mixtures of collinear and ultrasoft fields. This differs from  $U_n(x)$  which only connects collinear fields to each other.

It is important to note that the  $U_n$  and  $U_u$  gauge transformations are homogeneous in the power counting, so they do not change the order in  $\lambda$  for transformed operators. They are exact, there are no corrections to these transformations at higher orders in  $\lambda$ , and thus the power expansion will have gauge invariant operators at each order in  $\lambda$ .

The transformation of the fields yield transformations for objects that are built from the fields. An important case is the Wilson line  $W_n$  which is like the Fourier transform of  $W(x, -\infty)$ . In QCD a general Wilson line with the gauge field along a path will transform on each end as  $W(x, y) \rightarrow U(x)W(x, y)U^\dagger(x)$ . For the collinear gauge transformation we have fields in momentum space for labels, and position space representing residual momenta, and  $U_n^\dagger(-\infty) = 1$ , so the Wilson line transforms only on one side for collinear transformations. For ultrasoft transformations  $W_n(x)$  is actually a local operator with all fields at  $x$ , and the product of multiple  $\bar{n} \cdot A_n(x) \rightarrow U_{us}(x)\bar{n} \cdot A_n(x)U_{us}^\dagger(x)$  leads to one  $U_{us}$  and  $U_{us}^\dagger$  on the left and right. Thus with the matrix notation

$$\begin{aligned} \text{collinear :} & \quad W_n(x) \rightarrow \hat{U}_n(x)W_n(x), \\ \text{ultrasoft :} & \quad W_n(x) \rightarrow U_{us}(x)W_n(x)U_{us}^\dagger(x). \end{aligned} \quad (5.11)$$

It is useful to consider the correspondence between the appearance of the Wilson line  $W_n$  in operators, and the collinear gauge symmetry. If we consider our example of the heavy-to-light current then without the Wilson line the operator  $\bar{\xi}_n \Gamma h_v^{us}$  is not gauge invariant, transforming to  $\bar{\xi}_n U_n^\dagger \Gamma h_v^{us}$ . Here the  $\xi_n$  transforms because collinear gluons couple to  $\xi_n$  without taking it offshell, but  $h_v^{us}$  does not transform because this ultrasoft field can not interact with the collinear gluons while remaining near its mass shell. But recall that when the offshell collinear gluons are accounted for in matching onto the SCET operator that the  $\bar{n} \cdot A_n \sim \lambda^0$  gluons generate a Wilson line  $W_n$ , so the complete result from tree level matching is

$$J_{\text{SCET}} = \bar{\xi}_n W_n \Gamma h_v^{us}. \quad (5.12)$$

Now under a collinear gauge transformation  $J_{\text{SCET}} \rightarrow \bar{\xi}_n \hat{U}_n^\dagger \hat{U}_n W_n \Gamma h_v^{us} = \bar{\xi}_n W_n \Gamma h_v^{us}$ , so the current is collinear gauge invariant. Under an ultrasoft gauge transformation  $J_{\text{SCET}} \rightarrow \bar{\xi}_n U_{us}^\dagger U_{us} W_n U_{us}^\dagger \Gamma U_{us} h_v^{us} = \bar{\xi}_n W_n \Gamma h_v^{us}$ , so the current is also ultrasoft gauge invariant. Thus the leading order attachments of  $\bar{n} \cdot A_n$  gluons that lead to the Wilson line  $W_n$  are necessary to obtain a gauge invariant result. Furthermore, by gauge symmetry the fact that the product  $\bar{\xi}_n W_n$  appears in the operator will not be modified by loop corrections. We will take up what modifications can be generated by loop corrections in section 6.2 below.

Gauge symmetry forces gauge fields and derivatives to occur in the following combinations

$$\begin{aligned} in \cdot D &= in \cdot \partial + gn \cdot A_n + gn \cdot A_{us}, \\ iD_{n\perp}^\mu &= \mathcal{P}_\perp^\mu + gA_{n\perp}^\mu, \\ i\bar{n} \cdot D_n &= \bar{\mathcal{P}} + g\bar{n} \cdot A_n, \\ iD_{us}^\mu &= i\partial^\mu + gA_{us}^\mu. \end{aligned} \quad (5.13)$$

We see that gauge symmetry is a powerful tool in determining the structure of operators. It is reasonable to ask, is power counting and gauge invariance enough to fix the leading order Lagrangian  $\mathcal{L}_{n\xi}^{(0)}$  for  $\xi_n$ ? Only the operators  $in \cdot D$  and  $(1/\bar{\mathcal{P}})D_{n\perp}D_{n\perp}$  are  $\mathcal{O}(\lambda^2)$  and have the correct mass dimension. The latter will have the correct gauge transformation properties once we include  $W_n$ s. Nevertheless, nothing so far rules out the operator

$$\bar{\xi}_n iD_{n\perp}^\mu W_n \frac{1}{\bar{\mathcal{P}}} W_n^\dagger iD_{n\perp}^\mu \frac{\not{n}}{2} \xi_n \quad (5.14)$$

which is gauge invariant and has the correct  $\lambda$  scaling. To exclude this term we need to consider another symmetry principle, namely reparameterization invariance.



### 5.3 Reparamterization Invariance

Our choice of the  $n$  and  $\bar{n}$  reference vectors explicitly breaks Lorentz symmetry in SCET, much like  $v$  does in HQET. Part of this breaking is natural, SCET<sub>I</sub> is describing a collimated jet which explicitly picks out a corresponding  $n$ -collinear direction about which the field theory is describing fluctuations. There is also a part of the symmetry that is restored by the freedom we have in choosing our  $n$  and  $\bar{n}$  vectors, which is a reparameterization invariance (RPI). A second attribute of the reparameterization symmetry is the freedom we have in splitting momenta between label and residual components. We will explore these two in turn.

The only required property of a set of  $n$ ,  $\bar{n}$  basis vectors is that they satisfy

$$n^2 = \bar{n}^2 = 0, \quad n \cdot \bar{n} = 2. \quad (5.15)$$

Consequently a different choice for  $n$  and  $\bar{n}$  can yield a valid set of light-cone coordinates as long as our result still obeys (5.15). Specifically, there are three sets of transformations which can be made on a set of light-cone coordinates to obtain another, equally valid, set.

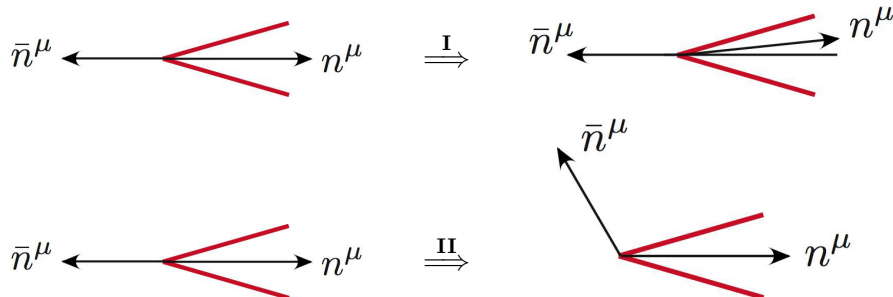
$$\begin{array}{ccc} \text{I} & \text{II} & \text{III} \\ n_\mu \rightarrow n_\mu + \Delta_\mu^\perp & n_\mu \rightarrow n_\mu & n_\mu \rightarrow e^\alpha n_\mu \\ \bar{n}_\mu \rightarrow \bar{n}_\mu & \bar{n}_\mu \rightarrow \bar{n}_\mu + \varepsilon_\mu^\perp & \bar{n}_\mu \rightarrow e^{-\alpha} \bar{n}_\mu \end{array} \quad (5.16)$$

where  $\bar{n} \cdot \varepsilon^\perp = n \cdot \varepsilon^\perp = \bar{n} \cdot \Delta^\perp = n \cdot \Delta^\perp = 0$ . The first two transformations are infinitesimal. The third is a finite transformation (where the form is simple), but can be made infinitesimal by expansion in  $\alpha$ . These transformations must leave a collinear momentum collinear in the same directions, so we can obtain the  $\lambda$ -scaling of these parameters by noting that:

$$\begin{aligned} \lambda^2 &\sim n \cdot p \rightarrow n \cdot p + \Delta^\perp \cdot p_\perp \implies \Delta^\perp \sim \lambda^1 \\ \lambda^0 &\sim \bar{n} \cdot p \rightarrow \bar{n} \cdot p + \varepsilon^\perp \cdot p_\perp \implies \varepsilon^\perp \sim \lambda^0 \\ \alpha &\sim \lambda^0 \end{aligned} \quad (5.17)$$

Thus only  $\Delta^\perp$  is constrained by the power counting, while large changes are allowed for  $\alpha$  and  $\varepsilon^\perp$ . These RPI transformations are a manifestation of the Lorentz symmetry which was broken by introducing the vectors  $n$  and  $\bar{n}$ . The five infinitesimal parameters  $\Delta_\mu^\perp$ ,  $\varepsilon_\mu^\perp$ , and  $\alpha$  correspond to the five generators of the Lorentz group which were broken by introducing the vectors  $n$  and  $\bar{n}$ . These generators are defined by  $\{n_\mu M^{\mu\nu}, \bar{n}_\mu M^{\mu\nu}\}$  or in terms of our standard light-cone coordinates  $Q_1^\pm = J_1 \pm K_2$ ,  $Q_2^\pm = J_2 \pm K_1$ , and  $K_3$ . Here  $M^{\mu\nu}$  are the usual 6 antisymmetric SO(3,1) generators.

If we start with our canonical basis choice  $n = (1, 0, 0, 1)$  and  $\bar{n} = (1, 0, 0, -1)$  then we can visualize the Type I and Type II transformations as changes in the directions orthogonal to the  $\hat{z}$  direction



and we can visualize Type III transformations as boosts in the  $\hat{z}$  direction. For Type I we can transform  $n$  by an  $\mathcal{O}(\lambda)$  amount, into another vector within this collinear sector, without changing any of the physics. For Type II we recall that the auxillary vector  $\bar{n}$  was chosen simply to enable us to decompose momenta, so there is a considerable freedom in its definition, and this corresponds to the freedom to make large transformations. (If we start with a more general choice for  $n$  and  $\bar{n}$  that satisfies Eq. (5.15) then the picture for the Type-III transformation is more complicated than a simple boost.)

The implications of the Type III transformation for SCET operators are very simple,  $n$  and  $\bar{n}$  must appear in operators either together, or with one factor of  $\bar{n}/n$  in both the numerator and denominator. That is, in one of the combinations

$$(A \cdot n)(B \cdot \bar{n}), \quad \frac{A \cdot n}{B \cdot n}, \quad \frac{A \cdot \bar{n}}{B \cdot \bar{n}} \quad (5.18)$$

where  $A^\mu$  and  $B^\mu$  are arbitrary 4-vectors.

In order to derive the complete set of transformation relations we must also determine how  $p_\perp^\mu$  transforms. Recall that the definition of  $p_\perp$  depends on  $n$  and  $\bar{n}$ , since it is orthogonal to  $n$  and  $\bar{n}$ , satisfying  $n \cdot p_\perp = 0 = \bar{n} \cdot p_\perp$ . We can work out its transformation by noting that the four vector  $p^\mu$  does not depend on the basis for coordinates. Using the Type-I transformation as an example

$$p^\mu = \frac{n^\mu}{2} \bar{n} \cdot p + \frac{\bar{n}^\mu}{2} n \cdot p + p_\perp^\mu \implies \frac{n^\mu}{2} \bar{n} \cdot p + \frac{\bar{n}^\mu}{2} n \cdot p + p_\perp^\mu + \frac{\Delta_\perp^\mu}{2} \bar{n} \cdot p + \frac{\bar{n}^\mu}{2} \Delta_\perp \cdot p_\perp + \delta_I(p_\perp^\mu) = p^\mu. \quad (5.19)$$

Thus  $p_\perp^\mu$  must transform as

$$p_\perp^\mu \xrightarrow{\mathbf{I}} p_\perp^\mu - \frac{\bar{n}^\mu}{2} \Delta_\perp \cdot p_\perp - \frac{\Delta_\perp^\mu}{2} \bar{n} \cdot p. \quad (5.20)$$

The projection relation  $(\not{n}\not{\bar{n}}/4)\xi_n = \xi_n$  also implies that  $\xi_n \rightarrow [1 + (\not{\Delta}^\perp \not{\bar{n}})/4]\xi_n$ . Similar relations can also be worked out for type-II transformations, for example

$$p_\perp^\mu \xrightarrow{\mathbf{II}} p_\perp^\mu - \frac{n^\mu}{2} \varepsilon_\perp \cdot p_\perp - \frac{\varepsilon_\perp^\mu}{2} n \cdot p. \quad (5.21)$$

Summarizing all the type-I and type-II transformations on vectors and fields (using  $D^\mu$  as a typical vector) we have

$$\begin{array}{c|c} \mathbf{I} & \mathbf{II} \\ \hline n \rightarrow n + \Delta^\perp & n \rightarrow n \\ \bar{n} \rightarrow \bar{n} & \bar{n} \rightarrow \bar{n} + \varepsilon^\perp \\ n \cdot D \rightarrow n \cdot D + \Delta^\perp \cdot D^\perp & n \cdot D \rightarrow n \cdot D \\ D_\mu^\perp \rightarrow D_\mu^\perp - \frac{\Delta_\mu^\perp}{2} \bar{n} \cdot D - \frac{\bar{n}^\mu}{2} \Delta^\perp \cdot D & D_\mu^\perp \rightarrow D_\mu^\perp - \frac{\varepsilon_\mu^\perp}{2} n \cdot D - \frac{n^\mu}{2} \varepsilon^\perp \cdot D \\ \bar{n} \cdot D \rightarrow \bar{n} \cdot D & \bar{n} \cdot D \rightarrow \bar{n} \cdot D + \varepsilon^\perp \cdot D^\perp \\ \xi_n \rightarrow \left(1 + \frac{1}{4} \not{\Delta}^\perp \not{\bar{n}}\right) \xi_n & \xi_n \rightarrow \left(1 + \frac{1}{2} \not{\varepsilon}^\perp \frac{1}{i\bar{n} \cdot D} i\not{D}_\perp\right) \xi_n \\ W_n \rightarrow W_n & W_n \rightarrow \left(1 - \frac{1}{i\bar{n} \cdot D} \varepsilon^\perp \cdot iD^\perp\right) W_n \end{array} \quad (5.22)$$

For type-III transformations  $p_\perp^\mu$  does not transform, and neither does  $W_n$ .

We can show that our leading order SCET Lagrangian

$$\mathcal{L}_{n\xi}^{(0)} = \xi_n i n \cdot D \frac{\not{n}}{2} \xi_n + \bar{\xi}_n i \not{D}_{n,\perp} \frac{1}{i\bar{n} \cdot D} i \not{D}_{n,\perp} \frac{\not{\bar{n}}}{2} \xi_n \quad (5.23)$$

is invariant under these transformations. Under a type-I transformation we have

$$\begin{aligned}\delta_{\text{I}}\mathcal{L}_{n\xi}^{(0)} &= \delta_{\text{I}}\left(\xi_n i\bar{n}\cdot D\frac{\not{n}}{2}\xi_n\right) + \delta_{\text{I}}\left(\bar{\xi}_n i\not{D}_{n,\perp}\frac{1}{i\bar{n}\cdot D}i\not{D}_{n,\perp}\frac{\not{n}}{2}\xi_n\right) \\ &= \bar{\xi}_n i\Delta^\perp\cdot D^\perp\frac{\not{n}}{2}\xi_n - \bar{\xi}_n i\Delta^\perp\cdot D^\perp\frac{\not{n}}{2}\xi_n \\ &= 0\end{aligned}\tag{5.24}$$

where to obtain the second line we used  $\not{n}^2 = 0$ , the orthogonal properties of the 4-vectors, and ignored quadratic combinations of the  $\Delta^\perp$  infinitesimal. Hence the SCET quark Lagrangian obtained from tree level matching is indeed invariaant under  $\delta_{\text{I}}$ . However, this Lagrangian is not completely determined by invariance under  $\delta_{\text{I}}$ . For example, the term we encountered at the end of the gauge symmetry section transforms as

$$\delta_{(I)}\left(\bar{\xi}_n iD_\mu^\perp\frac{1}{i\bar{n}\cdot D}iD^{\perp\mu}\frac{\not{n}}{2}\xi_n\right) = -\bar{\xi}_n i\Delta^\perp\cdot D\frac{\not{n}}{2}\xi_n\tag{5.25}$$

which is the same transformation as for the second term in (5.24). Consequently, we may replace the second term with this new term with no violation of power counting, gauge symmetry, or RPI type-I. This ambiguity is only resolved by using invariance under RPI of type-II. The detailed calculation is given in [7] with the final result that our Lagrangian  $\mathcal{L}_{n\xi}^{(0)}$  remains invariant under  $\delta_{\text{II}}$  while the term given in (5.14) does transforms in a way that can not be compensated by any other leading order term in the Lagrangian. Therefore our SCET<sub>I</sub> Lagrangian  $\mathcal{L}_{n\xi}^{(0)}$  is unique by power counting, gauge invariance, and reparameterization invariance. This also implies that its form is not modified by loop corrections. In general type-III RPI will restrict operators at the same order in  $\lambda$ , type-I restricts operators at different orders in  $\lambda$ , and type-II will restrict operators at both the same and different orders in  $\lambda$ .

Reparameterization invariance also manifests itself in the ambiguity of label and residual momenta decomposition. We can separate the total momenta

$$\bar{n}\cdot p = \bar{n}\cdot(p_\ell + p_r) \quad p_\perp^\mu = p_{\ell\perp}^\mu + p_{r\perp}^\mu\tag{5.26}$$

into  $p_\ell$  and  $p_r$  in different ways as long as we maintain the power counting. Specifically, a transformation that takes

$$\mathcal{P}^\mu \rightarrow \mathcal{P}^\mu + \beta^\mu \quad i\partial^\mu \rightarrow i\partial^\mu - \beta^\mu\tag{5.27}$$

implements this freedom. The transformation on  $i\partial^\mu$  is induced by the  $\beta$ -transformation of the fields, for example

$$\xi_{n,p}(x) \rightarrow e^{i\beta(x)}\xi_{n,p+\beta}(x).\tag{5.28}$$

The set of these  $\beta$  transformations also determines the space of equivalent decompositions  $\mathcal{I}$  that we mod out by when constructing pairs of label and residual momenta components  $(p_\ell, p_r)$  in  $\mathbb{R}^3 \times \mathbb{R}^4/\mathcal{I}$ . Invariance under this RPI requires the combination

$$\mathcal{P}^\mu + i\partial^\mu\tag{5.29}$$

to be grouped together for collinear fields. Since  $\bar{\mathcal{P}}$  and  $i\bar{n}\cdot\partial$  (and  $\mathcal{P}_\perp^\mu$  and  $i\partial_\perp^\mu$ ) appear at different orders in the power counting, this RPI connects the Wilson coefficients of operators at different orders in  $\lambda$ .

A natural question is how to gauge the connection between label and residual derivatives in (5.29). Recall that the gauge transformations for derivatives are

	collinear	ultrasoft
$iD_{n\perp} \rightarrow$	$U_c iD_{n\perp} U_c^\dagger$	$U_{us} iD_{n\perp} U_{us}^\dagger$
$i\bar{n}\cdot D_n \rightarrow$	$U_c i\bar{n}\cdot D_n U_c^\dagger$	$U_{us} i\bar{n}\cdot D_n U_{us}^\dagger$
$i\bar{n}\cdot D \rightarrow$	$U_c i\bar{n}\cdot D U_c^\dagger$	$U_{us} i\bar{n}\cdot D U_{us}^\dagger$
$iD_{us}^\mu \rightarrow$	$iD_{us}^\mu$	$U_{us} iD_{us}^\mu U_{us}^\dagger$

The most natural guess for the gauging of (5.29) would be

$$iD_{n\perp}^\mu + iD_{us\perp}^\mu, \quad i\bar{n} \cdot D_n + i\bar{n} \cdot D_{us}. \quad (5.30)$$

However, with the above transformations these combinations do not have uniform transformations under the gauge symmetries, since  $D_{us}$  does not transform under  $U_n$ . We can rectify this problem by introducing our Wilson line  $W_n$  into the combination of these derivatives. The unique result which preserves the SCET gauge symmetries without changing the power counting of the terms is

$$iD_\perp^\mu \equiv iD_{n\perp}^\mu + W_n iD_{n\perp}^{us,\mu} W_n^\dagger \quad (5.31)$$

$$i\bar{n} \cdot D \equiv i\bar{n} \cdot D_n + W_n i\bar{n} \cdot D_{us} W_n^\dagger, \quad (5.32)$$

where  $W_n$  transforms as  $W_n \rightarrow U_n W_n$ . Stripping off the regular derivative terms, the extra multi-gluon terms appearing in the formulae like  $A_\perp^\mu = A_{n\perp}^\mu + A_{us\perp}^\mu + \dots$  are the terms we denoted by ellipses in (4.9). These terms are necessary to form gauge invariant subleading operators.

Like in HQET, the RPI in SCET connects the Wilson coefficients of leading and  $\lambda$ -suppressed Lagrangians and external currents and operators. As an example, applying the connection to the term  $\bar{\xi}_n i\mathcal{D}_{n,\perp} W_n (1/\overline{\mathcal{P}}) W_n^\dagger i\mathcal{D}_{n,\perp} \xi_n$  in  $\mathcal{L}_{n\xi}^{(0)}$  yields the subleading Lagrangian that couples collinear quarks to  $A_\perp^{us}$  gluons,

$$\mathcal{L}_{n\xi}^{(1)} = (\bar{\xi}_n W_n) i\mathcal{D}_\perp^{us} \frac{1}{\overline{\mathcal{P}}} (W_n^\dagger i\mathcal{D}_{n,\perp} \xi_n) + (\bar{\xi}_n i\mathcal{D}_{n,\perp} W_n) \frac{1}{\overline{\mathcal{P}}} i\mathcal{D}_\perp^{us} (W_n^\dagger \xi_n). \quad (5.33)$$

The complete set of SCET<sub>I</sub> Lagrangian interactions up to  $\mathcal{O}(\lambda^2)$  can be found in Ref. [10].

## 5.4 Discrete Symmetries

After considering the residual form of Lorentz symmetry encoded in reparameterization invariance it is natural to consider how our SCET fields transform under  $C$ ,  $P$ , and  $T$  transformations. In this case we will satisfy ourselves with the transformations of the collinear field  $\xi_{n,p}$ . We have

$$C^{-1} \xi_{n,p}(x) C = -[\bar{\xi}_{n,-p}(x) \mathcal{C}]^T \quad (5.34)$$

$$P^{-1} \xi_{n,p}(x) P = \gamma_0 \xi_{\bar{n},\tilde{p}}(x_P)$$

$$T^{-1} \xi_{n,p}(x) T = \mathcal{T} \xi_{\bar{n},\tilde{p}}(x_T)$$

where  $n = (1, 0, 0, 1)$ ,  $\bar{n} = (1, 0, 0, -1)$ ,  $p \equiv (p^+, p^-, p^\perp)$ ,  $x \equiv (x^+, x^-, x^\perp)$ ,  $\mathcal{C}$  is the standard matrix induced by charge conjugation symmetry, and we have defined  $\tilde{p} = (p^-, p^+, -p^\perp)$  as well as  $x_P = (x^-, x^+, -x^\perp)$  and  $x_T = (-x^-, -x^+, x^T)$ .

## 5.5 Extension to Multiple Collinear Directions

For processes with more than one energetic hadron, or more than one energetic jet our list of degrees of freedom must include more than one type of collinear mode, and hence more than one type of collinear quark and collinear gluon. When two collinear modes in different directions interact, the resulting particle is offshell, and does not change the formulation of the leading order collinear Lagrangians. Therefore the Lagrangian with multiple collinear directions is

$$\mathcal{L}_{\text{SCET}_I}^{(0)} = \mathcal{L}_{us}^{(0)} + \sum_n \left[ \mathcal{L}_{n\xi}^{(0)} + \mathcal{L}_{ng}^{(0)} \right]. \quad (5.35)$$

for  $n_1, n_2, n_3, \dots$  collinear modes in the sum on  $n$ . The collinear modes are distinct only if

$$n_i \cdot n_j \gg \lambda^2 \quad \text{for } i \neq j. \quad (5.36)$$

We may understand this result by a counter argument: If a momentum  $p_2 = Qn_2$ , then  $n_1 \cdot p_2 = Qn_1 \cdot n_2 \sim \lambda^2$  iff  $n_1 \cdot n_2 \sim \lambda^2$ . Hence  $p_2$  is  $n_1$ -collinear, and  $n_2$  is not a distinct collinear direction from  $n_1$ . If  $n_i \cdot n_1 \sim \lambda^2$  then we say that  $n_i$  is within the RPI equivalence class  $[n_1]$  defined by the member  $n_1$ . Distinct collinear directions correspond to the different equivalence classes, and we only sum over distinct directions in Eq. (5.35).

Essentially all of the things we derived with one collinear direction get repeated when we have more than one collinear direction.

- For each light-like  $n_i$  we define an auxillary light-like  $\bar{n}_i$  where  $n_i \cdot \bar{n}_i = 2$ . Collinear momenta in the  $n_i$  direction are decomposed with the  $\{n_i, \bar{n}_i\}$  basis vectors since the components have a definite power counting:  $(n_i \cdot p, \bar{n}_i \cdot p, p_{n_i \perp}) \sim (\lambda^2, 1, \lambda)$ . Note that the meaning of  $\perp$  depends on which  $n_i$ -collinear sector we are discussing.
- There is a separate RPI for each  $n_i$ -collinear sector that only acts on the  $n_i$ -collinear fields, and on objects decomposed with the  $\{n_i, \bar{n}_i\}$  basis vectors. Here there is no simple connection to an overall Lorentz transformation because the fields in other sectors do not transform.
- There is a collinear gauge transformation  $U_{n_i}$  for each type of collinear field. Only the fields in the  $n_i$ -collinear direction transform (fields in other collinear sectors do not transform with  $U_{n_i}$  since such transformations would yield offshell momenta that are outside the effective theory).
- Matching calculations generate multiple collinear Wilson lines  $W_{n_i} = W_{n_i}[\bar{n}_i \cdot A_{n_i}]$ . The definitions are identical to Eq. (4.51) with  $n \rightarrow n_i$ ,  $\bar{n} \rightarrow \bar{n}_i$ , including  $\bar{P} \rightarrow \bar{n}_i \cdot \mathcal{P}$ . They are again always built only out of the  $\mathcal{O}(\lambda^0)$  gluon fields, and correspond to straight Wilson lines. These matching calculations lead to operators in SCET that are gauge invariant under  $U_{n_i}$  transformations.

As an example of the last point consider the process  $e^+e^- \rightarrow \gamma^* \rightarrow$  two-jets. The QCD current is  $J^\mu = \bar{\psi}\gamma^\mu\psi$ . By integrating out offshell fields to match onto SCET<sub>I</sub> we obtain the leading order current

$$J_{\text{SCET}}^\mu = (\bar{\xi}_{n_1} W_{n_1}) \gamma^\mu (W_{n_2}^\dagger \xi_{n_2}). \quad (5.37)$$

Here  $n_1$  and  $n_2$  are the directions of the two jets. The Wilson line  $W_{n_1} = W_{n_1}[\bar{n}_1 \cdot A_{n_1}]$  is generated by integrating out the attachment of  $\bar{n}_1 \cdot A_{n_1}$  gluons to  $n_2$ -collinear quarks and gluons, and analogously for  $W_{n_2}$ . The resulting operator in Eq. (7.29) is invariant under  $n_1$ -collinear,  $n_2$ -collinear, and ultrasoft gauge transformations. In general one can carry out all orders tree level matching computations to derive the presence of these Wilson lines. For situations with multiple lines in different directions these calculations are greatly facilitated by using the auxillary field method (see the appendices of [6, 8]).

## 6 Factorization from Mode Separation

One of the benefits of the SCET formalism is the clear separation of scales at the level of the Lagrangian and of operators that mediate hard interactions. We will explore the factorization between various types of modes in this section.

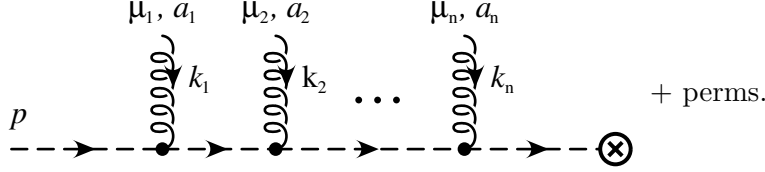


Figure 9: The attachments of ultrasoft gluons to a collinear quark line which are summed up into a path-ordered exponential.

### 6.1 Ultrasoft-Collinear Factorization

Recall that only the  $n \cdot A_{us}$  component couples to  $n$ -collinear quarks and gluons at leading order in  $\lambda$ . This is explicit in the Feynman rules in Figs. 6 and 7 where only  $n_\mu$  appears for the ultrasoft gluon with index  $\mu$ . Furthermore due to the multipole expansion the collinear particles only see the  $n \cdot k$  ultrasoft momentum of the  $n \cdot A_{us}$  gluons. For example, if we consider Fig. 9 with only one ultrasoft gluon then the collinear quark propagator is

$$\frac{\bar{n} \cdot p}{\bar{n} \cdot p n \cdot (p_r + k) + p_\perp^2 + i0} = \frac{\bar{n} \cdot p}{\bar{n} \cdot p n \cdot k + p^2 + i0} = \frac{\bar{n} \cdot p}{\bar{n} \cdot p n \cdot k + i0}, \quad (6.1)$$

where in the last equality we used the onshell condition  $p^2 = 0$  for the external collinear quark. Together with the  $n_\mu$  from the vertex this result corresponds to the eikonal propagator for the coupling of soft gluons to an energetic particle. The appropriate sign for the  $i0$  is determined by dividing through by  $\bar{n} \cdot p$  and noting the sign of this momentum, which differs for quark and antiquarks. Accounting for attachments to incoming or outgoing particles this leads to the four eikonal propagator results summarized in Fig. 10.

Now, we consider the case of multiple usoft gluon emission. Calculating within SCET the graphs in Fig. 9 gives  $\Gamma \tilde{Y}_n u_n$  where  $\Gamma$  is the structure at the  $\otimes$  vertex, and  $u_n$  is a collinear quark spinor. Here

$$\tilde{Y}_n = \sum_{m=0}^{\infty} \sum_{\text{perms}} \frac{(-g)^m n \cdot A^{a_1}(k_1) \cdots n \cdot A^{a_m}(k_m) T^{a_m} \cdots T^{a_1}}{n \cdot k_1 n \cdot (k_1 + k_2) \cdots n \cdot (\sum_i k_i)} \quad (6.2)$$

where all propagators are  $+i0$ . These eikonal propagators come from collinear quarks with offshellness  $\sim \lambda^2$ , which is near their mass shell, and hence are a property of fields in the EFT itself (as opposed to the Wilson lines  $W_n$  which were generated by matching onto the EFT). This corresponds to the momentum space formula for an ultrasoft Wilson line  $Y_n$ . In position space this formula becomes

$$Y_n(x) = \text{Pexp} \left[ ig \int_{-\infty}^0 ds n \cdot A_{us}^a(x + ns) T^a \right]. \quad (6.3)$$

It satisfies a defining equation and unitarity condition:

$$in \cdot D_{us} Y_n = 0, \quad Y_n^\dagger Y_n = 1. \quad (6.4)$$

For the case where the Wilson line is in the fundamental representation  $T^a \rightarrow T_{\alpha\beta}^a$ , while for a Wilson line in the adjoint representation  $T^a \rightarrow -if^{abc}$ . We will assume that all Wilson lines are in the fundamental representation and reserve the notation  $Y_n$  for this case. For the adjoint Wilson line we will use  $\mathcal{Y}_n$ .

When we wish to be specific in the notation for our Wilson lines to show whether they extend from  $-\infty$

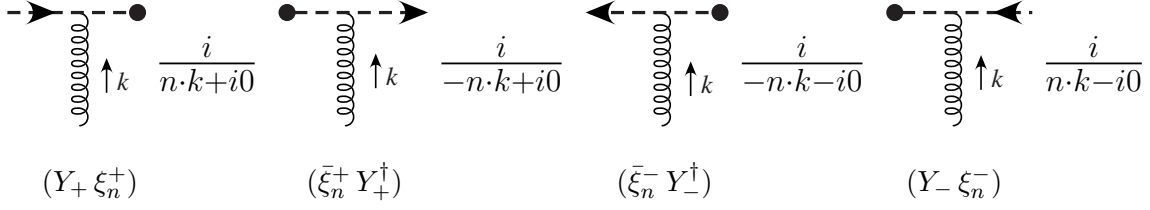


Figure 10: Eikonal  $i0$  prescriptions for incoming/outgoing quarks and antiquarks and the result that reproduces this with an ultrasoft Wilson line and sterile quark field.

or out to  $+\infty$ , and whether they are path-ordered or antipath-ordered, we will use the following notations

$$\begin{aligned}
 Y_{n+} &= \text{P exp} \left( ig \int_{-\infty}^0 ds n \cdot A_{us}(x + sn) \right), & Y_{n-} &= \bar{\text{P exp}} \left( -ig \int_0^{\infty} ds n \cdot A_{us}(x + sn) \right), \\
 Y_{n-}^\dagger &= \bar{\text{P exp}} \left( -ig \int_{-\infty}^0 ds n \cdot A_{us}(x + sn) \right), & Y_{n+}^\dagger &= \text{P exp} \left( ig \int_0^{\infty} ds n \cdot A_{us}(x + sn) \right).
 \end{aligned} \tag{6.5}$$

Here  $(Y_{n\pm})^\dagger = Y_{n\mp}^\dagger$ , and the subscript on  $Y_{n\pm}^\dagger$  should be read as  $(Y_{n\pm}^\dagger)_\pm$  rather than  $(Y_\pm)^\dagger$ . The  $+$  denotes Wilson lines obtained from attachments to quarks, and the  $-$  denotes Wilson lines from attachments to antiquarks. The Wilson lines obtained for various situations are shown in Fig. 10.

The generation of the Wilson line  $Y_n$  from the example above motivates us to consider whether all the leading order usoft-collinear interactions within SCET<sub>I</sub> (to all orders in  $\alpha_s$  and with loop corrections) can be encoded through the non-local interactions contained in the Wilson line  $Y_n(x)$ . To show that this is indeed the case we consider the BPS field redefinitions [6]

$$\xi_{n,p}(x) = Y_n(x) \xi_{n,p}^{(0)}(x), \quad A_{n,p}^\mu(x) = Y_n(x) A_{n,p}^{(0)\mu}(x) Y_n^\dagger(x). \tag{6.6}$$

They include in addition  $c_{n,p}(x) = Y_n(x) c_{n,p}^{(0)} Y_n^\dagger(x)$  for the ghost field in any general covariant gauge.

The defining equation for  $Y_n$  implies the operator equation

$$Y_n^\dagger in \cdot D_{us} Y_n = in \cdot \partial. \tag{6.7}$$

Also because the label operator  $\bar{\text{P}}$  commutes with  $Y_n$  the redefinition on  $\bar{n} \cdot A_n$  in (6.6) implies that

$$W_n \rightarrow Y_n W_n^{(0)} Y_n^\dagger, \tag{6.8}$$

where  $W_n^{(0)}$  is built from  $\bar{n} \cdot A_n^{(0)}$  fields. Implementing these transformations into our leading collinear quark Lagrangian we find

$$\begin{aligned}
 \mathcal{L}_{n\xi}^{(0)} &= \bar{\xi}_{n,p'} \left( in \cdot D + i \not{D}_{n\perp} \frac{1}{i\bar{n} \cdot D_n} i \not{D}_{n\perp} \right) \frac{\not{n}}{2} \xi_{n,p} \\
 &= \bar{\xi}_{n,p'} \left( in \cdot D_{us} + gn \cdot A_{n,q} + (\not{\mathcal{P}}_\perp + g A_{n,q\perp}) W \frac{1}{\mathcal{P}} W^\dagger (\not{\mathcal{P}}_\perp + g A_{n,q\perp}) \right) \frac{\not{n}}{2} \xi_{n,p} \\
 &= \bar{\xi}_{n,p'}^{(0)} Y^\dagger \left( in \cdot D_{us} + g Y n \cdot A_{n,q}^{(0)} Y^\dagger \right. \\
 &\quad \left. + (\not{\mathcal{P}}_\perp + g Y A_{n,q\perp}^{(0)} Y^\dagger) Y W^{(0)} Y^\dagger \frac{1}{\mathcal{P}} Y W^{(0)\dagger} Y^\dagger (\not{\mathcal{P}}_\perp + g A_{n,q\perp}^{(0)}) \right) \frac{\not{n}}{2} Y \xi_{n,p}^{(0)} \\
 &= \bar{\xi}_{n,p'}^{(0)} \left( in \cdot \partial + gn \cdot A_{n,q}^{(0)} + (\not{\mathcal{P}}_\perp + g A_{n,q\perp}^{(0)}) W^{(0)} \frac{1}{\mathcal{P}} W^{(0)\dagger} (\not{\mathcal{P}}_\perp + g A_{n,q\perp}^{(0)}) \right) \frac{\not{n}}{2} \xi_{n,p}^{(0)}, \tag{6.9}
 \end{aligned}$$

where the last line is completely independent of the usoft gluon field. With similar steps we can easily show that the collinear gluon Lagrangian  $\mathcal{L}_{ng}^{(0)}$  in (4.55) also completely decouples from the  $n \cdot A_{us}$  usoft gluon field. In summary, we see that the usoft gluons have completely decoupled from collinear particles in the leading order collinear Lagrangian  $\mathcal{L}_n^{(0)} = \mathcal{L}_{n\xi}^{(0)} + \mathcal{L}_{ng}^{(0)}$  via

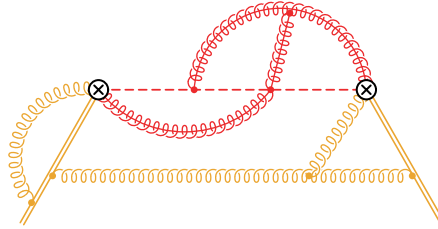
$$\mathcal{L}_n^{(0)}[\xi_{n,p}, A_{n,q}^\mu, n \cdot A_{us}] = \mathcal{L}_n^{(0)}[\xi_{n,p}^{(0)}, A_{n,q}^{(0)\mu}, 0]. \quad (6.10)$$

However, it is important to note that the usoft interactions for our collinear field have not disappeared, but have simply moved out of the Lagrangian and into the currents. We must make the field redefinition everywhere, including external operators and currents, as well as on interpolating fields for partons and hadrons. The field redefinition on the interpolating fields that describe incoming and outgoing states will determine whether the final usoft Wilson lines are  $Y_+$ ,  $Y_+^\dagger$ ,  $Y_-$ , or  $Y_-^\dagger$  since these interpolating field operators are localized either at  $-\infty$  or  $+\infty$ .

Eg.1: Consider our standard heavy-to-light current. Performing the field redefinitions we have

$$\begin{aligned} J^\mu &= \bar{\xi}_n W \Gamma^\mu h_v = \bar{\xi}_n^{(0)} Y_n^\dagger Y_n W^{(0)} Y_n^\dagger \Gamma^\mu h_v \\ &= \bar{\xi}_n^{(0)} W^{(0)} \Gamma^\mu Y_n^\dagger h_v. \end{aligned} \quad (6.11)$$

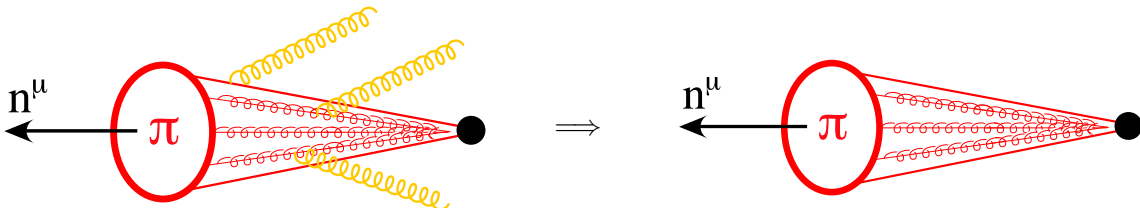
The last line gives us our first factorization result. Since  $\bar{\xi}_n$  is an outgoing quark, here  $Y_n^\dagger = Y_+^\dagger$ . As is necessary for effective theories, we will need to include a Wilson coefficient encoding higher energy dynamics, but we can already clearly see how different scales have separated into distinct gauge invariant quantities ( $\bar{\xi}_n^{(0)} W^{(0)}$ ) and  $(Y_n^\dagger h_v)$  at the level of operators. We can demonstrate this ultrasoft-collinear factorization diagrammatically by considering the time ordered product of two currents  $T J^\mu(x) J^{\dagger\nu}(0)$  (whose imaginary part is related to the inclusive decay rate). Rather than having diagrams with ultrasoft gluons coupling to collinear lines they decouple into distinct parts:



Eg.2: Consider a current that is a global color singlet within the  $n$ -collinear sector

$$J^\mu = (\bar{\xi}_n W) \Gamma^\mu W^\dagger \xi_n = (\bar{\xi}_n^{(0)} W^{(0)}) \Gamma^\mu (W^{(0)\dagger} \xi_n^{(0)}). \quad (6.12)$$

Here all the usoft gluons have cancelled using  $Y_n^\dagger Y_n = 1$ , so all the usoft gluons decouple at leading order. Diagrammatically we can imagine this current producing an energetic color singlet state like a collinear pion (ignoring the fact that we're in SCET<sub>I</sub> for a moment):





This decoupling is called color transparency, the long wavelength usoft gluons only see the overall color charge of the energetic fields in the pion, and hence cancel out for this color singlet object.

Eg.3: As a third example, consider our operator for  $e^+e^- \rightarrow$  dijets. Here we have two types of collinear fields,  $n_1$  and  $n_2$ , and the BPS field redefinitions give  $Y_{n_1}$  and  $Y_{n_2}$  ultrasoft Wilson lines:

$$J = (\bar{\xi}_{n_1} W_{n_1}) \Gamma(W_{n_2}^\dagger \xi_{n_2}) = (\bar{\xi}_{n_1}^{(0)} W_{n_1}^{(0)}) (Y_{n_1}^\dagger Y_{n_2}) \Gamma(W_{n_2}^{(0)\dagger} \xi_{n_2}^{(0)}). \quad (6.13)$$

This result involves the product of three factored sectors ( $n_1$ -collinear)(ultrasoft)( $n_2$ -collinear). Here the lines are both outgoing,  $Y_{n_1}^\dagger = Y_{n_1+}^\dagger$  and  $Y_{n_2} = Y_{n_2-}$ .

Remark: It is possible to formulate a gauge symmetry for the decoupled collinear fields via  $U_n^{(0)} = Y_n^\dagger(x) U_n(x) Y_n(x)$ , that then acts on the collinear (0) fields without ultrasoft components. However, there is not new content to this gauge symmetry beyond the ones we considered earlier.

## 6.2 Wilson Coefficients and Hard Factorization

As is standard in effective field theories, the high energy behavior of the theory is encoded in Wilson coefficients  $C$ . In SCET the Wilson coefficients can depend on the large momenta of collinear fields that are  $\mathcal{O}(\lambda^0)$ . Because of gauge symmetry the momenta appearing in  $C$  must be momenta for collinear gauge invariant products of fields. We can write  $C(\bar{\mathcal{P}}, \mu)$  where the large momenta is picked out by the label operator  $\bar{\mathcal{P}}$  which acts on these products of fields. For example, including this operator with our heavy-to-light current yields

$$(\bar{\xi}_n W_n) \Gamma^\mu h_v C(\bar{\mathcal{P}}^\dagger) = C(-\bar{\mathcal{P}}, \mu) (\bar{\xi}_n W_n) \Gamma^\mu h_v \quad (6.14)$$

(noting that  $\bar{\mathcal{P}}^\dagger > 0$  so we have picked a convenient sign). We have included parentheses around  $\bar{\xi}_n W_n$  because  $C(-\bar{\mathcal{P}}, \mu)$  must act on this product, since only the momentum of this combination is collinear gauge invariant. It is convenient to write this result as a convolution between a real number valued Wilson coefficient and an operator depending on a new label  $\omega$

$$\begin{aligned} (\bar{\xi}_n W) \Gamma^\mu h_v C(\bar{\mathcal{P}}^\dagger) &= \int d\omega C(\omega, \mu) [(\bar{\xi}_n W_n) \delta(\omega - \bar{\mathcal{P}}^\dagger) \Gamma^\mu h_v] \\ &= \int d\omega C(\omega, \mu) \mathcal{O}(\omega, \mu) \end{aligned} \quad (6.15)$$

where  $C(\omega, \mu)$  encodes the hard dynamics and  $\mathcal{O}(\omega, \mu)$  encodes the collinear and ultrasoft dynamics. Thus the hard dynamics is factorized from that of collinear fields, and this in general leads to convolutions since they both have  $\bar{n} \cdot p$  momenta that are  $\mathcal{O}(\lambda^0)$ .

We can show see that this hard-collinear factorization is a general result that can be applied to any SCET operator. Recall the following relations for  $W$

$$i\bar{n} \cdot D_n W_n = 0, \quad W_n^\dagger W_n = 1, \quad i\bar{n} \cdot D_n = W_n \bar{\mathcal{P}} W_n^\dagger, \quad 1/(i\bar{n} \cdot D_n) = W_n (1/\bar{\mathcal{P}}) W_n^\dagger. \quad (6.16)$$

These conditions imply the operator equations (for any integer  $k$ )

$$(i\bar{n} \cdot D_n)^k = W_n (\bar{\mathcal{P}})^k W_n^\dagger. \quad (6.17)$$

and we have for a general function  $f(\bar{\mathcal{P}})$  or  $f(i\bar{n} \cdot D_n)$

$$\begin{aligned} f(\bar{\mathcal{P}}) &= \int d\omega f(\omega) [\delta(\omega - \bar{\mathcal{P}})], \\ f(i\bar{n} \cdot D_n) &= W_n f(\bar{\mathcal{P}}) W_n^\dagger = \int d\omega f(\omega) [W \delta(\omega - \bar{\mathcal{P}}) W_n^\dagger]. \end{aligned} \quad (6.18)$$

If in general the hard dynamics leads to a function  $f$  of a large momentum  $\bar{\mathcal{P}}$ , then we have  $f(\bar{\mathcal{P}})$  if it acts on a  $n$ -collinear gauge invariant product of fields, and this relation shows that we can always represent this by a convolution of a Wilson coefficient  $f(\omega)$  which includes a  $\delta(\omega - \bar{\mathcal{P}})$  as part of the collinear operator. (If we act on fields that transform under a collinear gauge transformation then the same is true but with  $f(i\bar{n} \cdot D_n)$  and the extra Wilson lines are included in the operator.) For example, with our current for  $e^+e^- \rightarrow$  dijets we have

$$\int d\omega_1 d\omega_2 C(\omega_1, \omega_2) (\bar{\xi}_{n_1} W_{n_1}) \delta(\omega_1 - \bar{n}_1 \cdot \mathcal{P}^\dagger) \Gamma \delta(\omega_2 - \bar{n}_2 \cdot \mathcal{P}) (W_{n_2}^\dagger \xi_{n_2}). \quad (6.19)$$

Note that since the  $Y_n$  Wilson lines commute with  $\mathcal{P}^\mu$  we can perform the ultrasoft-collinear factorization by field redefinition after having determined the most general possible Wilson coefficient, and the results will be the same as we obtained prior to discussing Wilson coefficients. In general the function  $C(\omega_1, \omega_2)$  will be constrained by momentum conservation for the process under consideration, and any nontrivial dependence must be determined by matching calculations.

### 6.3 Operator Building Blocks

Our discussion of hard-collinear factorization in SCET in the previous section motivates setting up a more convenient notation for building operators out of products that are collinear gauge invariant. For the collinear quark field we define a “quark jet field” (SCET<sub>I</sub>) or “quark parton field” (SCET<sub>II</sub>)

$$\begin{aligned} \chi_n &\equiv W_n^\dagger \xi_n, \\ \chi_{n,\omega} &\equiv \delta(\omega - \bar{n} \cdot \mathcal{P}) (W_n^\dagger \xi_n), \end{aligned} \quad (6.20)$$

where the last expression has a definite  $\mathcal{O}(\lambda^0)$  momentum. With this notation our  $e^+e^- \rightarrow$  dijets operator becomes

$$\int d\omega_1 d\omega_2 C(\omega_1, \omega_2) \bar{\chi}_{n,\omega_1} \Gamma \chi_{n,\omega_2}. \quad (6.21)$$

For the gluon field we define a “gluon jet field” (SCET<sub>I</sub>) or “gluon parton field” (SCET<sub>II</sub>) as

$$\begin{aligned} \mathcal{B}_{n\perp}^\mu &\equiv \frac{1}{g} \left[ \frac{1}{\bar{n} \cdot \mathcal{P}} W_n^\dagger [i\bar{n} \cdot D_n, iD_{n\perp}^\mu] W_n \right], \\ \mathcal{B}_{n\perp,\omega}^\mu &= [\mathcal{B}_{n\perp}^\mu \delta(\omega - \bar{\mathcal{P}}^\dagger)], \end{aligned} \quad (6.22)$$

where the label operators and derivatives act only on the fields inside the outer square brackets. We can show that a complete basis of objects for building collinear operators at any order in  $\lambda$  is given by the three objects [14]

$$\chi_n, \quad \mathcal{B}_{n\perp}^\mu, \quad \mathcal{P}_{n\perp}^\mu. \quad (6.23)$$

Any other operators can be expressed in terms of these three objects. This basis is nice because the two gluon degrees of freedom in  $\mathcal{B}_{n\perp}^\mu$  can be taken as the physical polarizations. Indeed the expansion of  $\mathcal{B}_{n\perp}^\mu$  in terms of gluon fields yields

$$\mathcal{B}_{n\perp}^\mu = A_{n\perp}^\mu - \frac{q_\perp^\mu}{\bar{n} \cdot q} \bar{n} \cdot A_{n,q} + \dots, \quad (6.24)$$

where the ellipses denote terms with  $\geq 2$  collinear gluon fields. In addition to the building blocks in (6.23), operators will also of course involve functions of  $\bar{\mathcal{P}} = \bar{n} \cdot \mathcal{P}$  that appear as Wilson coefficients.

To see that Eq. (6.23) gives a complete basis we start by noting that the  $\perp$  covariant derivative is redundant. If we consider it sandwiched by Wilson lines, then

$$i\mathcal{D}_n^{\perp\mu} \equiv W_n^\dagger iD_{n\perp}^\mu W_n = \mathcal{P}_{n\perp}^\mu + g\mathcal{B}_{n\perp}^\mu. \quad (6.25)$$

To show this we manipulate the operator as follows

$$\begin{aligned} W_n^\dagger iD_{n\perp}^\mu W_n &= \mathcal{P}_{n\perp}^\mu + [W_n^\dagger iD_{n\perp}^\mu W_n] \\ &= \mathcal{P}_{n\perp}^\mu + \left[ \frac{1}{\bar{n} \cdot \mathcal{P}} \bar{n} \cdot \mathcal{P} W_n^\dagger iD_{n\perp}^\mu W_n \right] = \mathcal{P}_{n\perp}^\mu + \left[ \frac{1}{\bar{n} \cdot \mathcal{P}} W_n^\dagger i\bar{n} \cdot D_n iD_{n\perp}^\mu W_n \right] \\ &= \mathcal{P}_{n\perp}^\mu + \left[ \frac{1}{\bar{n} \cdot \mathcal{P}} W_n^\dagger [i\bar{n} \cdot D_n, iD_{n\perp}^\mu] W_n \right] = \mathcal{P}_{n\perp}^\mu + g\mathcal{B}_{n\perp}^\mu. \end{aligned} \quad (6.26)$$

The outer square brackets indicate that derivatives act only on objects inside. In the second line we used  $\bar{n} \cdot \mathcal{P} = W_n^\dagger i\bar{n} \cdot D_n W_n$ , and in the last line we used that fact that within the square brackets  $[i\bar{n} \cdot D_n W_n] = 0$  so that we could write the result as a commutator.

We can also remove  $in \cdot \partial$  derivatives by using the equations of motion for quarks and gluons. For instance the collinear quark equations of motion can be written as

$$in \cdot \partial \chi_n = -(gn \cdot \mathcal{B}_n) \chi_n - (i\mathcal{D}_n^\perp) \frac{1}{\bar{n} \cdot \mathcal{P}} (i\mathcal{D}_n^\perp) \chi_n, \quad (6.27)$$

where  $\mathcal{D}_{n\perp}^\mu$  is given in terms of basis objects by (6.25), and where

$$n \cdot \mathcal{B}_n \equiv \frac{1}{g} \left[ \frac{1}{\mathcal{P}} W_n^\dagger [i\bar{n} \cdot D_n, in \cdot D_n] W_n \right]. \quad (6.28)$$

The gluon equations motion allow us to eliminate  $n \cdot \mathcal{B}_n$  in terms of basis objects as

$$n \cdot \mathcal{B}_n = -\frac{2\mathcal{P}_{n\perp}^\nu}{\bar{n} \cdot \mathcal{P}} \mathcal{B}_\nu^{n\perp} + \frac{2}{\bar{n} \cdot \mathcal{P}} g^2 T^A \sum_f [\bar{\chi}_n^f T^A \not{n} \chi_n^f] + \dots, \quad (6.29)$$

where the ellipses denote a term that involves two  $\mathcal{B}_{n\perp}$ s. The gluon equation of motion also allow us to eliminate  $in \cdot \partial \mathcal{B}_{n\perp}^\mu$  in terms of the basic building blocks, much like for the quark term. Finally, objects like  $g\mathcal{B}_{\perp\perp}^{\mu\nu} \equiv [1/(\bar{n} \cdot \mathcal{P}) W^\dagger [iD_{n\perp}^\mu, iD_{n\perp}^\nu] W]$  and  $g\mathcal{B}_{\perp 2}^\mu \equiv [1/(\bar{n} \cdot \mathcal{P}) W^\dagger [iD_{n\perp}^\mu, in \cdot D_n] W]$  can again be eliminated in terms of the building blocks with manipulations similar to those in (6.26), and with the use of (6.29).

We do still need all of the original ultrasoft fields and operators, including ultrasoft covariant derivatives and field strengths. The ultrasoft equations of motion (equivalent to the QCD equations of motion) can be used to reduce the basis for these operators. It is worth remarking about the connections between our building blocks in Eq. (6.23) and the ultrasoft operators that come from RPI and gauge covariance. Multiplying the identities in (5.32) with Wilson lines on both sides we find

$$\begin{aligned} iW_n^\dagger iD_\perp^\mu W_n &= iD_{n\perp}^\mu + iD_{\text{us}\perp}^\mu = \mathcal{P}_{n\perp}^\mu + g\mathcal{B}_{n\perp}^\mu + iD_{\text{us}\perp}^\mu, \\ iW_n^\dagger i\bar{n} \cdot D W_n &= \bar{n} \cdot \mathcal{P} + i\bar{n} \cdot D_{\text{us}}^\mu. \end{aligned} \quad (6.30)$$

Thus factors of  $\mathcal{P}_{n\perp}^\mu$  and  $\bar{n} \cdot \mathcal{P}$  that appear in operators will be connected to higher order operators with these ultrasoft covariant derivatives.

## 7 Wilson Coefficients and Hard Dynamics

We now turn to the dynamics of SCET at one loop. An interesting aspect of loops in the effective theory is that often a full QCD loop graph has more than one counterpart with similar topology in SCET. We will compare the SCET one loop calculation for a single hard interaction current with the one loop calculation in QCD. Our goal is to understand the IR and UV divergences in SCET and the corresponding logarithms, as well as understanding how the terms not associated to divergences are treated.

In our analysis we will use the same regulator for infrared divergences, and show that the IR divergences in QCD and SCET exactly agree, which is a validation check on the EFT. The difference determines the Wilson coefficient for the SCET operator that encodes the hard dynamics. This matching result is independent of the choice of infrared regulator as long as the same regulator is used in the full and effective theories. Finally, the SCET calculation contains additional UV divergences, beyond those in full QCD, and the renormalization and anomalous dimension determined from these divergences will sum up double Sudakov logarithms.

We will give two examples of matching QCD onto SCET, the  $b \rightarrow s\gamma$  transition, and  $e^+e^- \rightarrow 2$ -jets. The first example has the advantage of involving only one collinear sector, but the disadvantage of requiring some familiarity with Heavy Quark Effective theory for the treatment of the  $b$  quark and involving contributions from two Dirac structures. The second example only involves jets with a single Dirac structure, but has two collinear sectors. In both cases we will use Feynman gauge for all gluons, and dimensional regularization with  $d = 4 - 2\epsilon$  for all UV divergences (denoting them as  $1/\epsilon$ ). To regulate the IR divergences we will take the strange quark offshell,  $p^2 \neq 0$ . For IR divergences associated purely with the heavy quark we will use dimensional regularization (denoting them  $1/\epsilon_{\text{IR}}$  to distinguish from the UV divergences).

### 7.1 $b \rightarrow s\gamma$ , SCET Loops and Divergences

As a 1-loop example consider the heavy-to-light currents for  $b \rightarrow s\gamma$ . Although there are several operators in the full electroweak Hamiltonian, for simplicity we will just consider the dominant dipole operator  $J_{\mu\nu}^{\text{QCD}} F^{\mu\nu}$  where  $F_{\mu\nu}$  is the photon field strength and the quark tensor current is

$$J^{\text{QCD}} = \bar{s} \Gamma b, \quad \Gamma = \sigma^{\mu\nu} P_R. \quad (7.1)$$

In SCET the corresponding current (for the original Lagrangian, prior to making the  $Y_n$  field redefinition) was

$$J^{\text{SCET}} = (\bar{\xi}_n W) \Gamma h_v C(v \cdot n \bar{\mathcal{P}}^\dagger) = \int d\omega C(\omega) \bar{\chi}_{n,\omega} \Gamma h_v. \quad (7.2)$$

In general because of the presence of the vectors  $v^\mu$  and  $n^\mu$  there can be a larger basis of Dirac structures  $\Gamma$  for the SCET current (we will see below that at one-loop there are in fact two non-zero structures for the SCET tensor current). Note that the factor of  $v \cdot n$  makes it clear that the current preserves type-III RPI. We will set  $v \cdot n = 1$  in the following.

Together with the QCD and (leading order) SCET Lagrangians, we can carry out loop calculations with these two currents. First lets consider loop corrections in QCD. We have a wavefunction renormalization graph for the heavy quark denoted  $b$ , and one for the massless (strange) quark denoted  $q$ :



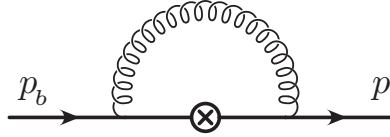
This gives the wavefunction renormalization factors  $Z_{\psi_b}$  and  $Z_\psi$  respectively. In the ‘‘on-shell’’ scheme which includes both the UV divergences and the finite residues these  $Z$ -factors are

$$\begin{aligned} Z_{\psi_b} &= 1 - \frac{\alpha_s C_F}{4\pi} \left[ \frac{1}{\epsilon} + \frac{2}{\epsilon_{\text{IR}}} + 3 \ln \frac{\mu^2}{m_b^2} + 4 \right], \\ Z_\psi &= 1 - \frac{\alpha_s C_F}{4\pi} \left[ \frac{1}{\epsilon} - \ln \frac{-p^2}{\mu^2} + 1 \right]. \end{aligned} \quad (7.3)$$

(If one instead uses  $\overline{\text{MS}}$  for the wavefunction renormalization factors, then the finite residues still show up in the final result for the S-matrix element due to the LSZ formula.) The remaining diagram is a vertex graph for the tensor current  $J^{\text{QCD}}$ . At tree level the matrix element gives

$$V_{\text{qcd}}^0 = \bar{u}_s(p) P_R i\sigma^{\mu\nu} u_b(p_b) \quad (7.4)$$

while the one-loop diagram



gives

$$\begin{aligned} V_{\text{qcd}}^1 &= -\frac{\alpha_s C_F}{4\pi} \left[ \ln^2 \left( \frac{-p^2}{m_b^2} \right) + 2 \ln \left( \frac{-p^2}{m_b^2} \right) - \frac{2}{\epsilon} + \frac{1}{2} \ln \left( \frac{-p^2}{\mu^2} \right) + 2 \ln \frac{\mu}{\omega} - 3 \ln \frac{\mu}{m_b} + f_1(1 - \hat{q}^2) \right] \bar{u}_s P_R i\sigma^{\mu\nu} u_b \\ &+ \frac{\alpha_s C_F}{4\pi} f_2(1 - \hat{q}^2) \bar{u}_s P_R \left( \frac{p^\mu \gamma^\nu - p^\nu \gamma^\mu}{m_b} \right) u_b, \end{aligned} \quad (7.5)$$

where we have kept  $p^2 \neq 0$  only for the IR singularities, and set it to zero whenever it is not needed to regulate an IR divergence. The variable  $\hat{q}^2 = (p_b - p)^2/m_b^2 = 1 - 2p_b \cdot p/m_b^2$  and the functions appearing in Eq. (7.5) are

$$f_1(x) = \ln(x) + \frac{2}{(1-x)} \ln(x) + 2\text{Li}_2(1-x) + \pi^2, \quad f_2(x) = \frac{4}{(1-x)} \ln(x). \quad (7.6)$$

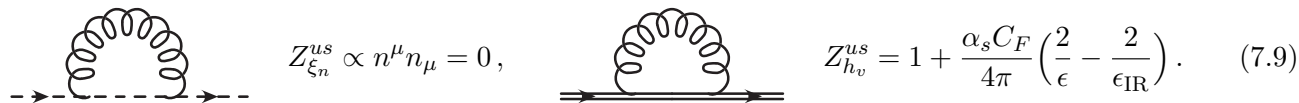
Unlike for the conserved vector current, in QCD for the tensor current the sum of vertex and wavefunction graphs still contains a  $1/\epsilon$  UV divergence. Hence this QCD local current operator requires an additional counterterm not related to strong coupling renormalization, and it is given by

$$Z_{\text{tensor}} = 1 + \frac{\alpha_s C_F}{4\pi} \frac{1}{\epsilon}. \quad (7.7)$$

Adding together the QCD vertex graph and the contributions from the three  $Z$ 's, and replacing the kinematic variable  $\hat{q}^2 = 1 - \bar{n} \cdot p/m_b = 1 - \omega/m_b$ , the sum gives

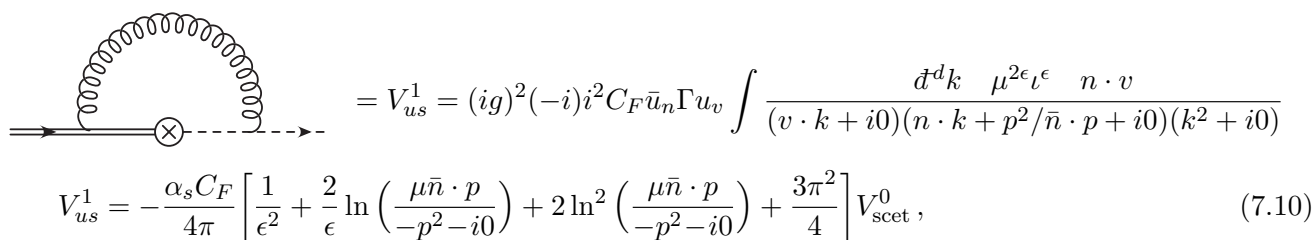
$$\begin{aligned} \text{QCD Sum} &= V_{\text{qcd}}^1 + \left[ \frac{1}{2}(Z_{\psi_b} - 1) + \frac{1}{2}(Z_\psi - 1) + (Z_{\text{tensor}}^{-1} - 1) \right] V_{\text{qcd}}^0 \\ &= -\bar{u}_s \Gamma u_b \frac{\alpha_s C_F}{4\pi} \left[ \ln^2 \left( \frac{-p^2}{\omega^2} \right) + \frac{3}{2} \ln \left( \frac{-p^2}{\omega^2} \right) + \frac{1}{\epsilon_{\text{IR}}} + \ln \left( \frac{\mu^2}{\omega^2} \right) + f_1 \left( \frac{\omega}{m_b} \right) + \frac{5}{2} \right] \\ &+ \frac{\alpha_s C_F}{4\pi} f_2 \left( \frac{\omega}{m_b} \right) \bar{u}_s P_R \left( \frac{p^\mu \gamma^\nu - p^\nu \gamma^\mu}{m_b} \right) u_b, \end{aligned} \quad (7.8)$$

Next consider the ultrasoft loops in SCET. In Feynman gauge the ultrasoft wavefunction renormalization of the collinear quark vanishes, since the couplings are both proportional to  $n^\mu$ , and  $n^2 = 0$ . The ultrasoft wavefunction renormalization of the heavy quark is just the HQET wavefunction renormalization. We summarize these two results as:



$$Z_{\xi_n}^{us} \propto n^\mu n_\mu = 0, \quad Z_{h_v}^{us} = 1 + \frac{\alpha_s C_F}{4\pi} \left( \frac{2}{\epsilon} - \frac{2}{\epsilon_{\text{IR}}} \right). \quad (7.9)$$

We can already note that the  $1/\epsilon_{\text{IR}}$  pole in  $Z_{h_v}^{us}$  matches up with the IR pole in  $Z_{\psi_b}$  in full QCD (and this is the only IR divergence that we are regulating with dimensional regularization). In addition to wavefunction renormalization there is an ultrasoft vertex diagram for the SCET current. Using the on-shell condition  $v \cdot p_b = 0$  for the incoming  $b$ -quark, and the SCET propagator from Eq. (4.43) for a line with injected ultrasoft momentum, we have



$$V_{us}^1 = (ig)^2 (-i) i^2 C_F \bar{u}_n \Gamma u_v \int \frac{d^d k \mu^{2\epsilon} \iota^\epsilon n \cdot v}{(v \cdot k + i0)(n \cdot k + p^2/\bar{n} \cdot p + i0)(k^2 + i0)}$$

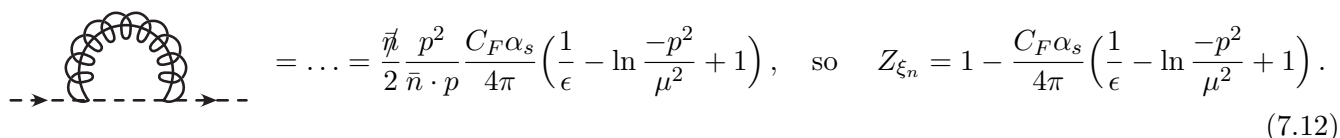
$$V_{us}^1 = -\frac{\alpha_s C_F}{4\pi} \left[ \frac{1}{\epsilon^2} + \frac{2}{\epsilon} \ln \left( \frac{\mu \bar{n} \cdot p}{-p^2 - i0} \right) + 2 \ln^2 \left( \frac{\mu \bar{n} \cdot p}{-p^2 - i0} \right) + \frac{3\pi^2}{4} \right] V_{\text{sct}}^0, \quad (7.10)$$

where the tree level SCET amplitude is

$$V_{\text{sct}}^0 = \bar{u}_n \Gamma u_v, \quad (7.11)$$

and  $\iota^\epsilon = (4\pi)^{-\epsilon} e^{\epsilon\gamma_E}$  ensures that the scale  $\mu$  has the appropriate normalization for the  $\overline{\text{MS}}$  scheme. Note that this graph is independent of the current's Dirac structure  $\Gamma$ . On the heavy quark side the heavy-quark propagator gives a  $P_v = (1 + \not{v})/2$ , but this commutes with the HQET vertex Feynman rule and hence yields a projector on the HQET spinor,  $P_v u_v = u_v$ . On the light quark side the propagator gives a  $\not{v}/2$  and the vertex gives a  $\not{v}/2$  to yield the projector  $P_n = (\not{v}\not{\bar{n}})/4$  acting on the light-quark spinor,  $P_n u_n = u_n$ . Hence whatever  $\Gamma$  is inserted at the current vertex is also the Dirac structure that appears between spinors in the answer for the loop graph. For this heavy-to-light current this feature is actually true for all loop diagrams in SCET, the spin structure of the current is preserved by loops diagrams in the EFT. For ultrasoft diagrams it happens by a simple generalization of the arguments above, while for collinear diagrams the interactions only appear on the collinear quark side of the  $\Gamma$ , so we just need to know that they do not induce additional Dirac matrices. (This is ensured by chirality conservation in the EFT.)

Lets finally consider the one loop diagrams with a collinear gluon. There is no wavefunction renormalization diagram for the heavy quark, since the collinear gluon does not couple to it. There is a wavefunction renormalization graph for the light-collinear quark



$$= \dots = \frac{\not{v} p^2}{2 \bar{n} \cdot p} \frac{C_F \alpha_s}{4\pi} \left( \frac{1}{\epsilon} - \ln \frac{-p^2}{\mu^2} + 1 \right), \quad \text{so} \quad Z_{\xi_n} = 1 - \frac{C_F \alpha_s}{4\pi} \left( \frac{1}{\epsilon} - \ln \frac{-p^2}{\mu^2} + 1 \right). \quad (7.12)$$

We have not written out the SCET loop integrand, but it follows in a straightforward manner from using the collinear quark and gluon propagators and vertex Feynman rules from Fig. (6). Note that the result for  $Z_{\xi_n}$  is the same as the full theory  $Z_\psi$ . This occurs because for the wavefunction graph there is no connection

to the ultrasoft modes or the hard production vertex, and by itself a single collinear sector is just a boosted version of full QCD (and  $Z_\psi$  is independent of this boost). There are also no subtleties related to zero-bin subtractions for this graph (the subtraction integrands are power suppressed and therefore the subtraction vanishes). There is also a diagram generated by the two-quark two-gluon Feynman rule, but this tadpole type diagram vanishes with our choice of regulators. There is also a tadpole type diagram where two gluons are taken out of the Wilson lines in the vertex, which also vanishes, ie.

$$= 0, \quad = 0. \quad (7.13)$$

The last diagram we must consider is the collinear vertex graph with an attachment from the Wilson line going to the collinear quark propagator,

$$= V_n^1 = -ig^2 C_F \bar{u}_n \Gamma u_v \mu^{2\epsilon} \ell^\epsilon \sum_{\substack{k_\ell \neq 0 \\ k_\ell \neq -p_\ell}} \int \frac{d^d k_r}{(\bar{n} \cdot k_\ell)(k^2)(k+p)^2}$$

$$= -ig^2 C_F \bar{u}_n \Gamma u_v \hat{V}_n^1. \quad (7.14)$$

Here each momentum has been split into label and residual components  $k = (k_\ell^\mu, k_r^\mu)$  and  $p = (p_\ell^\mu, p_r^\mu)$ . There are no +-momenta in the label components, and the only residual component for the external  $p$  is its +-momentum. For reasons that will soon become apparent, we have used a short hand notation for the relativistic collinear gluon and quark propagators, which in fact contain a mixture of label and residual momenta,

$$k^2 = k_r^+ k_\ell^- - \vec{k}_\ell^\perp{}^2, \quad (k+p)^2 = (k_r^+ + p_r^+)(k_\ell^- + p_\ell^-) - (\vec{k}_\ell^\perp + \vec{p}_\ell^\perp)^2, \quad (7.15)$$

and are homogeneous in the power counting with  $k^2 \sim p^2 \sim \lambda^2$ . We have also introduced the notation with a hat,  $\hat{V}_n^1$ , for the collinear loop integrand.

In general in collinear loop integrals there can be a nontrivial interplay between the Wilson coefficients and the large collinear loop integration, because both depend on a momentum that is the same size in the power counting, namely the large minus momenta,  $k^- \sim Q$ . When matching at one-loop,  $\mathcal{O}(\alpha_s)$ , in some cases the tree level hard matching coefficient we insert might be independent of the loop momentum  $k^-$ . In this case we can insert it back into the calculation only at the end. Even in this case it must be included when considering the renormalization group evolution, because the sharing of large momenta can lead to convolutions in the RG evolution equations. We will meet an example of this type later on when we discuss the running of parton distributions for a collinear proton. For our example of the heavy-to-light current for  $b \rightarrow s\gamma$ , things are actually simple for a different reason. The SCET operator in Eq. (7.2) contains only a single gauge invariant product of collinear fields,  $(\bar{\xi}_n W)$ , and the Wilson coefficient only depends on the overall outgoing momentum of this product. Therefore if we include a coefficient into our diagram in Eq. (7.14) it gives only dependence on the total external momentum

$$C[\bar{n} \cdot (p+k) + \bar{n} \cdot (-k)] = C(\bar{n} \cdot p). \quad (7.16)$$

This result remains true for collinear loop diagrams at higher orders, so the coefficient can always be treated as multiplicative for this current, and the coefficient is always evaluated with the total --momentum

of the collinear jet, which in this case is  $\bar{n} \cdot p = m_b$ . Indeed, even when we have collinear fields for multiple directions, the large momenta are still fixed by the external kinematics *as long as we have only one (gauge invariant product of) collinear fields in each direction*. In this case the Wilson coefficient for the hard dynamics remains multiplicative in momentum space. (And we remark that this is the case that is predominantly studied for amplitudes for LHC processes with an exclusive number of jets. In general the coefficient will still be a matrix in color space once we have enough colored particles to give more than one possibility for making an overall color singlet (4 particles). There is only one possibility for the current example and hence no matrix in color space.) When we have more than one block of gauge invariant collinear fields in the same collinear direction then this will no longer be true, there will be momentum convolutions between the hard coefficient  $C$  and the collinear parts of the SCET operator.

To perform the collinear loop integration in Eq. (7.14) we should follow the rules from section 4.5 on combining label and residual momenta. As a first pass we will ignore the 0-bin restrictions  $k_\ell \neq 0, -p_\ell$ . In this case we can apply the simple rule from Eq. (4.60). Results following this rule in SCET<sub>I</sub> are often called the naive collinear integrals. Since only momenta of external collinear particles appear in the loop integrand the multipole expansion is trivial for this integral, and this gives the same result that we would have obtained by ignoring the split into label and residual momenta from the start:

$$\begin{aligned} \hat{V}_n^{1 \text{ naive}} &= \mu^{2\epsilon} \ell^\epsilon \int \frac{\bar{d}^d k (n \cdot \bar{n})(\bar{n} \cdot (p+k))}{(\bar{n} \cdot k) k^2 (k+p)^2} \\ &= \frac{i}{(4\pi)^2} \left[ \frac{2}{\epsilon^2} + \frac{2}{\epsilon} + \frac{2}{\epsilon} \ln \left( \frac{\mu^2}{-p^2} \right) + \ln^2 \left( \frac{\mu^2}{-p^2} \right) + 2 \ln \left( \frac{\mu^2}{-p^2} \right) + 4 - \frac{\pi^2}{6} \right]. \end{aligned} \quad (7.17)$$

This result for the loop integral can be obtained either with standard Feynman parameter rules or by contour integration in  $k^+$  or  $k^-$ . Feynman parameter tricks and other equations that are useful for doing loop integrals in SCET are summarized in Appendix E.

Having assembled results for all the SCET loop graphs we can now add them up to obtain the bare SCET result

$$\text{Sum SCET} = V_{us}^1 + V_n^1 + \left[ \frac{1}{2}(Z_{h_v}^{us} - 1) + \frac{1}{2}(Z_{\xi_n} - 1) \right] V_{\text{scet}}^0, \quad (7.18)$$

and then compare with the full QCD calculation, setting the renormalized coupling  $g^2 = 4\pi\alpha_s(\mu)$ . For the moment we still will label our SCET result as naive since it ignores the 0-bin restrictions. If we examine the IR divergences encoded in the  $\ln(-p^2)$  factors (and the  $1/\epsilon_{\text{IR}}$  from the heavy quark wavefunction renormalization) then we find for  $\Gamma = P_R i\sigma^{\mu\nu}$  that at leading order  $V_{\text{qcd}}^0 = V_{\text{scet}}^0$  and

$$\begin{aligned} (\text{Sum QCD})^{\text{ren}} &= -\frac{\alpha_s C_F}{4\pi} \left[ \ln^2 \left( \frac{-p^2}{m_b^2} \right) + \frac{3}{2} \ln \left( \frac{-p^2}{m_b^2} \right) + \frac{1}{\epsilon_{\text{IR}}} + \dots \right] V_{\text{scet}}^0 + \dots, \\ (\text{Sum SCET})^{\text{naive}} &= -\frac{\alpha_s C_F}{4\pi} \left[ \ln^2 \left( \frac{-p^2}{m_b^2} \right) + \frac{3}{2} \ln \left( \frac{-p^2}{m_b^2} \right) + \frac{1}{\epsilon_{\text{IR}}} - \frac{1}{\epsilon^2} - \frac{5}{2\epsilon} - \frac{2}{\epsilon} \ln \left( \frac{\mu}{m_b} \right) + \dots \right] V_{\text{scet}}^0. \end{aligned} \quad (7.19)$$

Thus the results match up in the IR (as long as the remaining  $1/\epsilon$  terms in the SCET result can be interpreted as UV divergences). To obtain this result for the sum of the SCET diagrams there is an important cancellation between the collinear and ultrasoft diagrams,  $\ln(-p^2/\mu^2)/\epsilon - \ln[-p^2/(\mu\bar{n} \cdot p)]/\epsilon = \ln(\bar{n} \cdot p/\mu)/\epsilon = -\ln(\mu/m_b)/\epsilon$ . The cancellation of the  $\ln(-p^2)$  dependence in this  $1/\epsilon$  pole is crucial both to match the IR divergences correctly in QCD, and in order for the remaining  $1/\epsilon$  pole to possibly have an ultraviolet interpretation. The remaining  $\mu$  dependence on  $\bar{n} \cdot p = m_b$  in the  $1/\epsilon$  pole is fine because this



is the large momentum that the Wilson coefficient anyway depends on. This same cancellation also has a reflection in the double logarithms where the  $\ln(\mu^2)$  dependence cancels out from the  $\ln^2(-p^2)$  dependent term. Again this cancellation is important for the matching of IR divergences with the full theory.

The final catch is related to our use of the naive collinear integrand is the interpretation of the  $1/\epsilon$  poles from the collinear loop integral. The  $1/\epsilon$  divergences from the ultrasoft vertex diagram are clearly determined to be of UV origin (from large euclidean momenta or large light-like momenta). However in the collinear vertex diagram with the naive integral one of the divergences actually comes from  $\bar{n} \cdot k \rightarrow 0$ , and hence is of IR origin. This IR region is actually already correctly accounted for by the ultrasoft diagram where the heavy quark propagator is time-like,  $v \cdot k + i0$ , as it should be in the infrared region. In this region the original propagator does not behave like  $\bar{n} \cdot k$ . The  $\bar{n} \cdot k$  term which comes from the collinear Wilson line  $W$  is instead the appropriate approximation for large  $\bar{n} \cdot k$ , rather than small  $\bar{n} \cdot k$ . Thus the issue with the naive collinear loop integral for the vertex diagram is that it double counts an IR region accounted for by the ultrasoft diagram. This double accounting is removed once we properly consider the 0-bin subtraction contributions. Therefore we apply now the rule with the 0-bin subtractions  $k_\ell \neq 0, -p_\ell$  using Eq.(4.64) to obtain

$$\hat{V}_n^1 = \mu^{2\epsilon} \int \bar{d}^d k \left[ \frac{(n \cdot \bar{n}) \bar{n} \cdot (p+k)}{(\bar{n} \cdot k) k^2 (k+p)^2} - \frac{(n \cdot \bar{n}) \bar{n} \cdot p}{(\bar{n} \cdot k) k^2 (\bar{n} \cdot p n \cdot k + p^2)} \right] = \hat{V}_n^{1,\text{naive}} - \hat{V}_n^{1,0\text{bin}}. \quad (7.20)$$

It is easy to see where the 0-bin integrand comes from because it can be obtained from the appropriate ultrasoft scaling limit of the naive collinear integrand. For  $k_\ell \neq 0$  we have a subtraction for the region  $k_\ell \sim \lambda^2$  where we only keep terms up to those scaling as  $\lambda^{-8}$ , which gives precisely the integrand in Eq. (7.20) denoted as  $\hat{V}_n^{1,0\text{bin}}$ . The terms with  $n \cdot k$  and  $\bar{n} \cdot k$  in the denominator count as  $\lambda^2$ , while the term with  $k^2 \sim \lambda^4$  to give the eight powers that compensate the  $d^d k \sim \lambda^8$  for the subtraction. Note that we have kept the offshellness  $0 \neq p^2 \sim \lambda^2$  since it is the same order as the  $(\bar{n} \cdot p)(n \cdot k)$  term. The other subtraction is  $k_\ell \neq -p_\ell$  so we have the subtraction region  $k_\ell + p_\ell \sim \lambda^2$ . For this case one of the factors in the denominator is  $\bar{n} \cdot k \rightarrow -\bar{n} \cdot p \sim \lambda^0$  (and there is suppression from the numerator as well) so there is no contribution at  $\mathcal{O}(\lambda^{-8})$ .

Being more careful about the UV ( $1/\epsilon$ ) and IR ( $1/\epsilon_{\text{IR}}$ ) divergences we find

$$\begin{aligned} \hat{V}_n^{1,\text{naive}} &= \frac{i}{(4\pi)^2} \left[ \frac{2}{\epsilon_{\text{IR}} \epsilon} + \frac{2}{\epsilon} + \frac{2}{\epsilon_{\text{IR}}} \ln \frac{\mu^2}{-p^2} + \left( \frac{2}{\epsilon} - \frac{2}{\epsilon_{\text{IR}}} \right) \ln \frac{\mu}{\bar{n} \cdot p} + \ln^2 \frac{\mu^2}{-p^2} + 2 \ln \frac{\mu^2}{-p^2} + 4 - \frac{\pi^2}{6} \right], \\ \hat{V}_n^{1,0\text{bin}} &= \frac{i}{(4\pi)^2} \left[ \frac{2}{\epsilon} - \frac{2}{\epsilon_{\text{IR}}} \right] \left[ \frac{1}{\epsilon} + \ln \frac{\mu^2}{-p^2} - \ln \frac{\mu}{\bar{n} \cdot p} \right], \\ V_n^1 &= \frac{\alpha_s C_F}{4\pi} \left[ \frac{2}{\epsilon^2} + \frac{2}{\epsilon} + \frac{2}{\epsilon} \ln \left( \frac{\mu^2}{-p^2} \right) + \ln^2 \left( \frac{\mu^2}{-p^2} \right) + 2 \ln \left( \frac{\mu^2}{-p^2} \right) + 4 - \frac{\pi^2}{6} \right]. \end{aligned} \quad (7.21)$$

So we see that the subtraction cancels the  $\bar{n} \cdot q \rightarrow 0$  IR singularities  $1/\epsilon_{\text{IR}}$  in the first line. The UV divergences arising from  $\bar{n} \cdot q \rightarrow \infty$  are independent of the IR regulator and just depend on the UV regulator  $\epsilon$ . Since the 0-bin contribution is scaleless with our choice of regulators, taking  $\epsilon_{\text{IR}} = \epsilon$  and ignoring this subtraction would give us the correct answer. Nevertheless, even with this regulator the 0-bin contribution is still important to obtain the correct physical interpretation for the divergences.<sup>6</sup>

Since the final result after subtracting the 0-bin contribution is the same as in Eq. (7.17) with the  $1/\epsilon$  poles all now known to be UV, we can determine the appropriate UV counterterm to renormalize the SCET current. Defining

$$C^{\text{bare}}(\omega, \epsilon) = Z_C(\mu, \omega, \epsilon) C(\mu, \omega) = C + (Z_C - 1)C, \quad (7.22)$$

<sup>6</sup>For other less inclusive calculations or for other choices of regulators (such as  $\Omega_\perp^2 \leq \vec{k}_\perp^2 \leq \Lambda_\perp^2$ ,  $\Omega_\perp^2 \leq (k^-)^2 \leq \Lambda_\perp^2$ ) the subtractions are even more crucial to obtain the correct result and have the UV divergences independent of the IR regulator.

and adding the counterterm graph with  $(Z_C - 1)C$  to cancel the  $1/\epsilon$  poles in  $\overline{\text{MS}}$  gives

$$Z_C(\mu, \omega, \epsilon) = 1 - \frac{C_F \alpha_s(\mu)}{4\pi} \left( \frac{1}{\epsilon^2} + \frac{1}{\epsilon} \ln \frac{\mu^2}{\omega^2} + \frac{5}{2\epsilon} \right) + \mathcal{O}(\alpha_s^2). \quad (7.23)$$

(Where by momentum conservation  $\omega = m_b$ .) We can now add up the collinear and ultrasoft loop graphs to obtain the final renormalized SCET result, and compare with the renormalized QCD result

$$\begin{aligned} (\text{Sum QCD})^{\text{ren}} &= -\frac{\alpha_s C_F}{4\pi} \left[ \frac{1}{\epsilon_{\text{IR}}} + \ln^2 \left( \frac{-p^2}{\omega^2} \right) + \frac{3}{2} \ln \left( \frac{-p^2}{\omega^2} \right) + 2 \ln \left( \frac{\mu}{\omega} \right) + f_1 \left( \frac{\omega}{m_b} \right) + \frac{5}{2} \right] V_{\text{scet}}^0 \\ &\quad + \frac{\alpha_s C_F}{4\pi} f_2 \left( \frac{\omega}{m_b} \right) \bar{u}_s P_R \left( \frac{p^\mu \gamma^\nu - p^\nu \gamma^\mu}{m_b} \right) u_b, \\ (\text{Sum SCET})^{\text{ren}} &= V_{us}^1 + V_n^1 + \left[ \frac{1}{2} (Z_{hv}^{us} - 1) + \frac{1}{2} (Z_{\xi_n} - 1) + (Z_C - 1) \right] V_{\text{scet}}^0 \\ &= -\frac{\alpha_s C_F}{4\pi} \left[ \frac{1}{\epsilon_{\text{IR}}} + \ln^2 \left( \frac{-p^2}{\omega^2} \right) + \frac{3}{2} \ln \left( \frac{-p^2}{\mu^2} \right) - 2 \ln^2 \left( \frac{\mu}{\omega} \right) + \frac{11\pi^2}{12} - \frac{7}{2} \right] V_{\text{scet}}^0. \end{aligned} \quad (7.24)$$

From these two results we see that the renormalized QCD and SCET have the same infrared divergences. The difference of these results is determined by ultraviolet physics and determines the one-loop matching result for the  $\overline{\text{MS}}$  Wilson coefficients  $C_1(\mu, \omega, m_b)$  and  $C_2(\mu, \omega, m_b)$  that multiply the SCET operator in Eq. (7.2) for the Dirac structures  $\Gamma = \Gamma_1 = P_R i \sigma^{\mu\nu}$  and  $\Gamma = \Gamma_2 = P_R (n^\mu \gamma_\perp^\nu - n^\nu \gamma_\perp^\mu)$  respectively. Only the Dirac structure  $\Gamma_1$  was present at tree-level, while  $\Gamma_2$  is generated at one-loop. Taking the difference of the above two results and simplifying we find

$$\begin{aligned} C_1(\mu, \omega, m_b) &= 1 - \frac{C_F \alpha_s(\mu)}{4\pi} \left[ 2 \ln^2 \left( \frac{\mu}{\omega} \right) + 5 \ln \left( \frac{\mu}{\omega} \right) + f_1 \left( \frac{\omega}{m_b} \right) - \frac{11\pi^2}{12} + 6 \right], \\ C_2(\mu, \omega, m_b) &= \frac{C_F \alpha_s(\mu)}{4\pi} \frac{\omega}{2m_b} f_2 \left( \frac{\omega}{m_b} \right). \end{aligned} \quad (7.25)$$

## 7.2 $e^+e^- \rightarrow 2\text{-jets}$ , SCET Loops

In this section we perform the matching from QCD onto SCET for the process  $e^+e^- \rightarrow 2\text{-jets}$ . This matching will be independent of the details of the kinematical constraints that are used to enforce that we really are restricting ourselves to have only 2 jets in the final state, which will all be contained in the long distance dynamics of the effective theory. Indeed, the fact that we can successfully carry out this matching at the amplitude level makes it clear that it does not depend on which constraints we put on the phase space of the 2-jet final state. Once again, it will also be independent of the choice of IR regulator as long as the same regulator is used in both the QCD and SCET calculations. We will use Feynman gauge in both QCD and SCET, and take  $d = 4 - 2\epsilon$  to regulate UV divergences and offshellness for the quark and antiquark,  $p_q^2 = p_{\bar{q}}^2 = p^2 \neq 0$ , to regulate all IR divergences.

In full QCD, the production of hadrons in  $e^+e^-$  collisions occurs via an s-channel exchange of a virtual photon or a  $Z$  boson. The coupling is either via a vector or an axial vector current and is therefore given by

$$J^{\text{QCD}} = \bar{q} \Gamma_i q, \quad \Gamma_V = g_V \gamma^\mu, \quad \Gamma_A = g_A \gamma^\mu \gamma^5, \quad (7.26)$$

where  $g_{V,A}$  contain the electroweak couplings for the photon or  $Z$ -boson (for a virtual photon  $g_V = e_q$  the electromagnetic charge of the quark  $q$ , and  $g_A = 0$ ). In SCET the current involves collinear quarks in the

back-to-back  $n$  and  $\bar{n}$  directions

$$J^{\text{SCET}} = (\bar{\xi}_{\bar{n}} W_{\bar{n}}) \Gamma_i C(\mathcal{P}_{\bar{n}}^\dagger, \mathcal{P}_n, \mu) (W_n^\dagger \xi_n) = \int d\omega d\omega' C(\omega, \omega') \bar{\chi}_{\bar{n}, \omega'} \Gamma_i \chi_{n, \omega}. \quad (7.27)$$

By reparametrization invariance of type-III the dependence on the label operators can only be in the combination  $\omega\omega'$  inside  $C$ , so

$$C(\omega, \omega') = C(\omega\omega'). \quad (7.28)$$

Finally in the CM frame momentum conservation fixes  $\omega = \omega' = Q$ , the CM energy of the  $e^+e^-$  pair, so we can write

$$J^{\text{SCET}} = C(Q^2) (\bar{\xi}_{\bar{n}} W_{\bar{n}}) \Gamma_i (W_n^\dagger \xi_n), \quad (7.29)$$

and the matching calculation in this section will determine the renormalized  $\overline{\text{MS}}$  Wilson coefficient  $C(Q^2, \mu^2)$ . In this case there is only one relevant Dirac structure  $\Gamma_i$  in SCET for each of the vector and axial-vector currents.

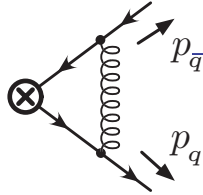
We again begin by calculating the full theory diagrams. As in the case of  $B \rightarrow X_s \gamma$  we need the wave function contributions for the light quarks, in this case one for the quark and one for the anti-quark. Both wave function contributions are the same as the results obtained before

$$Z_\psi = 1 - \frac{\alpha_s C_F}{4\pi} \left[ \frac{1}{\epsilon} - \ln \frac{-p^2}{\mu^2} + 1 \right]. \quad (7.30)$$

The remaining vertex graph can again be calculated in a straightforward manner. At tree level we find

$$V_{\text{qcd}}^0 = \bar{u}(p_n) \Gamma_i v_{\bar{n}}(p_{\bar{n}}) \quad (7.31)$$

while the one loop vertex diagram



gives

$$\begin{aligned} V_{\text{qcd}}^1 &= \mu^{2\epsilon} \iota^\epsilon \int \frac{d^d k}{(2\pi)^d} ig \bar{u}(p_q) \gamma^\alpha T^A \frac{i(\not{k} + \not{p}_q)}{(k + p_q)^2} \Gamma_i \frac{i(\not{k} - \not{p}_{\bar{q}})}{(k - p_{\bar{q}})^2} ig \gamma_\alpha T^A v(p_{\bar{q}}) \frac{-i}{k^2} \\ &= -ig^2 C_F \mu^{2\epsilon} \int \frac{d^d k}{(2\pi)^d} \bar{u}(p_q) \frac{\gamma^\alpha (\not{k} + \not{p}_q) \Gamma_i (\not{k} - \not{p}_{\bar{q}}) \gamma_\alpha}{(k + p_q)^2 (k - p_{\bar{q}})^2 k^2} v(p_{\bar{q}}) \\ &= \frac{\alpha_s C_F}{4\pi} \left[ \frac{1}{\epsilon} - 2 \ln^2 \frac{p^2}{Q^2} - 4 \ln \frac{p^2}{Q^2} - \ln \frac{(-Q^2 - i0)}{\mu^2} - \frac{2\pi^2}{3} \right] \bar{u}(p_q) \Gamma_i v(p_{\bar{q}}). \end{aligned} \quad (7.32)$$

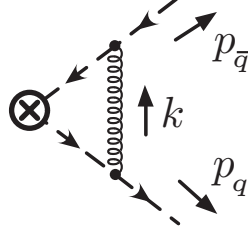
Here  $\iota^\epsilon = (4\pi)^{-\epsilon} e^{\epsilon\gamma_E}$  ensures that the scale  $\mu$  has the appropriate normalization for the  $\overline{\text{MS}}$  scheme. Adding the QCD diagrams we find

$$\begin{aligned} \text{QCD Sum} &= V_{\text{qcd}}^1 + 2 \left[ \frac{1}{2} (Z_\psi - 1) \right] V_{\text{qcd}}^0 \\ &= \frac{\alpha_s C_F}{4\pi} \left[ -2 \ln^2 \frac{p^2}{Q^2} - 3 \ln \frac{p^2}{Q^2} - 1 - \frac{2\pi^2}{3} \right] \bar{u}(p_q) \Gamma_i v(p_{\bar{q}}). \end{aligned} \quad (7.33)$$

As before, we next consider the loops in SCET. The wave function renormalization for the collinear quark is the same as in the previous section, and we find

$$Z_\xi^{us} = 0, \quad Z_\xi = 1 - \frac{C_F \alpha_s}{4\pi} \left( \frac{1}{\epsilon} - \ln \frac{-p^2}{\mu^2} + 1 \right). \quad (7.34)$$

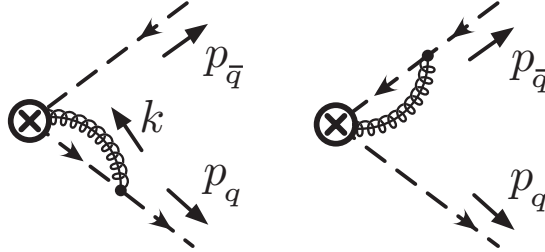
The tree level amplitude in SCET is  $V_{\text{scet}}^0 = \bar{u}_n(p_q) \Gamma_i v_{\bar{n}}(p_{\bar{q}})$ , and to leading order  $V_{\text{qcd}}^0 = V_{\text{scet}}^0$ . The ultrasoft vertex graph in SCET involves an exchange between the  $n$ -collinear and  $\bar{n}$ -collinear quarks,



and is given by

$$\begin{aligned} V_{\text{usoft}}^1 &= \mu^{2\epsilon} \ell^\epsilon \int \frac{d^d k}{(2\pi)^d} \bar{u}_n \left( ig \frac{\not{n}}{2} n^\alpha T^A \right) \frac{i \not{k}}{2} \frac{\bar{n} \cdot p_q}{\bar{n} \cdot p_q n \cdot k + p_q^2} \Gamma_i \frac{i \not{k}}{2} \frac{(-n \cdot p_{\bar{q}})}{n \cdot p_{\bar{q}} \bar{n} \cdot k + p_{\bar{q}}^2} \left( ig \frac{\not{\bar{n}}}{2} \bar{n}_\alpha T^A \right) v_{\bar{n}} \frac{(-i)}{k^2} \\ &= ig^2 C_F \mu^{2\epsilon} \ell^\epsilon \left( \bar{u}_n \frac{\not{n} \not{\bar{n}}}{4} \Gamma_i \frac{\not{\bar{n}} \not{n}}{4} v_{\bar{n}} \right) \int \frac{d^d k}{(2\pi)^d} \frac{n \cdot \bar{n}}{\left( n \cdot k + \frac{p_q^2}{\bar{n} \cdot p_q} \right) \left( \bar{n} \cdot k + \frac{p_{\bar{q}}^2}{n \cdot p_{\bar{q}}} \right) k^2} \\ &= \frac{\alpha_s C_F}{4\pi} \left[ -\frac{2}{\epsilon^2} + \frac{2}{\epsilon} \ln \frac{-p^4}{\mu^2 Q^2} - \ln^2 \frac{-p^4}{\mu^2 Q^2} - \frac{\pi^2}{2} \right] \bar{u}_n(p_q) \Gamma_i v_{\bar{n}}(p_{\bar{q}}). \end{aligned} \quad (7.35)$$

There are two possible collinear vertex graphs which involve a contraction between the  $W_n[\bar{n} \cdot A_n]$  Wilson line and a  $n$ -collinear quark, and another between the  $W_{\bar{n}}[n \cdot A_{\bar{n}}]$  Wilson line and the  $\bar{n}$ -collinear quark



For the first diagram, we find

$$\begin{aligned} V_{\text{coll}}^1 &= \mu^{2\epsilon} \ell^\epsilon \int \frac{d^d k}{(2\pi)^d} ig \bar{u}_n \left[ n^\alpha + \frac{\not{p}_\perp \gamma_\perp^\alpha}{\bar{n} \cdot p} + \frac{\gamma_\perp^\alpha (\not{p}_\perp + \not{k}_\perp)}{\bar{n} \cdot (p+k)} - \frac{\not{p}_\perp (\not{p}_\perp + \not{k}_\perp)}{\bar{n} \cdot p \bar{n} \cdot (p+k)} \right] \frac{\not{n}}{2} T^A \\ &\quad \times i \frac{\not{n}}{2} \frac{\bar{n} \cdot (p+k)}{(p+k)^2} \left( -g \frac{\bar{n}_\alpha}{\bar{n} \cdot k} T^A \right) \Gamma_i v_{\bar{n}} \frac{(-i)}{k^2} \\ &= -ig^2 C_F \mu^{2\epsilon} \ell^\epsilon \int \frac{d^d k}{(2\pi)^d} \frac{(n \cdot \bar{n}) \bar{n} \cdot (p+k)}{\bar{n} \cdot k (p+k)^2 k^2} \bar{u}_n \Gamma_i v_{\bar{n}} \\ &= \frac{\alpha_s C_F}{4\pi} \left[ \frac{2}{\epsilon^2} + \frac{2}{\epsilon} - \frac{2}{\epsilon} \ln \frac{-p^2}{\mu^2} + \ln^2 \frac{-p^2}{\mu^2} - 2 \ln \frac{-p^2}{\mu^2} + 4 - \frac{\pi^2}{6} \right] \bar{u}_n(p_q) \Gamma_i v_{\bar{n}}(p_{\bar{q}}). \end{aligned} \quad (7.36)$$

One can easily show that the second collinear vertex diagram gives the same result as the first diagram. Furthermore the collinear integral here is identical to the one for  $b \rightarrow s\gamma$  in Eq. (7.14). The result in

Eq. (7.36) is for the naive integrand, since it does not include the 0-bin subtraction contribution. But the 0-bin subtraction terms here are scaleless as in Eq. (7.21), and hence the final result in Eq. (7.36) is correct with the interpretation of the  $1/\epsilon$  divergences as UV.

Adding the SCET diagrams we find after some straightforward manipulations

$$\begin{aligned} \text{SCET Sum} &= V_{\text{usoft}}^1 + 2V_{\text{coll}}^1 + 2\left[\frac{1}{2}(Z_\xi - 1)\right]V_{\text{scet}}^0 \\ &= \frac{\alpha_s C_F}{4\pi} \left[ \frac{2}{\epsilon^2} + \frac{3}{\epsilon} - \frac{2}{\epsilon} \ln \frac{-Q^2}{\mu^2} + 2 \ln^2 \frac{\mu^2}{-p^2} - \ln^2 \frac{\mu^2 Q^2}{-p^4} + 3 \ln \frac{\mu^2}{-p^2} + 7 - \frac{5\pi^2}{6} \right] \bar{u}_n \Gamma_i v_{\bar{n}} \\ &= \frac{\alpha_s C_F}{4\pi} \left[ \frac{2}{\epsilon^2} + \frac{3}{\epsilon} - \frac{2}{\epsilon} \ln \frac{-Q^2}{\mu^2} - 2 \ln^2 \frac{p^2}{Q^2} + \ln^2 \frac{-Q^2}{\mu^2} - 3 \ln \frac{p^2}{Q^2} - 3 \ln \frac{-Q^2}{\mu^2} + 7 - \frac{5\pi^2}{6} \right] \bar{u}_n \Gamma_i v_{\bar{n}}. \end{aligned} \quad (7.37)$$

Comparing the  $\ln(p^2)$  dependence in the final line to the QCD amplitude in Eq. (7.33) We can see that SCET reproduces all IR divergences of the form  $\ln p^2/Q^2$ , and that the matching coefficient is therefore independent of IR divergences as it should. However, while the matrix element of the full QCD current is UV finite (since it is a conserved current), the matrix element in the effective theory is UV divergent and therefore needs to be renormalized. Defining a renormalized coupling by

$$C(Q, \epsilon) = Z_C(\mu, Q, \epsilon)C(\mu, Q) = C + (Z_C - 1)C \quad (7.38)$$

the renormalization constant that cancels the divergences in Eq. (7.37) is

$$Z_C = 1 + \frac{C_F \alpha_s(\mu)}{4\pi} \left[ -\frac{2}{\epsilon^2} - \frac{3}{\epsilon} + \frac{2}{\epsilon} \ln \left( \frac{-Q^2 - i0}{\mu^2} \right) \right]. \quad (7.39)$$

Taking the difference between the renormalized matrix elements in full QCD and SCET,

$$(\text{QCD sum})^{\text{ren}} = \frac{\alpha_s C_F}{4\pi} \left[ -2 \ln^2 \frac{p^2}{Q^2} - 3 \ln \frac{p^2}{Q^2} - 1 - \frac{2\pi^2}{3} \right] \bar{u}(p_n) \Gamma_i v(p_{\bar{n}}), \quad (7.40)$$

$$(\text{SCET sum})^{\text{ren}} = \frac{\alpha_s C_F}{4\pi} \left[ -2 \ln^2 \frac{p^2}{Q^2} + \ln^2 \frac{-Q^2}{\mu^2} - 3 \ln \frac{p^2}{Q^2} - 3 \ln \frac{-Q^2}{\mu^2} + 7 - \frac{5\pi^2}{6} \right] \bar{u}_n \Gamma_i v_{\bar{n}},$$

we obtain the matching result for Wilson coefficient of the operator in Eq. (7.29) at one-loop order

$$C(\mu, Q) = 1 + \frac{C_F \alpha_s(\mu)}{4\pi} \left[ -\ln^2 \left( \frac{-Q^2 - i0}{\mu^2} \right) + 3 \ln \left( \frac{-Q^2 - i0}{\mu^2} \right) - 8 + \frac{\pi^2}{6} \right]. \quad (7.41)$$

Note that the only momentum dependence in the Wilson coefficient is in logarithms of the ratio of the renormalization scale to the hard scale  $Q$ . This dependence signals that it captures offshell physics from the hard scale  $Q$  that we are integrating out. If we choose the renormalization scale to be equal to  $Q$ , we find that all logarithms vanish

$$C(Q, Q) = 1 + \frac{C_F \alpha_s(Q)}{4\pi} \left[ -8 + \frac{7\pi^2}{6} - 3i\pi \right]. \quad (7.42)$$

Sometimes it is useful to avoid inducing large factors of  $\pi$  in the non-logarithmic terms, which can be accomplished by using a complex scale,  $\mu = -iQ$ . Here this gives

$$C(-iQ, Q) = 1 + \frac{C_F \alpha_s(-iQ)}{4\pi} \left[ -8 + \frac{\pi^2}{6} \right]. \quad (7.43)$$

For dijet observables described by the current in Eq. (7.29) the cross section is obtained by squaring the amplitude, and will depend on a hard function defined by

$$H(\mu, Q) = |C(\mu, Q)|^2. \quad (7.44)$$

Thus the imaginary contributions in  $C(\mu, Q)$  cancel out for these observables.

### 7.3 Summing Sudakov Logarithms

With the information from either of the last two sections, we can calculate the anomalous dimensions of the operators or Wilson coefficients. Taking

$$0 = \mu \frac{d}{d\mu} C^{\text{bare}}(\epsilon) = \mu \frac{d}{d\mu} [Z_C(\mu, \epsilon) C(\mu)] = \left[ \mu \frac{d}{d\mu} Z_C(\mu, \epsilon) \right] C(\mu) + Z_C(\mu, \epsilon) \left[ \mu \frac{d}{d\mu} C(\mu) \right], \quad (7.45)$$

we see that the anomalous dimension is defined by a derivative of the counterterm

$$\mu \frac{d}{d\mu} C(\mu) = \left[ -Z_C^{-1}(\mu, \epsilon) \mu \frac{d}{d\mu} Z_C(\mu, \epsilon) \right] C(\mu) \equiv \gamma_C(\mu) C(\mu). \quad (7.46)$$

To calculate the  $\mu$  derivative we should recall the result for the derivative of the strong coupling in  $d$  dimensions

$$\mu \frac{d}{d\mu} \alpha_s(\mu, \epsilon) = -2\epsilon \alpha_s(\mu, \epsilon) + \beta[\alpha_s], \quad (7.47)$$

where  $\beta[\alpha_s]$  is the standard  $d = 4$  QCD beta function written in terms of  $\alpha_s(\mu, \epsilon)$ .

Lets apply this to our two examples in turn. The counterterm for the  $b \rightarrow s\gamma$  current is

$$Z_C^\gamma = 1 - \frac{\alpha_s(\mu) C_F}{4\pi} \left( \frac{1}{\epsilon^2} + \frac{2}{\epsilon} \ln \frac{\mu}{\omega} + \frac{5}{2\epsilon} \right). \quad (7.48)$$

Using the definition of  $\gamma_C$  in Eq. (7.46) we find

$$\begin{aligned} \gamma_C^\gamma(\mu, \omega, \epsilon) &= -\frac{1}{Z_C^\gamma} \mu \frac{d}{d\mu} Z_C^\gamma = \mu \frac{d}{d\mu} \frac{C_F \alpha_s(\mu, \epsilon)}{4\pi} \left( \frac{1}{\epsilon^2} + \frac{2}{\epsilon} \ln \frac{\mu}{\omega} + \frac{5}{2\epsilon} \right) \\ &= \frac{C_F \alpha_s(\mu, \epsilon)}{4\pi} \left( -\frac{2}{\epsilon} - 4 \ln \frac{\mu}{\omega} - 5 + \frac{2}{\epsilon} \right) + \mathcal{O}(\alpha_s^2), \\ \gamma_C^\gamma(\mu, \omega) &= -\frac{\alpha_s(\mu)}{4\pi} \left( 4C_F \ln \frac{\mu}{\omega} + 5C_F \right), \end{aligned} \quad (7.49)$$

where we differentiated both  $\alpha_s(\mu)$  and the explicit  $\ln(\mu)$ , noting that the  $1/\epsilon$  terms cancel to yield a well defined anomalous dimension in the  $\epsilon \rightarrow 0$  limit which is given on the last line.

Similarly, the counterterm for the  $e^+e^- \rightarrow \text{dijets}$  current is

$$Z_C^{2\text{jet}} = 1 + \frac{C_F \alpha_s(\mu)}{4\pi} \left[ -\frac{2}{\epsilon^2} - \frac{3}{\epsilon} + \frac{2}{\epsilon} \ln \left( \frac{-Q^2 - i0}{\mu^2} \right) \right], \quad (7.50)$$

so the anomalous dimension is obtained by

$$\begin{aligned} \gamma_C^{2\text{jet}}(\mu, Q, \epsilon) &= -\frac{1}{Z_C^{2\text{jet}}} \mu \frac{d}{d\mu} Z_C^{2\text{jet}} = \mu \frac{d}{d\mu} \frac{C_F \alpha_s(\mu, \epsilon)}{4\pi} \left[ \frac{2}{\epsilon^2} + \frac{3}{\epsilon} + \frac{2}{\epsilon} \ln \left( \frac{\mu^2}{-Q^2 - i0} \right) \right] \\ &= \frac{C_F \alpha_s(\mu, \epsilon)}{4\pi} \left[ \frac{-4}{\epsilon} - 6 - 4 \ln \left( \frac{\mu^2}{-Q^2 - i0} \right) + \frac{4}{\epsilon} \right] + \mathcal{O}(\alpha_s^2), \\ \gamma_C^{2\text{jet}}(\mu, Q) &= -\frac{\alpha_s(\mu)}{4\pi} \left[ 4C_F \ln \left( \frac{\mu^2}{-Q^2 - i0} \right) + 6C_F \right]. \end{aligned} \quad (7.51)$$

Again in the last line we have taken the  $\epsilon \rightarrow 0$  limit. Note the similarity in the form of the anomalous dimensions for our two examples of Wilson coefficients. Both anomalous dimension equations for  $C(\mu)$  are homogeneous linear differential equations because in both cases the operator mixes back into itself.

An interesting feature of anomalous dimensions in SCET is the presence of a single logarithm,  $\ln(\mu)$ . It can be shown by the consistency of SCET, or by consistency of top-down versus bottom-up evolution using a factorization theorem for a process with Sudakov logarithms, that no terms with more than a single logarithm can appear in anomalous dimensions. The coefficient of this single logarithm is related to the cusp anomalous dimension that governs the renormalization of Wilson lines that meet at a cusp angle  $\beta_{ij}$  between lines along the four vectors  $n_i$  and  $n_j$ , where  $\cosh \beta_{ij} = n_i \cdot n_j / [|n_i| |n_j|]$ . In the light-like limit  $n_i^2, n_j^2 \rightarrow 0$  we have  $\beta_{ij} \rightarrow \infty$ . The cusp anomalous dimension is linear in  $\beta_{ij}$  in this limit, which yields a logarithmic dependence on  $2n_i \cdot n_j / [|n_i| |n_j|]$  since  $\cosh \beta_{ij} \simeq e^{\beta_{ij}}/2$ . This single logarithm is the same one encountered in Eqs. (7.49) and (7.50), where the divergence has been handled by the renormalization procedure, and hence has become a  $\ln(\mu)$ . Indeed, if we consider making the BPS field redefinition for the dijet current we get  $Y_n^\dagger Y_{\bar{n}}$ , so it is clear that our ultrasoft diagrams involve two light-like Wilson lines meeting at a cusp. In the case of the collinear diagrams we have a Wilson line  $W_n$  that meets up with a collinear quark  $\xi_n$ , and in doing so also effectively forms a cusp.

The all orders form for the anomalous dimension of our two example currents is

$$\begin{aligned} \gamma_C(\mu, \omega) &= -a_C \Gamma_{\text{cusp}}[\alpha_s(\mu)] \ln\left(\frac{\mu}{\omega_C}\right) - \gamma_C[\alpha_s(\mu)], \\ \Gamma_{\text{cusp}}[\alpha_s] &= \sum_{k=1}^{\infty} \left(\frac{\alpha_s}{4\pi}\right)^k \Gamma_k^{\text{cusp}}, \quad \gamma_C[\alpha_s] = \sum_{k=1}^{\infty} \left(\frac{\alpha_s}{4\pi}\right)^k \gamma_k^C, \end{aligned} \quad (7.52)$$

where  $\Gamma_{\text{cusp}}[\alpha_s]$  is called the cusp-anomalous dimension, and the one-loop result has  $\Gamma_1^{\text{cusp}} = 4$ . The constant prefactor  $a_C$ , the dimensionful variable  $\omega_C$ , and the non-cusp anomalous dimension  $\gamma_C[\alpha_s]$  all depend on the particular current under consideration. In order to solve the anomalous dimension equation we should decide what terms must be kept at each order in perturbation theory that we would like to consider. Counting  $\alpha_s \ln(\mu) \sim 1$ , the correct grouping for obtaining the leading-log (LL), next-to-leading log (NLL), etc., results is

$$\gamma_C(\mu, \omega) \sim [\alpha_s \ln(\mu)]_{\text{LL}} + [\alpha_s + \alpha_s^2 \ln(\mu)]_{\text{NLL}} + [\alpha_s^2 + \alpha_s^3 \ln(\mu)]_{\text{NNLL}} + \dots \quad (7.53)$$

Thus we see that the cusp-anomalous dimension with the  $\ln(\mu)$  is required at one-higher order than the non-cusp anomalous dimension. (Typically this is not a problem due to the universal form of the cusp contribution, and the fact that its coefficients are known to 3-loop order for QCD, that is up to  $\Gamma_3^{\text{cusp}}$ .) To solve the first order differential equation involving  $\gamma_C$  we also must specify a boundary condition for  $C(\mu, \omega)$ . At both LL and NLL order the tree-level boundary condition suffices, while at NNLL we need the one-loop boundary condition, etc.

Lets solve the generic anomalous dimension at LL order where

$$\mu \frac{d}{d\mu} \ln C(\mu, \omega) = -4a_C \frac{\alpha_s(\mu)}{4\pi} \ln\left(\frac{\mu}{\omega}\right) = -\frac{a_C \alpha_s(\mu)}{\pi} \ln\left(\frac{\mu}{\omega}\right). \quad (7.54)$$

This equation may be solved for specific quantum field theories. For QED without massless fermions the coupling does not run, and with the tree-level boundary condition  $C(\mu = \omega, \omega) = 1 + \mathcal{O}(\alpha_s)$  we have

$$C(\mu, \omega) = \exp\left[-a_C \frac{\alpha}{2\pi} \ln^2\left(\frac{\mu}{\omega}\right)\right]. \quad (7.55)$$

This result involves an exponential of a double logarithm, and is often referred to as the Sudakov form factor. The suppression encoded in this result is related to the restrictions in phase space that are intrinsic for the allowed types of radiation that our operators can emit. The Sudakov form factor also gives the

probability of evolving without branching in a parton shower. For QCD we must also account for the running of the coupling, and at LL order we can use the LL  $\beta$ -function,

$$\mu \frac{d}{d\mu} \alpha_s(\mu) = -\frac{\beta_0}{2\pi} \alpha_s^2(\mu), \quad \beta_0 = \frac{11}{3} C_A - \frac{4}{3} T_F n_f. \quad (7.56)$$

Together Eqs. (7.54) and (7.56) are a coupled set of differential equations. The easiest way to solve these two equations is to use the second one to implement a change of variable for the first by noting that

$$d \ln \mu = \frac{d\alpha_s}{\beta[\alpha_s]} = -\frac{2\pi}{\beta_0} \frac{d\alpha_s}{\alpha_s^2}, \quad \ln\left(\frac{\mu}{\omega}\right) = -\frac{2\pi}{\beta_0} \int_{\alpha_s(\omega)}^{\alpha_s(\mu)} \frac{d\alpha}{\alpha^2}. \quad (7.57)$$

Using the more generic boundary condition which fixes the coefficient at the scale  $\mu_0$ ,  $C(\mu_0, \omega) = 1 + \mathcal{O}(\alpha_s)$  we then have

$$\begin{aligned} \ln C(\mu, \omega) &= -\left(\frac{2\pi}{\beta_0}\right)^2 \int_{\alpha_s(\mu_0)}^{\alpha_s(\mu)} \frac{d\alpha_s}{\alpha_s^2} \frac{a_C \alpha_s}{\pi} \int_{\alpha_s(\omega)}^{\alpha_s} \frac{d\alpha}{\alpha^2} \\ &= -\frac{4\pi a_C}{\beta_0^2} \int_{\alpha_s(\mu_0)}^{\alpha_s(\mu)} \frac{d\alpha_s}{\alpha_s} \left[ -\frac{1}{\alpha_s} + \frac{1}{\alpha_s(\omega)} \right] \\ &= -\frac{4\pi a_C}{\beta_0^2} \left[ \frac{1}{\alpha_s(\mu)} - \frac{1}{\alpha_s(\mu_0)} + \frac{1}{\alpha_s(\omega)} \ln\left(\frac{\alpha_s(\mu)}{\alpha_s(\mu_0)}\right) \right] \\ &= -\frac{4\pi a_C}{\beta_0^2 \alpha_s(\mu_0)} \left( \frac{1}{z} - 1 + \ln z \right) - \frac{2a_C}{\beta_0} \ln\left(\frac{\omega}{\mu_0}\right) \ln z, \end{aligned} \quad (7.58)$$

where in the last line we used  $1/\alpha_s(\omega) = 1/\alpha_s(\mu_0) + \frac{\beta_0}{2\pi} \ln(\omega/\mu_0)$ , and defined

$$z \equiv \frac{\alpha_s(\mu)}{\alpha_s(\mu_0)}. \quad (7.59)$$

The solution is therefore

$$C(\mu, \omega) = \exp \left[ -\frac{4\pi a_C}{\beta_0^2 \alpha_s(\mu_0)} \left( \frac{1}{z} - 1 + \ln z \right) \right] \left( \frac{\omega}{\mu_0} \right)^{-2a_C \ln z / \beta_0}. \quad (7.60)$$

This result sums the infinite tower of leading-logarithms in the exponent which are of the form,  $C \sim \exp(-\alpha_s L^2 - \alpha_s^2 L^3 - \alpha_s^3 L^4 - \dots)$ , where the coefficients here are schematic and  $L = \ln(\mu/\mu_0)$  is a potentially large logarithm. Again this result is called the Sudakov form factor with a running coupling. Note that the form of the series obtained by expanding in the argument of the exponent is much simpler than what we would obtain by expanding the exponent itself. At each order in resummed perturbation theory the terms that are determined by solving the anomalous dimension equation can be classified by the simpler series that appears in the exponential as follows

$$\ln C \sim \left[ -L \sum_k (\alpha_s L)^k \right]_{\text{LL}} + \left[ \sum_k (\alpha_s L)^k \right]_{\text{NLL}} + \left[ \sum_k \alpha_s (\alpha_s L)^k \right]_{\text{NNLL}} + \dots \quad (7.61)$$

A natural question to ask is how generic are the two examples treated so far in this section? It turns out that much of the structure here is quite generic for cases like our examples, where the  $\omega$  variables are fixed by external kinematics. This will occur for any operator that involves only one building block,  $\chi_n$  or  $\mathcal{B}_{n\perp}^\mu$ , for each collinear direction  $n$ . For example, with four collinear directions we have the operator

$$\int d\omega_1 d\omega_2 d\omega_3 d\omega_4 C(\omega_1, \omega_2, \omega_3, \omega_4) \left[ \bar{\chi}_{n_1, \omega_1} \Gamma_{\mu\nu} \mathcal{B}_{n_2\perp, \omega_2}^\mu \mathcal{B}_{n_3\perp, \omega_3}^\nu \chi_{n_4, \omega_4} \right] \quad (7.62)$$



and again the  $\omega_i$ 's will be fixed by momenta that are external to collinear loops. An example where this would not be true is if we had the same collinear direction  $n$  in two or more of our building blocks, such as

$$\int d\omega_1 d\omega_2 C(\omega_1, \omega_2) [\bar{\chi}_{n, \omega_1} \not{n} \chi_{n, \omega_2}]. \quad (7.63)$$

For this operator one combination of  $\omega_1$  and  $\omega_2$  will be fixed by momentum conservation, while the other combination will involve collinear loop momenta. This will lead to anomalous dimension equations of a more complicated form, involving convolutions such as

$$\mu \frac{d}{d\mu} C(\mu, \omega) = \int d\omega' \gamma(\mu, \omega, \omega') C(\mu, \omega'). \quad (7.64)$$

Indeed, the operator in Eq. (7.64) is responsible for several classic evolution equations: i) DIS where we have DGLAP evolution for the parton distribution functions  $f_{i/p}(\xi)$ , ii) hard exclusive processes like  $\gamma^* \pi^0 \rightarrow \pi^0$  where we have Brodsky-Lepage evolution for the light-cone meson distributions  $\phi_\pi(x)$ , and iii) the deeply virtual Compton scattering process  $\gamma^* p \rightarrow \gamma p'$  where the evolution is a combination of both of these. It is interesting that all of these processes are sensitive to different projections of the evolution of the single operator given in Eq. (7.64). We will carry out an example of an evolution equation with a convolution in the next section, where we consider DIS and the DGLAP equation.

## 8 Deep Inelastic Scattering

**(ROUGH)** DIS is a rich subject, so for the purpose of these notes we will treat only aspects related to factorization and the renormalization group evolution with SCET. In particular we will demonstrate the factorization of momentum by showing that the forward DIS scattering amplitude can be written as an integral over hard coefficients times parton distribution functions.

### 8.1 Factorization of Amplitude

The scattering process is depicted in the figure. The hard scale  $Q$  of the process is defined by the photon

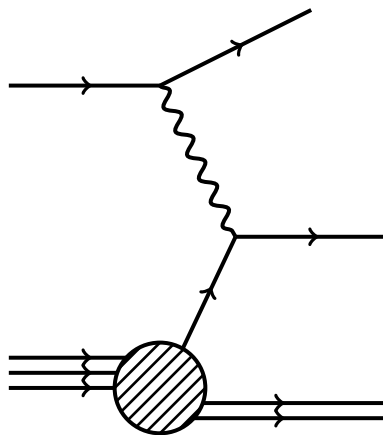


Figure 11: Deep Inelastic Scattering

momentum  $q^\mu$

$$q^2 = -Q^2 \quad (8.1)$$

and satisfies  $Q^2 \gg \Lambda^2$ . Our Bjorken variable  $x$  is defined in the standard way

$$x = \frac{Q^2}{2p \cdot q} \quad (8.2)$$

and with momentum conservation defined by  $p^\mu + q^\mu = p_X^\mu$ , we have

$$p_X^2 = \frac{Q^2}{x}(1-x) + m_p^2. \quad (8.3)$$

With this result we may determine the various energy regions of the process

Regions	Description
$(\frac{1}{x} - 1) \sim 1 \implies p_X^2 \sim Q^2$	Standard OPE Region
$(\frac{1}{x} - 1) \sim \frac{\Lambda}{Q} \implies p_X^2 \sim Q\Lambda$	Endpoint Region
$(\frac{1}{x} - 1) \sim \frac{\Lambda^2}{Q^2} \implies p_X^2 \sim \Lambda^2$	Resonance Region

### Describe Parton Variables

We will consider our scattering process in the standard OPE region so that the final state has  $p_X^2$  of order  $Q^2$  and can consequently be integrated out. Conversely, the proton with its comparatively small invariant mass  $p^2 \sim \Lambda^2$  may be treated as a collinear field. We analyze the process in the **Breit Frame** in which the perpendicular momentum component of  $q^\mu$  is zero with

$$q^\mu = \frac{Q}{2}(\bar{n}^\mu - n^\mu). \quad (8.4)$$

The proton and final state momentum are then

$$p^\mu = \frac{n^\mu}{2}\bar{n} \cdot p + \frac{\bar{n}^\mu}{2}n \cdot p \quad (8.5)$$

$$= \frac{n^\mu}{2}\bar{n} \cdot p + \frac{\bar{n}^\mu}{2}\frac{m_p^2}{\bar{n} \cdot p} \quad (8.6)$$

$$= \frac{n^\mu}{2}\frac{Q}{x} + \dots \quad (8.7)$$

$$p_X^\mu = p^\mu + q^\mu \quad (8.8)$$

$$= \frac{n^\mu}{Q} + \frac{\bar{n}^\mu}{2}Q\frac{(1-x)}{x}. \quad (8.9)$$

The cross section for DIS in terms of leptonic and hadronic tensors is

$$d\sigma = \frac{d^3k'}{2|\vec{k}'|(2\pi)^3} \frac{\pi e^4}{sQ^4} L^{\mu\nu}(k, k') W_{\mu\nu}(p, q) \quad (8.10)$$

where  $k$  and  $k'$  are the incoming and outgoing lepton momenta, respectively, and we have defined  $q \equiv k' - k$ , and  $s \equiv (p + k)^2$ .  $L^{\mu\nu}(k, k')$  is the leptonic tensor computed using standard QFT methods and  $W_{\mu\nu}(p, q)$  is the hadronic tensor which will occupy us in this section.  $W_{\mu\nu}$  is related to the imaginary part of the DIS scattering amplitude by

$$W_{\mu\nu}(p, q) = \frac{1}{\pi} \text{Im} T_{\mu\nu} \quad (8.11)$$

where

$$T_{\mu\nu}(p, q) = \frac{1}{2} \sum_{\text{spin}} \langle p | \hat{T}_{\mu\nu}(q) | p \rangle \quad \hat{T}_{\mu\nu}(q) = i \int d^4x e^{iqx} T[J_\mu(x) J_\nu(0)]. \quad (8.12)$$

Taking  $J_\mu$  to be an electromagnetic current, we may write

$$T_{\mu,\nu}(p, q) = \left(-g_{\mu\nu} + \frac{q_\mu q_\nu}{q^2}\right) T_1(x, Q^2) + \left(p_\mu + \frac{q_\mu}{2x}\right) \left(p_\nu + \frac{q_\nu}{2x}\right) T_2(x, Q^2). \quad (8.13)$$

which satisfies current conservation, P, C, and T symmetries. Matching the  $\hat{T}_{\mu\nu}(q)$  onto the most general leading order SCET operator for collinear fields in the  $n^\mu$  direction and satisfying current conservation  $q^\mu \hat{T}_{\mu\nu}$  we have

$$\hat{T}^{\mu\nu} \rightarrow \frac{g_\perp^{\mu\nu}}{Q} \left(O_1^{(i)} + \frac{O_1^g}{Q}\right) + \frac{(n^\mu + \bar{n}^\mu)(n^\nu + \bar{n}^\nu)}{Q} \left(O_2^{(i)} + \frac{O_2^g}{Q}\right) \quad (8.14)$$

where

$$O_j^{(i)} = \overline{\xi_{n,p}^i} W \frac{\not{n}}{2} C_j^{(i)}(\bar{\mathcal{P}}_+, \bar{\mathcal{P}}_-) W^\dagger \xi_{n,p}^i \quad (8.15)$$

$$O_j^g = \text{Tr}[W^\dagger B_\perp^\lambda W C_j^g(\bar{\mathcal{P}}_+, \bar{\mathcal{P}}_-) W^\dagger B_{\perp\lambda} W] \quad (8.16)$$

$$(8.17)$$

with  $igB_\perp^\lambda$  and  $\bar{\mathcal{P}}_\pm$  defined as

$$igB_\perp^\lambda \equiv [i\bar{n} \cdot D_n, iD_{n,\perp}^\lambda], \quad \bar{\mathcal{P}}_\pm = \bar{\mathcal{P}}^\dagger \pm \bar{\mathcal{P}}. \quad (8.18)$$

The subscripts  $j$  in  $O_j^{(i)}$  are arbitrary labels, similar to those found in (8.13), which differentiate the two parts of  $\hat{T}_{\mu\nu}$ . The superscript  $(i)$  defines the flavor ( $u, d, s$ , etc.) of quarks and the superscript  $g$  in  $O_j^g$  stands for a gluon. In accord with their labels,  $O_j^{(i)}$  will lead to the quark and anti-quark PDF and  $O_j^g$  will lead to the gluon PDF. The placement of factors of  $\frac{1}{Q}$  is done in order to yield dimensionless Wilson coefficients. The fact that these Wilson coefficients are dimensionless can be understood by realizing that according to (8.12),  $\hat{T}_{\mu\nu}$  has mass dimension 2.

In (8.14) there are both quark and gluon operators. However, with  $\hat{T}_{\mu\nu}$  defined in terms of an electromagnetic current we can focus on the quarks and treat the gluons as an higher order contribution so that  $\hat{T}_{\mu\nu}$  becomes

$$\hat{T}^{\mu\nu} \rightarrow \frac{g_\perp^{\mu\nu}}{Q} O_1^{(i)} + \frac{(n^\mu + \bar{n}^\mu)(n^\nu + \bar{n}^\nu)}{Q} O_2^{(i)}. \quad (8.19)$$

Returning to the quark operator  $O_j^{(i)}$ , we may introduce a convolution to separate the hard coefficients from the long distance operators

$$O_j^{(i)} = \int d\omega_1 d\omega_2 C_j^{(i)}(\omega_+, \omega_-) [(\bar{\xi}_n W)_{\omega_1} \delta(\omega_1 - \bar{\mathcal{P}}^\dagger) \frac{\not{n}}{2} (W^\dagger \xi_n)_{\omega_2} \delta(\omega_2 - \mathcal{P})] \quad (8.20)$$

where  $\omega_\pm = \omega_1 \pm \omega_2$ . Our hope is to connect this operator to the PDF as a clear demonstration of factorization. The PDF for quarks is given by

$$f_{i/p}(\xi) = \int dy e^{-2i\xi\bar{n}\cdot py} \langle p | \bar{\xi}(y) W(y, -y) \not{n} \xi(y) | p \rangle \quad (8.21)$$

and the PDF for anti-quarks is simply  $\bar{f}_{i/p}(\xi) = -f_{i/p}(-\xi)$ . In momentum space, we can write the matrix element in (8.21) as

$$\langle p | \bar{\xi}(y) W(y, -y) \not{n} \xi(y) | p \rangle = \langle p | (\bar{\xi}_n W)_{\omega_1} \not{n} (W^\dagger \xi_n)_{\omega_2} | p \rangle \quad (8.22)$$

$$= 4\bar{n} \cdot p \int_0^1 d\xi \delta(\omega_-) \quad (8.23)$$

$$\times [\delta(\omega_+ - 2\xi\bar{n} \cdot p) f_{i/p}(\xi) - \delta(\omega_+ + 2\bar{n} \cdot p) \bar{f}_{i/p}(\xi)]. \quad (8.24)$$

The delta function over  $\omega_-$  sets  $\omega_1 = \omega_2$ . The other set of delta functions ensure that for  $\omega_+ > 0$  we use quark PDF  $f_{i/p}(z)$ . and for  $\omega_+ < 0$  we use anti-quark PDF  $\bar{f}_{i/p}(z)$ . Using these results we may rewrite our operator  $O_j^{(i)}$  including spin averages as

$$\frac{1}{2} \sum_{\text{spin}} \langle p | O_j^{(i)} | p \rangle = \frac{1}{4} \int d\omega_1 d\omega_2 C_j^{(i)}(\omega_+, \omega_-) [(\bar{\xi}_n W)_{\omega_1} \delta(\omega_1 - \bar{\mathcal{P}}^\dagger) \not{n}(W^\dagger \xi_n)_{\omega_2} \delta(\omega_2 - \mathcal{P})] \quad (8.25)$$

$$= \frac{1}{4} \int d\omega_1 d\omega_2 C_j^{(i)}(\omega_+, \omega_-) 4\bar{n} \cdot p \quad (8.26)$$

$$\times \int_0^1 d\xi \delta(\omega_-) [\delta(\omega_+ - 2\xi\bar{n} \cdot p) f_{i/p}(\xi) - \delta(\omega_+ + 2\bar{n} \cdot p) \bar{f}_{i/p}(\xi)] \quad (8.27)$$

$$= \bar{n} \cdot p \int_0^1 [C_j^i(2\bar{n} \cdot p\xi, 0) f_{i/p}(\xi) - C_j^i(-2\bar{n} \cdot p\xi, 0) \bar{f}_{i/p}(\xi)]. \quad (8.28)$$

Now, by charge conjugation invariance (reference), we have  $C(-\omega_+, \omega_-) = -C(\omega_+, \omega_-)$  so that the final form of the spin averaged matrix element is

$$\frac{1}{2} \sum_{\text{spin}} \langle p | O_j^{(i)} | p \rangle = \bar{n} \cdot p \int_0^1 C_j^i(2\bar{n} \cdot p\xi, 0) [f_{i/p}(z\xi) + \bar{f}_{i/p}(z\xi)]. \quad (8.29)$$

We note that although we are using SCET<sub>II</sub> no soft gluons have appeared in our analysis. This fact can be understood by observing that our original operator

$$O_j^{(i)} = \bar{\xi}_{n,p}^i W \frac{\not{n}}{2} C_j^{(i)}(\bar{\mathcal{P}}_+, \bar{\mathcal{P}}_-) W^\dagger \xi_{n,p}^i$$

is a color singlet and therefore decouples from any color-charge changing (i.e. gluon) interactions. With (8.29) we have the necessary result for a demonstration of factorization. Now all that is left to do is perform the matching of the full field theoretic operators  $T_1(x, Q^2)$  and  $T_2(x, Q^2)$  onto the operators  $O_j^{(i)}$ . Recalling our formula for  $T_{\mu\nu}$  in terms of  $\hat{T}_{\mu\nu}$ , we have

$$T^{\mu\nu} = \frac{1}{2} \sum_{\text{spin}} \langle p | \hat{T}^{\mu\nu} | p \rangle \quad (8.30)$$

$$= \frac{g_\perp^{\mu\nu}}{Q} \frac{1}{2} \sum_{\text{spin}} \langle p | O_j^{(i)} | p \rangle + \frac{4n^\mu n^\nu}{Q} \frac{1}{2} \sum_{\text{spin}} \langle p | O_j^{(i)} | p \rangle. \quad (8.31)$$

This is the SCET amplitude. The QCD amplitude is

$$T_{\mu,\nu}^{SCET}(p, q) = \left( -g_{\mu\nu} + \frac{q_\mu q_\nu}{q^2} \right) T_1(x, Q^2) + \left( p_\mu + \frac{q_\mu}{2x} \right) \left( p_\nu + \frac{q_\nu}{2x} \right) T_2(x, Q^2) \quad (8.32)$$

Writing this result in light-cone coordinates and using the Ward Identity ( $q_\nu L^{\mu\nu} = q_\mu L^{\mu\nu} = 0$ ), and the fact that all terms proportional to  $(\bar{n}_\mu - n_\mu) = \frac{2q_\mu}{Q}$  become zero upon contraction with  $L_{\mu\nu}$ , we have

$$T_{\mu\nu}^{QCD} = -g_{\mu\nu\perp} T_1(x, Q^2) + n_{\mu\nu} \left( \frac{Q^2}{4x^2} T_2(x, Q^2) - T_1(x, Q^2) \right) \quad (8.33)$$

We refer the reader to [?] for a full derivation of this result. Matching  $T^{QCD}$  onto  $T^{SCET}$ , yields the relations

$$-\frac{1}{2Q} \sum_{\text{spin}} \langle p | O_j^{(i)} | p \rangle = T_1(x, Q^2) \quad (8.34)$$

$$\frac{2}{Q} \sum_{\text{spin}} \langle p | O_j^{(i)} | p \rangle = \left( \frac{Q^2}{4x^2} T_2(x, Q^2) - T_1(x, Q^2) \right) \quad (8.35)$$

which, upon inversion, gives

$$T_1(x, Q^2) = -\frac{1}{2Q} \sum_{\text{spin}} \langle p | O_j^{(i)} | p \rangle \quad (8.36)$$

$$= -\frac{1}{x} \int_0^1 d\xi C_1^i(2\bar{n} \cdot p\xi, 0) [f_{i/p}(\xi) + \bar{f}_{i/p}(\xi)] \quad (8.37)$$

$$T_2(x, Q^2) = \frac{8x^2}{Q^3} \sum_{\text{spin}} \langle p | O_j^{(i)} | p \rangle - \frac{2x^2}{Q^3} \sum_{\text{spin}} \langle p | O_j^{(i)} | p \rangle \quad (8.38)$$

$$= \frac{4x}{Q^2} \int_0^1 d\xi \left( 4C_2^{(i)}(2\bar{n} \cdot p\xi, 0) - C_1^{(i)}(2\bar{n} \cdot p\xi, 0) \right) [f_{i/p}(\xi) + \bar{f}_{i/p}(\xi)]. \quad (8.39)$$

$$(8.40)$$

where in the Breit Frame  $x = \frac{Q^2}{2p \cdot q} = \frac{Q^2}{\bar{n} \cdot p n \cdot q} = \frac{Q}{\bar{n} \cdot p}$ . With the definition

$$H_j(z) \equiv C_j(2Qz, 0, Q, \mu), \quad (8.41)$$

where the hard scale  $Q$  and the  $\mu$  dependence has been made explicit, we have the final result

$$T_1(x, Q^2) = -\frac{1}{x} \int_0^1 d\xi H_1^{(i)}\left(\frac{\xi}{x}\right) [f_{i/p}(\xi) + \bar{f}_{i/p}(\xi)] \quad (8.42)$$

$$T_2(x, Q^2) = \frac{4x}{Q^2} \int_0^1 d\xi \left[ 4H_2^{(i)}\left(\frac{\xi}{x}\right) - H_1^{(i)}\left(\frac{\xi}{x}\right) \right] [f_{i/p}(\xi) + \bar{f}_{i/p}(\xi)] \quad (8.43)$$

where the sum over  $i$  is implicit.

### **Remarks**

- This result represents the general (to all orders in  $\alpha_s$ ) factorization for DIS. As promised we have the computable hard coefficients  $H_i$  weighted by the universal non-perturbative PDFs  $f_{i/p}$  and  $\bar{f}_{i/p}$ .
- The coefficients  $C_j$  are dimensionless and can therefore only have  $\alpha_s(\mu) \ln(\mu/Q)$  dependence on  $Q$ . This result is in accord with Bjorken Scaling.
- The  $\mu$  in  $H_i(\mu)$  and  $f_{i/p}(\mu)$  is typically called the factorization scale  $\mu = \mu_F$ . There is also the renormalization scale as in  $\alpha_s(\mu_R)$ . In SCET  $\mu$  is both the renormalization and factorization scale, since the same parameter  $\mu$  is responsible for the running of the EFT coupling  $\alpha_s(\mu)$  and for the EFT coupling  $C_j(\mu)$ .
- When we consider the tree level matching onto the wilson coefficients we find that  $C_2 = 0$  implying the Callan-Gross relation

$$\frac{W_1}{W_2} = \frac{Q^2}{4x^2} \quad (8.44)$$

and that

$$C_1(\omega_+) = 2e^2 Q_i^2 \left[ \frac{Q}{(\omega_+ - 2Q) + i\epsilon} - \frac{Q}{(-\omega_+ - 2Q) + i\epsilon} \right] \quad (8.45)$$

$$H_1 = -e^2 Q_i^2 \delta \left( \frac{\xi}{x} - 1 \right) \quad (8.46)$$

## 8.2 Renormalization of PDF

**(ROUGH)** In this section we calculate the anomalous dimension of the parton distribution function. We define the PDF as

$$f_q(\xi) = \langle p_n | \bar{\chi}_n(0) \frac{\not{n}}{2} \chi_{n,\omega}(0) | p_n \rangle \quad (8.47)$$

where  $\omega = \xi \bar{n} \cdot p_n > 0$ . Since we have a forward matrix element there is no need to consider a momentum label  $\omega'$  on  $\bar{\chi}_n$ , by momentum conservation it would be fixed to  $\omega' = \omega$ . We renormalize our PDF in our EFT framework with dimensional regularization, noting that there are only collinear fields and no ultrasoft interactions for this example. Collinear loop processes can change  $\omega$  (or  $\xi$ ) and also the type of parton. The renormalized PDF operators are given in terms of bare operators as

$$f_i^{\text{bare}}(\xi) = \int d\xi' Z_{ij}(\xi, \xi') f_j(\xi', \mu). \quad (8.48)$$

The  $\mu$  independence of the bare operators  $f_i^{\text{bare}}(\xi)$  yields an RGE for the renormalized operators in  $\overline{\text{MS}}$ ,

$$\mu \frac{d}{d\mu} f_i(\xi, \mu) = \int d\xi' \gamma_{ij}(\xi, \xi') f_j(\xi', \mu) \quad (8.49)$$

where

$$\gamma_{ij} = - \int d\xi'' Z_{ii'}^{-1}(\xi, \xi'') \mu \frac{d}{d\mu} Z_{i'j}(\xi'', \xi'). \quad (8.50)$$

At 1-loop we can take  $Z_{ii'}^{-1}(\xi, \xi'') = \delta_{ii'} \delta(\xi - \xi'') + \dots$  so that

$$\gamma_{ij}^{\text{1-loop}} = -\mu \frac{d}{d\mu} [Z_{ij}(\xi, \xi')]^{\text{1-loop}} \quad (8.51)$$

Computing the PDF at tree level, we obtain

$$= \underbrace{\bar{u}_n \frac{\not{n}}{2} u_n}_{p^-} \delta(\omega - p^-) = \delta(1 - \omega/p^-) \quad (8.52)$$

At the 1-loop level there are multiple contributions the first contribution yields the computation

$$= -ig^2 C_F \int d^d l \frac{p^-(d-2)l_1^2}{[l^2 + i0]^2 [(l-p)^2 + i0]} \delta(l^- - \omega) \frac{\mu^{2\epsilon} e^{\epsilon\gamma_E}}{(4\pi)^\epsilon} \quad (8.53)$$

$$= \frac{2g^2}{(4\pi)^2} (1-\epsilon)^2 \Gamma(\epsilon) e^{\epsilon\gamma_E} (1-z)\theta(z)\theta(1-z) \left( \frac{A}{\mu^2} \right)^{-\epsilon} \quad (8.54)$$

$$= \frac{\alpha_s C_F}{\pi} (1-z)\theta(z)\theta(1-z) \left[ \frac{1}{2\epsilon} - 1 - \frac{1}{2} \ln(A/\mu^2) \right] \quad (8.55)$$

where  $A = -p^+p^-z(1-z)$  with  $z = \omega/p^-$ . The next contribution is given by

$$= 2ig^2C_F \int \frac{d^d l}{(l^- - p^-)l^2(l-p)^2} \overbrace{[\delta(l^- - \omega)]}^{\text{real}} - \overbrace{[\delta(p^- - \omega)]}^{\text{virtual}} \quad (8.56)$$

$$= \frac{C_F\alpha_s(\mu)}{\pi} e^{\epsilon\gamma_E} \Gamma(\epsilon) \left[ \frac{z\theta(z)\theta(1-z)}{(1-z)^{1+\epsilon}} \left( \frac{-p^-p^+z - i0}{\mu^2} \right)^{-\epsilon} \right. \quad (8.57)$$

$$\left. - \delta(1-z) \left( \frac{-p^-p^+z - i0}{\mu^2} \right)^{-\epsilon} \frac{\Gamma(2-\epsilon)\Gamma(-\epsilon)}{\Gamma 2 - 2\epsilon} \right] \quad (8.58)$$

We can simplify this result with use of the distribtuion identity.

$$\frac{\theta(1-z)}{(1-z)^{1+\epsilon}} = -\frac{\delta(1-z)}{\epsilon} + \mathcal{L}_0(1-z) - \epsilon\mathcal{L}_1(1-z) + \dots \quad (8.59)$$

where the plus function  $\mathcal{L}_n(x)$  is defined as

$$\mathcal{L}_n(x) = \left[ \frac{\theta(x) \ln^n(x)}{x} \right] \quad (8.60)$$

and satisfies the following identities

$$\int_0^1 dx \mathcal{L}_n(x) = 0, \quad \int_0^1 \mathcal{L}_n(x)g(x) = \int_0^1 dx \frac{\ln^n x}{x} [g(x) - g(0)]. \quad (8.61)$$

With this replacement we find that the  $1/\epsilon^2$  terms in the real and virtual terms cancel and the remaining  $1/\epsilon$  is UV divergent. In the end the explicit contribution of this process is

$$= \frac{C_F\alpha_s(\mu)}{\pi} \left[ \{\delta(1-z) + z\theta(z)\mathcal{L}_0(1-z)\} \left( \frac{1}{\epsilon} + \ln \frac{\mu^2}{-p^+p^-z - i0} \right) \right. \quad (8.62)$$

$$\left. - z\mathcal{L}_2(1-z)\theta(z) + \delta(1-z) \left( 2 - \frac{\pi^2}{6} \right) \right]. \quad (8.63)$$

The last contribution to the renormalized PDF is the wavefunction renormalization of the external fermions.

$$F_i g() = \delta(1-z)(Z_\psi - 1) = \frac{\alpha_s C_F}{\pi} \left[ -\frac{1}{4\epsilon} - \frac{1}{4} - \frac{1}{4} \ln \left( \frac{\mu^2}{-p^+p^- - i0} \right) \right] \delta(1-z) \quad (8.64)$$

There are additional contributions from diagrams such as those in (), but we will ignore these by assuming that the operator is not a flavor singlet. Summing the various contributions, we have

$$\begin{aligned} \text{Sum} &= \frac{C_F\alpha_s(\mu)}{\pi} \left[ \left\{ \frac{3}{4}\delta(1-z) + z\theta(z)\mathcal{L}_0(1-z) + \right. \right. \\ &\quad \left. \left. + \frac{(1-z)}{2}\theta(z)\theta(1-z) \right\} \left( \frac{1}{\epsilon} + \ln \frac{\mu^2}{-p^+p^-z_i0} \right) + \text{finite function of } z \right] \\ &= \frac{C_F\alpha_s(\mu)}{\pi} \left[ \underbrace{\frac{1}{2} \left( \frac{1+z^2}{1-z} \right)}_{\text{Determines } Z_{qq}^{1\text{-loop}}} + \left( \frac{1}{\epsilon} + \ln \frac{\mu^2}{-p^+p^-z_i0} \right) + \dots \text{finite function of } z \right] \quad (8.65) \end{aligned}$$

If we let the total momentum of the hadronic state be  $\hat{p}^-$ . Then define  $p^-/\hat{p}^- = \xi^-$ . So that

$$z = \frac{\omega}{p^-} = \frac{\xi \hat{p}^-}{\xi' \hat{p}^-} = \frac{\xi}{\xi'} \quad (8.66)$$

Then our  $Z_{qq}^{1\text{-loop}}$  becomes

$$Z_{qq}^{1\text{-loop}} = \delta(1-z) + \frac{1}{\epsilon} \frac{\alpha_s(\mu)}{2\pi} C_F \theta z \theta(1-z) \left( \frac{1+z^2}{1-z} \right)_+ \quad (8.67)$$

And usng

$$\gamma_{ij} = -\mu \frac{d}{d\mu} \mathcal{Z}_{ij}(z, \mu), \quad \mu \frac{d}{d\mu} \alpha_s(\mu) = -2\epsilon \alpha_s(\mu) + \beta[\alpha_s(\mu)] \quad (8.68)$$

we then obtain the our final result

$$\gamma_{qq}(\xi, \xi') = \frac{C_F \alpha_s \mu}{\pi} \frac{\theta(\xi' - \xi) \theta(1 - \xi')}{\xi'} \left( \frac{1+z^2}{1-z} \right)_+ \quad (8.69)$$

which is the Aliterelli - Parisi (DGLAP) quark anomalous dimension at one-loop.

### 8.3 General Discussion on Appearance of Convolutions in SCET<sub>I</sub> and SCET<sub>II</sub>

## 9 Dijet Production, $e^+e^- \rightarrow 2$ jets

**(ROUGH)**

The production of jets at an  $e^+e^-$  collider has historically been very important. Measurements of various jet in  $e^+e^-$  collisions were used to validate QCD as the correct theory of the strong interaction, and to this day, even 10 years after the LEP has been turned off, measurements of event shape distributions are being used to study the nature of the strong interaction and to determine fundamental constants of nature such as the coupling constant of the strong interaction.

The dominant kinematical situation in  $e^+e^- \rightarrow$  jets is to produce two jets, but of course a larger number of jets can be obtained by the emission of additional hard strongly interacting particles. In this section we will discuss the production of two jets in  $e^+e^-$  collisions, which is to say the production of energetic particles in two back-to-back directions, accompanied only by usoft radiation in arbitrary regions of phase space.

Clearly, the question whether we have 2 or more jets has to be determined on an event by event basis, and there are many possible observables which can distinguish 2-jet events from events with more than 2 jets. The most natural definition might be to use a jet finding algorithm, and select those events with exactly two hard jets as defined by this algorithm. However, there is another set of observables which can be used to identify 2-jet events, and which are much easier to analyze theoretically. This class of observables are called event shapes, with the most well known event shape variable being thrust. In this section, we will only discuss the thrust distribution in  $e^+e^-$  collisions, but it should be clear from the discussion how one can extend the results to other event shape variables or other 2-jet observables.

### 9.1 Kinematics, Expansions, and Regions

The thrust of an event is defined as follows:

$$T = \max_{\vec{n}_T} \frac{\sum_i |\vec{p}_i \cdot \vec{n}_T|}{\sum_i |\vec{p}_i|} \quad (9.1)$$



The sum over  $i$  runs over all particles in the final state, and the direction  $\vec{n}_T$  is called the thrust axis. To fully understand this equation, let's first ignore the  $\max_{\vec{n}_T}$  and pick a fixed direction  $\vec{n}_T$ . Thrust is then defined by summing the absolute value of the projections of the momenta of all particles onto the thrust axis, and divide by the sum over the magnitude of all momenta. In the situation where the momenta of all particles are aligned (or anti-aligned) exactly with the thrust axis, the magnitude of the projection onto the thrust axis is exactly equal to the magnitude of the momentum itself, such that one obtains  $T = 1$ . Thus, energetic particles that are collinear or anti-collinear to the thrust axis give  $T \approx 1$ . Soft particles with vanishing momentum do not contribute to the thrust, since their contributions vanish in the numerator and denominators. Thus, events with  $T \approx 1$  only contain particles which are either collinear or anti-collinear to the thrust axis, or are usoft, and are therefore 2-jet like and can be described by SCET<sub>I</sub>. For later convenience we will often choose the variable

$$\tau = 1 - T \quad (9.2)$$

instead of  $T$  itself. In this case the 2-jet case corresponds to  $\tau \rightarrow 0$ , while  $\tau$  away from zero corresponds to three or more jets.

To make the connection of thrust with SCET even more obvious, we will define the two four-vectors

$$n^\mu = (1, \vec{n}_T), \quad \bar{n}^\mu = (1, -\vec{n}_T) \quad (9.3)$$

Using this definition, we can write

$$\begin{aligned} T &= \frac{Q - \sum_{i \in R} n \cdot p_i - \sum_{i \in L} \bar{n} \cdot p_i}{Q} \\ \Rightarrow \tau &= \frac{\sum_{i \in R} n \cdot p_i + \sum_{i \in L} \bar{n} \cdot p_i}{Q} \end{aligned}$$

## 9.2 Factorization

The thrust distribution in the full theory is given by summing over all final states in the event, and projecting each event onto its value of thrust, defined by (9.1)

$$\frac{d\sigma}{d\tau} = \frac{1}{2Q^2} \sum_X |M(e^+e^- \rightarrow X)|^2 (2\pi)^4 \delta^4(q - p_X) \delta(\tau - \tau(X)). \quad (9.4)$$

Here  $M(e^+e^- \rightarrow X)$  is the full QCD matrix element to produce the final state  $X$  from the collisions of an  $e^+e^-$  pair.

To obtain the expression in SCET, we need to match the full QCD matrix element onto operators in SCET. As was already discussed in Section Since we only consider final states with energetic particles collinear to either the direction  $n^\mu$  or  $\bar{n}^\mu$ , the appropriate operator in SCET is

$$O_{n\bar{n}} = \bar{\chi}_{\bar{n}} \Gamma \chi_n \quad (9.5)$$

where  $\chi_n$  is the gauge invariant quark jet field introduced in (6.20) and  $\Gamma$  is a Dirac structure that describes the production of a  $q\bar{q}$  field from a  $\gamma/Z$  boson. Thus, the matching from full QCD onto SCET can be written as

$$M(e^+e^- \rightarrow X) = C_{n\bar{n}} \langle 0 | O_{n\bar{n}} | X \rangle \quad (9.6)$$

such that we can write

$$\frac{d\sigma}{d\tau} = \frac{1}{2Q^2} \sum_n |C_{n\bar{n}}|^2 \sum_X |\langle 0 | O_{n\bar{n}} | X \rangle|^2 (2\pi)^4 \delta^4(q - p_X) \delta(\tau - \tau(X)) \quad (9.7)$$

$$\frac{d\sigma}{dM^2 d\bar{M}^2} = \sigma_0 H(Q, \mu) \int dl^+ dl^- J_n(M^2 - Ql_{,\mu}^+) J_{\bar{n}}(\bar{M}^2 - Ql_{,\mu}^-) S(l^+, l^-) \quad (9.8)$$

### 9.3 Perturbative Results

### 9.4 Results with Resummation

## 10 SCET II

**(ROUGH)** When soft gluons interact with collinear particles, the resulting particle has momentum  $Q(\lambda, 1, \lambda)$  and is therefore off the SCET mass shell.

$$q = q_s + q_c \sim Q(\lambda, 1, \lambda) \rightarrow q^2 = Q^2 \lambda \gg (Q\lambda)^2 \quad (10.1)$$

Consequently, these offshell particles can be integrated out of the theory. Analogous to our definition of the ultra-soft wilson line, we can define a soft wilson line  $S[n \cdot A_s]$  resulting from integrating out the offshell particles.

$$S_n = \left[ \sum_{\text{perms}} \exp \left( -g \frac{1}{n \cdot} \mathcal{P} n \cdot A_{s,q} \right) \right] \quad (10.2)$$

Aslo, similar to the usoft case, gauge invariance restricts the placement of factors of  $S$  in operators. For example, we use our canonical heavy to light (soft to collinear) current. under soft and collinear gauge transformations, the fields transform as

$$\text{soft: } h_v \rightarrow U_s h_v \quad \xi_{n,p} \rightarrow \xi_{n,p} \quad (10.3)$$

$$\text{collinear: } h_v \rightarrow h_v \quad \xi_{n,p} \rightarrow \mathcal{U}_{p-Q} \xi_{n,Q} \quad (10.4)$$

The fact that our standard current  $J = \bar{\xi}_{n,p} W_n \Gamma^\mu h_v$  is not gauge invariant under the soft transformations suggests that it is an incomplete description of the physics of this process. We can make this current soft gauge invariant by including the soft Wilson line. The soft Wilson line  $S_n$  transforming as

$$S_n \rightarrow U_s S \quad (10.5)$$

makes the current

$$J = \bar{\xi}_{n,p} W \Gamma^\mu S^\dagger h_v \quad (10.6)$$

gauge invariant. We may also build up this current by a diagrammatic analysis. Necessary to the procedure is the fact that only  $n \cdot A_{us}$  component of the usoft gluon builds up  $S$  (EXPLANATION) and only the  $\bar{n} \cdot A_{n,q}$  component of the collinear gluon build up  $W$ . The simplest diagram for soft- collinear coupling, where collinear and soft gluons take the quarks off-shell is given in

Diagram.

This diagram yields the current

$$\text{Fig } () = -g^2 \frac{n^\mu}{n \cdot q_s} \frac{\bar{n}^\nu}{\bar{n} \cdot q_c} \bar{\xi}_{n,q} T^a \Gamma T^b h_v. \quad (10.7)$$

But we have a problem. This current appears to have the color factors  $a$  and  $b$  in the wrong order. With  $a$  representing soft gluons and  $b$  representing collinear gluons this current appears to be derived from the

operator  $\bar{\xi}_{n,p} S^\dagger \Gamma^\mu W h_v$  which is not equivalent to (10.6) because  $S$  and  $W$  do not commute. This apparent problem is solved by considering the remaining two diagrams of the same order as this one

Diagrams.

These diagrams both yield the current

$$\text{Fig}() = \text{Fig}() = \frac{g^2}{2} i f^{abc} T^c \frac{n^\mu}{n \cdot q^s} \frac{\bar{n}^\nu}{\bar{n} \cdot q_c} \bar{\xi}_{n,p} \Gamma h_v. \quad (10.8)$$

Adding the three graphs together, reverses the order of the color indices (by virtue of  $[T^a, T^b] = i f^{abc}$ ) to give

$$\text{Fig}() + \text{Fig}() + \text{Fig}() = -g^2 \frac{n^\mu}{n \cdot q_s} \frac{\bar{n}^\nu}{\bar{n} \cdot q_c} \bar{\xi}_{n,q} T^b \Gamma T^a h_v \quad (10.9)$$

which is the correct ordering for the gauge invariant current in (10.6). This procedure can be extended to all orders as in (Reference).

We may construct SCET operators by another method using SCET<sub>I</sub>. The basis of the procedure comes from the fact that soft-modes in SCET<sub>II</sub> and usoft modes in SCET<sub>I</sub> have the same momentum; it is only the collinear fields which have distinct momenta. The exact procedure for obtaining SCET<sub>II</sub> is

1. Match QCD onto SCET<sub>I</sub>
2. Redefine fields with the usoft wilson line  $Y_n$  so that usoft interactions are only present in currents
3. Match SCET<sub>I</sub> onto SCET<sub>II</sub> by taking  $Y_n \rightarrow S_n$ .

As an example of the above procedure we may construct the SCET<sub>II</sub> current postulate above.

1. Matching QCD onto SCET<sub>I</sub>

$$J = \bar{u} \Gamma^\mu b \rightarrow J_I = (\bar{\xi}_n W) \Gamma^\mu h_v \quad (10.10)$$

2. Redefining fields so that usoft interactions are only present in currents

$$J_I = (\bar{\xi}_n^{(0)} W^{(0)}) \Gamma^\mu Y^\dagger h_v \quad (10.11)$$

3. Matching SCET<sub>I</sub> onto SCET<sub>II</sub> by taking  $Y_n \rightarrow S_n$ .

$$J_{II} = (\bar{\xi}_n^{(0)} W^{(0)}) \Gamma^\mu S^\dagger h_v \quad (10.12)$$

## 11 SCET<sub>II</sub> Applications

**(ROUGH)** In this section we will apply the SCET<sub>II</sub> formalism developed in previous sections to various processes to illustrate the formalism

- $\gamma^* \gamma \rightarrow \pi^0$
- $B \rightarrow D\pi$
- The Massive Gauge Boson Sudakov Form Factor
- $p_T$  distribution in Higgs production

- Jet broadening

A distinguishing feature of these processes is whether they involve a new type of divergence that requires a renormalization procedure, known as rapidity divergences. The first two processes do not, while the last three do. We will discuss these divergences in detail for the massive gauge boson form factor, and then be very brief about the last two examples.

### 11.1 $\gamma^*\gamma \rightarrow \pi^0$

#### 11.2 $B \rightarrow D\pi$

**(ROUGH)** As another exclusive scattering process, we analyze  $B \rightarrow D\pi$ . We may use the SCET framework here because the hard scales  $Q = \{m_b, m_c, E_\pi\} \gg \Lambda_{QCD}$ . At the scale  $\mu \sim m_b$  the QCD operators represented by the weak Hamiltonian are

$$H_W = \frac{4G_F}{\sqrt{2}} V_{ud}^\dagger V_{cb} [C_0^F(\mu_0) O_0(\mu_0) + C_8^F(\mu_0) O_8(\mu_0)] \quad (11.1)$$

where

$$O_0 = [\bar{c}\gamma^\mu P_L b][\bar{d}\gamma_\mu P_L u] \quad (11.2)$$

$$O_8 = [\bar{c}\gamma^\mu P_L T^a b][\bar{d}\gamma_\mu P_L T^a u]. \quad (11.3)$$

We want to factorize the matrix element  $\langle D\pi | O_{0,8} | B \rangle$ . We can represent this factorization diagrammatically as (INSERT FIG) where there are no gluons between  $\pi$  quarks and  $B/D$  quarks. For this process we expect a  $B \rightarrow D$  form factor (Isgur-Wise form factor) and a pion wavefunction/distribution. This factorization will be possible because the particles  $B$  and  $D$  have soft momentum scaling and  $\pi$  has collinear scalings. Specifically  $p_c^2 \sim \Lambda^2$  and we therefore use SCET<sub>II</sub> to describe this process.

First, matching the QCD Hamiltonian onto SCET we need the operators

$$Q_0^{1,5} = [\bar{h}_{v'}^{(c)} \Gamma_h^{1,5} h_v^{(b)}] [\bar{\xi}_{n,p}^{(d)} W \Gamma_l C_0(\bar{\mathcal{P}}_+) W^\dagger \xi_{n,p}^{(u)}] \quad (11.4)$$

$$Q_8^{1,5} = [\bar{h}_{v'}^{(c)} \Gamma_h^{1,5} T^a h_v^{(b)}] [\bar{\xi}_{n,p}^{(d)} W \Gamma_l C_8(\bar{\mathcal{P}}_+) T^a W^\dagger \xi_{n,p}^{(u)}] \quad (11.5)$$

where  $\Gamma_h^1 = \frac{\not{h}}{2}$ ,  $\Gamma_h^5 = \frac{\not{h}}{2} \gamma_5$  and  $\Gamma_l = \frac{\not{h}}{4} (1 - \gamma_5)$ . Note that the two operators  $O_0$  and  $O_8$  can both produce any of the  $Q_{0,8}^{1,5}$  operators. Now, implementing field redefinitions to factor usoft effects (remember we can start with SCET<sub>I</sub> to derive SCET<sub>II</sub> results) we have

$$\begin{aligned} \xi_{n,p} &= Y \xi_{n,p}^{(0)} \\ W &= Y W^{(0)} Y^\dagger \end{aligned}$$

These redefinitions are easily implemented in  $Q_0^{1,5}$ . They simply take

$$[\bar{\xi}_{n,p'}^{(d)} W \Gamma_l C_0(\bar{\mathcal{P}}_+) W^\dagger \xi_{n,p}^{(u)}] \rightarrow [\bar{\xi}_{n,p'}^{(d)(0)} W^{(0)} \Gamma_l C_0(\bar{\mathcal{P}}_+) W^{(0)\dagger} \xi_{n,p}^{(u)(0)}] \quad (11.6)$$

where we used the fact that  $Y$  commutes with the wilson coefficient  $C_0(\bar{\mathcal{P}}_+)$ . This argument cannot be applied to  $Q_8^{1,5}$  because  $Y$ , containing generators of its own, does not commute with  $T^a$ . However, by making use of the color identity

$$T^a \otimes Y^\dagger T^a Y = Y T^a Y^\dagger \otimes T^a \quad (11.7)$$

then we may move all usoft wilson lines into the usoft part of the operator yielding

$$Q_{\mathbf{8}}^{1,5} = [\bar{h}_{v'}^{(c)} \Gamma_h^{1,5} Y T^a Y^\dagger h_v^{(b)}] [\bar{\xi}_{n,p'}^{(d)} W \Gamma_l C_8(\bar{\mathcal{P}}_+) T^a W^\dagger \xi_{n,p}^{(u)}]. \quad (11.8)$$

Matching this SCET<sub>I</sub> result onto SCET<sub>II</sub> by the replacements  $Y \rightarrow S$  and  $\xi^{(0)} \rightarrow \xi$ ,  $W^{(0)} \rightarrow W$ , we have

$$Q_{\mathbf{0}}^{1,5} = [\bar{h}_{v'}^{(c)} \Gamma_h^{1,5} h_v^{(b)}] [\bar{\xi}_{n,p'}^{(d)} W \Gamma_l C_0(\bar{\mathcal{P}}_+) W^\dagger \xi_{n,p}^{(u)}] \quad (11.9)$$

$$Q_{\mathbf{8}}^{1,5} = [\bar{h}_{v'}^{(c)} \Gamma_h^{1,5} Y T^a Y^\dagger h_v^{(b)}] [\bar{\xi}_{n,p'}^{(d)} W \Gamma_l C_8(\bar{\mathcal{P}}_+) T^a W^\dagger \xi_{n,p}^{(u)}]. \quad (11.10)$$

Now, taking the matrix elements between the appropriate hadronic states we have

$$\langle \pi_n^- | \bar{\xi}_n W \Gamma_l C_0(\bar{\mathcal{P}}_+) W^\dagger \xi_n | 0 \rangle = \frac{i}{2} f_\pi E_\pi \int_0^1 dx C(2E_\pi(2x-1)) \phi_\pi(x) \quad (11.11)$$

$$\langle D_{v'} \pi_n^- | \bar{h}_{v'} \Gamma h_v | B \rangle = N' \xi(\omega_0, \mu). \quad (11.12)$$

We are able to achieve this factorization because with  $B$ ,  $D$  purely soft and  $\pi$  purely collinear there are no contractions between soft and collinear fields. So we find that our final factorization result is

$$\langle \pi D | H_W | B \rangle = i N \xi(\omega_0, \mu) \int_0^1 C(2E_\pi(2x-1), \mu) \phi_\pi(x, \mu) + O(\Lambda/Q) \quad (11.13)$$

where  $\xi(\omega_0, \mu)$  is the Isgur-Wise function at maximum recoil and

$$\omega_0 = \frac{m_B^2 - m_D^2}{2m_B} \quad (11.14)$$

This result also applies to other  $B$  decays such as

$$\begin{aligned} \bar{B}^0 &\rightarrow D^+ \pi^-, & \bar{B}^0 &\rightarrow D^{*+} \pi^-, & \bar{B}^0 &\rightarrow D^+ \rho^- \\ \bar{B}^- &\rightarrow D^0 \pi^-, & B^- &\rightarrow D^{*0} \pi^-, & \bar{B}^0 &\rightarrow D^+ \rho^- \end{aligned}$$

### 11.3 Massive Gauge Boson Form Factor & Rapidity Divergences

#### 11.4 $p_T$ Distribution for Higgs Production & Jet Broadening

## 12 More SCET<sub>I</sub> Applications

(ROUGH)

In this section we will apply the SCET formalism developed in previous sections to a few additional processes that either use SCET<sub>I</sub> or a combination of both SCET<sub>I</sub> and SCET<sub>II</sub> (where the more complicated part of the factorization occurs within SCET<sub>I</sub>). In particular we will consider

- $B \rightarrow X_s \gamma$
- Drell-Yan  $p\bar{p} \rightarrow l^+ l^- X$ : inclusive, endpoint, and isolated factorization theorems

12.1  $B \rightarrow X_s \gamma$ 

**(ROUGH)** In this section we treat the inclusive weak radiative decay  $B \rightarrow X_s \gamma$ . This decay is defined by the effective Hamiltonian

$$\mathcal{H} = -\frac{4G_F}{\sqrt{2}} V_{tb} V_{ts}^* C_7 \mathcal{O}_7, \quad \mathcal{O}_7 = \frac{e}{16\pi^2} m_b \bar{s} \sigma_{\mu\nu} F^{\mu\nu} P_R b \quad (12.1)$$

with  $F^{\mu\nu}$  the electromagnetic field tensor and  $P_R = \frac{1}{2}(1 + \gamma_5)$ . The decay is defined such that the photon momentum is opposite the collinear jet i.e.  $q_\mu = E_\gamma \bar{n}_\mu$ .

The photon energy spectrum of the decay is

$$\frac{1}{\Gamma_0} \frac{d\Gamma}{dE_\gamma} = \frac{4E_\gamma}{m_b^3} \left( -\frac{1}{\pi} \right) \text{Im} T(E_\gamma) \quad (12.2)$$

where

$$T(E_\gamma) = \frac{i}{m_b} \int d^4x e^{-iqx} \langle \bar{B}_v | T J_\mu^\dagger(x) J^\mu(0) | \bar{B}_v \rangle \quad (12.3)$$

Is the forward scattering amplitude with EM current  $J_\mu = \bar{s} i \sigma_{\mu\nu} q^\nu P_R b$ .

We will consider the endpoint region of the decay in which nearly all of the final state energy is in the photon. Analyzing this process in the rest frame of  $B$ , we find that the final momentum  $X$

$$p_X^\mu = p_B^\mu - q^\mu \quad (12.4)$$

$$= \frac{m_b}{2} (n^\mu + \bar{n}^\mu) - E_\gamma \bar{n}^\mu \quad (12.5)$$

$$= m_b \frac{\bar{n}^\mu}{2} + \frac{\bar{n}^\mu}{2} (m_b - 2E_\gamma). \quad (12.6)$$

Defining our endpoint region by

$$\frac{m_b}{2} - E_\gamma \leq \Lambda_{QCD} \quad (12.7)$$

gives us a mass squared scale of

$$p_X^2 \simeq m_b \Lambda = m_b^2 \frac{\Lambda}{m_b} = m_b^2 \lambda^2 \quad (12.8)$$

where in the last line we took  $\lambda = \sqrt{\frac{\Lambda}{m_b}}$ . Taking  $m_b$  as  $Q$  it is clear that this process is described by SCET<sub>I</sub>. Specifically,  $X$  will be represented by collinear gluons and quarks while  $B$  will be represented by heavy (usoft) quark. Our principal goal is to demonstrate how the effects of momentum scales are factorized in the formula for the photon energy spectrum. To this end we will prove that (12.2) can be factorized as

$$\frac{1}{\Gamma_0} \frac{d\Gamma}{dE_\gamma} = H(m_b, \mu) \int_{2E_\gamma - m_b}^\Lambda dk^+ S(k^+, \mu) J(k^+ + m_b - 2E_\gamma, \mu) \quad (12.9)$$

where  $H(m_b, \mu)$  is a calculable quantity arising from hard scale dynamics;  $S(k^+, \mu)$  is a non-perturbative soft function; and  $J(k^+)$  represents collinear gluons and quarks and is called the jet function.

We begin by matching the QCD current onto SCET to obtain

$$J_\mu = -E_\gamma e^{i(\bar{\mathcal{P}} \frac{n}{2} + \mathcal{P}_\perp - m_b v) \cdot x} C(\bar{\mathcal{P}}, \mu) \bar{\xi}_{n,p} W \gamma_\mu^\perp P_L h_v \quad (12.10)$$

$$= -E_\gamma C(m_b, \mu) \bar{\xi}_{n,p} W \gamma_\mu^\perp P_L h_v \quad (12.11)$$

where in the second line we used the label momentum conservation to set  $\bar{\mathcal{P}} = m_b$  and  $\mathcal{P}_\perp = 0$ . Inserting this result into (12.3), we may write

$$\frac{4E_\gamma}{m_b^3} T(E_\gamma) \equiv H(m_b, \mu) T_{\text{eff}}(E_\gamma, \mu) \quad (12.12)$$

where

$$T_{\text{eff}} = i \int d^4x e^{i(m_b \frac{\bar{n}}{2} - q) \cdot x} \langle \bar{B}_v | \text{T} J_{\text{eff}}^\mu(x) J_{\mu \text{eff}} | \bar{B}_v \rangle. \quad (12.13)$$

This gives us a hard amplitude of

$$H(m_b, \mu) = \frac{4E_\gamma^3}{m_b^3} |C(m_b, \mu)|^2. \quad (12.14)$$

Next, we decouple soft gluons from collinear fields by implementing the standard field redefinitions

$$\xi_{n,p} \rightarrow Y \xi_{n,p}^{(0)} \quad W \rightarrow Y W^{(0)} Y^\dagger \quad (12.15)$$

thus giving us a new effective current:

$$J_{\text{eff}}^\mu = \bar{\xi}_n^{(0)} W^{(0)} \gamma_\mu^\perp P_L Y^\dagger h_v. \quad (12.16)$$

Substituting this result into (12.13) gives us

$$T_{\text{eff}} = i \int d^4x e^{i(m_b \frac{\bar{n}}{2} - q) \cdot x} \langle \bar{B}_v | \text{T} [\bar{h}_v Y P_R \gamma_\mu^\perp W^{(0)\dagger} \xi_{n,p}^{(0)}(x) [\bar{\xi}_{n,p}^{(0)} W^{(0)} \gamma_\mu^\perp P_L Y^\dagger h_v](0) | \bar{B}_v \rangle \quad (12.17)$$

$$= - \int d^4x \int \frac{d^4k}{(2\pi)^4} e^{i(m_b \frac{\bar{n}}{2} - q - k) \cdot x} \langle \bar{B}_v | \text{T} [\bar{h}_v Y](x) P_R \gamma_\mu^\perp \frac{\not{n}}{2} \gamma_\mu^\perp P_L [Y^\dagger h_v](0) | \bar{B}_v \rangle J_P(k) \quad (12.18)$$

$$= \frac{1}{2} \int d^4x \int \frac{d^4k}{(2\pi)^4} e^{i(m_b \frac{\bar{n}}{2} - q - k) \cdot x} \langle \bar{B}_v | \text{T} [\bar{h}_v Y](x) [Y^\dagger h_v](0) | \bar{B}_v \rangle J_P(k), \quad (12.19)$$

where we defined

$$i \int \frac{d^4k}{(2\pi)^4} \langle 0 | \text{T} [W^{(0)\dagger} \xi_{n,p}^{(0)}(x) [\bar{\xi}_{n,p}^{(0)} W^{(0)}](0) | 0 \rangle \quad (12.20)$$

with the label  $P$  representing the sum of the label momentum carried by the collinear fields. (Additional Derivation)? Now, noting that  $J_P$  only depends on the  $k^+$  component of residual momentum  $k$ , we may do the  $k^-$  and  $k^+$  integrals thus putting  $x$  on the light cone

$$\begin{aligned} T_{\text{eff}} &= \frac{1}{2} \int d^4x e^{i(m_b \frac{\bar{n}}{2} - q) \cdot x} \delta(x^+) \delta(x_\perp) \int \frac{dk_\perp}{2\pi} e^{-\frac{i}{2} k_+ x^-} \langle \bar{B}_v | \text{T} [\bar{h}_v Y](x) [Y^\dagger h_v](0) | \bar{B}_v \rangle J_P(k^+) \\ &= \frac{1}{2} \int dk^+ J_P(k^+) \int \frac{dx^-}{4\pi} e^{-\frac{i}{2} (2E_\gamma - m_b + k^+) x^-} \langle \bar{B}_v | \text{T} [\bar{h}_v Y] \left( \frac{n}{2} x^- \right) [Y^\dagger h_v](0) | \bar{B}_v \rangle. \end{aligned} \quad (12.21)$$

Focusing on the heavy fields, we may then define

$$\begin{aligned}
S(k^+) &\equiv \frac{1}{2} \int \frac{dx^-}{4\pi} e^{-\frac{i}{2}l^+x^-} \langle \bar{B}_v | T[\bar{h}_v Y] (\frac{n}{2}x^-) [Y^\dagger h_v](0) | \bar{B}_v \rangle & (12.22) \\
&= \frac{1}{2} \int \frac{dx^-}{4\pi} e^{-\frac{i}{2}l^+x^-} \langle \bar{B}_v | T e^{x^- \frac{n}{2} \cdot \partial} [\bar{h}_v Y](0) [Y^\dagger h_v](0) | \bar{B}_v \rangle \\
&= \frac{1}{2} \int \frac{dx^-}{4\pi} e^{-\frac{i}{2}l^+x^-} \langle \bar{B}_v | T[\bar{h}_v Y](0) e^{-x^- \frac{n}{2} \cdot \partial} [Y^\dagger h_v](0) | \bar{B}_v \rangle \\
&= \frac{1}{2} \int \frac{dx^-}{4\pi} e^{-\frac{i}{2}l^+x^-} \langle \bar{B}_v | T \bar{h}_v Y e^{\frac{ix^-}{2} n \cdot \partial} Y^\dagger h_v | \bar{B}_v \rangle \\
&= \frac{1}{2} \int \frac{dx^-}{4\pi} e^{-\frac{i}{2}l^+x^-} \langle \bar{B}_v | T \bar{h}_v e^{i\frac{x^-}{2} (in \cdot D_{us})} h_v | \bar{B}_v \rangle \\
&= \frac{1}{2} \langle \bar{B}_v | \bar{h}_v \delta(in \cdot D_{us} - l^\dagger) h_v | \bar{B}_v \rangle. & (12.23)
\end{aligned}$$

The Soft function  $S(k^+)$  is non-perturbative and encodes information about the usoft dynamics of the  $B$  meson. (12.22) shows that we may interpret this result as giving the probability of finding a heavy quark  $b$  inside the  $\bar{B}$  meson carrying a residual momentum of  $k^+$ . Defining  $J(k^+) = -\frac{1}{\pi} \text{Im} J_P(k^+)$  and using (12.12), (12.21), (12.22) in (12.2), we have the final result

$$\boxed{\frac{1}{\Gamma_0} \frac{d\Gamma}{dE_\gamma} = \underbrace{H(m_b, \mu)}_{p^2 \sim m_b^2 \text{ Hard}} \int_{2E_\gamma - m_b}^{\bar{\Lambda}} dl^+ \underbrace{S(l^+)}_{p^2 \sim \Lambda^2 \text{ Usoft}} \underbrace{J(l^+ + m_b - 2E_\gamma)}_{p^2 \sim m_b \Lambda \text{ Collinear}}} \quad (12.24)$$

## 12.2 Drell-Yan: $pp \rightarrow Xl^+l^-$

**(ROUGH)** Our final example will be the Drell-Yan (DY) process  $p\bar{p} \rightarrow Xl^+l^-$ . This is a protypic LHC process. The kinematics of this process can be described by the following set of equations.

$$p_A + p_B = p_X + q \quad (12.25)$$

$$E_{cm}^2 = (p_A + p_B)^2 \quad \text{Collision Energy} \quad (12.26)$$

$$q^2 \quad : \quad \text{Hard scale of the problem} \quad (12.27)$$

$$\tau \equiv q^2/E_{cm}^2 \leq 1 \quad (12.28)$$

$$Y = \frac{1}{2} \ln \left( \frac{p_b \cdot q}{p_a \cdot q} \right) \quad \text{Total lepton rapidity (angular variable)} \quad (12.29)$$

And the analogs of the Bjorken Variables from DIS:

$$x_a \equiv \sqrt{\tau} e^Y, \quad x_b \equiv \sqrt{\tau} e^{-Y}, \quad (12.30)$$

where  $\tau \leq x_{a,b} \leq 1$ . We study this process int three distinct energy regions

$$\begin{aligned}
\cdot \text{Inclusive:} & \quad \tau \sim 1 \quad p_x^2 \sim q^2 \sim E_{cm}^2 \quad x_{a,b} \sim 1, \xi_{a,b} \sim 1 \\
\cdot \text{Endpoint:} & \quad \tau \rightarrow 1 \quad p_x^2 \ll q^2 \rightarrow E_{cm}^2 \quad x_{a,b} \rightarrow 1, \xi_{a,b} \rightarrow 1 \\
\cdot \text{Isolated:} & \quad \tau \rightarrow 0 \quad p_x^2 \gg q^2 \quad x_{a,b} \rightarrow 0, \xi_{a,b} \rightarrow 0
\end{aligned} \quad (12.31)$$

We now analyze these specific processes in detail.

**Inclusive** In this case this process represents an  $SCET_I$  problem of hard-collinear factorization. we have



a 4-quark operator in SCET, which after a Fierz Identity becomes,

$$[(\bar{\xi}_n W_n) \frac{\not{n}}{2} (W_n^\dagger \xi_n)] [(\bar{\xi}_{\bar{n}} W_{\bar{n}}) \frac{\not{n}}{2} (W_{\bar{n}}^\dagger \xi_{\bar{n}})] \quad (12.32)$$

**Remarks:**

- $T^A \otimes T^A$  octet structure vanishes under  $\langle p_n | \cdot | p_n \rangle$
- When we take  $\xi_n \rightarrow Y_n \xi_n$  for coupling to soft gluons, the soft wilson lines cancel out.
- This operator encodes information about the PDF because both

$$\langle p_n | \chi_{n,\omega} \frac{\not{n}}{2} \chi_{n,\omega'} | p_n \rangle \quad \text{and} \quad \langle p_{\bar{n}} | \chi_{\bar{n},\omega} \frac{\not{n}}{2} \chi_{\bar{n},\omega'} | p_{\bar{n}} \rangle \quad (12.33)$$

are defined as PDFs. These PDFs contribute to the differential cross section for this process:

$$\frac{1}{\sigma_0} \frac{d\sigma}{dq^2 dY} = \sum_{i,j} \int_{x_a}^1 \frac{d\xi_a}{\xi_a} \int_{x_b}^1 \frac{d\xi_b}{\xi_b} H_{ij}^{\text{incl}} \left( \frac{x_a}{\xi_a}, \frac{x_b}{\xi_b}, q^2, \mu \right) f_i(\xi_a, \mu) f_j(\xi_b, \mu) \quad (12.34)$$

$$= \left[ 1 + \mathcal{O} \left( \frac{\Lambda_{QCD}}{\sqrt{q^2}} \right) \right]. \quad (12.35)$$

- As a last important caveat, we note that Glauber Gluons cancel out at leading order. However, proving this result is out of the scope of our current discussion.

**Threshold Limit** In the threshold limit only the terms of  $H_{ij}^{\text{incl}}$  most singular in  $1 - \tau$  contribute.

$$H_{ij}^{\text{incl}} \rightarrow S_{q\bar{q}}^{\text{thr}} \left[ \sqrt{q^2} \left( 1 - \frac{\tau}{q_a q_b} \right), \mu \right] H_{ij}(q^2, \mu) [1 + \mathcal{O}(1 - \tau)] \quad (12.36)$$

where  $i, j = u\bar{u}, d\bar{d}, \dots$ . The interpretation when we take  $\xi_{a,b} \rightarrow 1$  is that one parton in each proton carries all the momentum. This is not the dominant LHC region.

**Isolated DY** The isolated case of DY allows forward jets to carry away part of  $E_{cm}$ , so  $\xi_{a,b} \rightarrow 1$ . It also restricts the central region to still only have soft radiation (the signal region is background free). To guarantee this requires an experimental observation. **Observable:**  $p_X = B_a + B_b$ . There are two hemispheres perpendicular to the beam axis.

$$B_a^+ = n_a \cdot B_a = \sum_{k \in a} n_a \cdot p_k \quad (12.37)$$

$$= \sum_{k \in a} E_k (1 + \tanh Y_k) e^{-2Y_k} \quad (12.38)$$

We expect the plus momenta for  $n$ -collinear radiation to be small. We find that this is indeed the case because

$$B_a^+ \leq Q e^{-2Y_{\omega t}} \ll Q \quad (12.39)$$

and there is an identical expression for  $B_b^+$ . For the  $n$ -collinear proton (a) and jet (a), we do not merely get a PDF from the hard-collinear-soft factorization. We get something new called a beam function. The

differential cross section for this process can be written as

$$\begin{aligned} \frac{1}{\sigma_0} \frac{d\sigma}{dq^2 dY dB_a^+ dB_b^+} &= \sum_{ij} H_{ij}(q^2, \mu) \int dk_a^+ dk_b^+ Q^2 B_i[\omega_a(B_a^+ - k_a^+), x_a, \mu] B_j[\omega_b(B_b^+ - k_b^+), x_b, \mu] \\ &\times S_{i\text{hemi}}(k_a^+, k_b^+, \mu) \left[ 1 + \mathcal{O}\left(\frac{\Lambda_{QCD}}{Q}, \frac{\sqrt{B_{a,b}\omega_{a,b}}}{Q}\right) \right] \end{aligned} \quad (12.40)$$

where  $\omega_{a,b} = x_{a,b} E_{cm}$  and  $B_i$  is defined as our "Beam Function."

$$B_q(\omega b^+, \omega/\hat{p}^-, \mu) = \frac{\theta(\omega)}{\omega} \int \frac{dy^-}{4\pi} e^{ib^+ y/2} \langle p_n(\hat{p}^-) | \bar{\chi}_n(y^- \frac{n}{2}) \delta(\omega - \bar{\mathcal{P}}) \frac{\bar{\eta}}{2} \chi_n(0) | p_n(\hat{p}^-) \rangle \quad (12.41)$$

We recall the definitions of jet function

$$\langle 0 | \bar{\chi}_{n,\omega}(y^- \frac{n}{2}) \frac{\bar{\eta}}{2} \chi_n(0) | 0 \rangle \quad (12.42)$$

and pdf

$$\langle p | \bar{\chi}_{n,\omega}(0) \frac{\bar{\eta}}{2} \chi_n(0) | p \rangle \quad (12.43)$$

We see that the Jet Function is a mix of both. The proton is a collinear field in SCET<sub>II</sub> and the jet is collinear in SCET<sub>I</sub>. Matching SCET<sub>I</sub> to SCET<sub>II</sub> gives us

$$B_i(t, x, \mu) = \sum_i \int_x^1 \frac{d\xi}{\xi} \mathcal{I}_{ij}(t, \frac{x}{\xi}, \mu) f_j(\xi, \mu) \left[ 1 + \mathcal{O}\left(\frac{\Lambda_{QCD}^2}{t}\right) \right] \quad (12.44)$$

$$b_a^\mu = (\xi - x) E_{cm} \frac{n_a}{2} + b_a^+ \frac{\bar{n}_a}{s} + b_{a\perp} \quad (12.45)$$

At tree level the Beam Function is simply

$$B_i(t, x, \mu) = \delta(t) f_i(x, \mu) \quad (12.46)$$

as in the pdf case we can write the RGE for the beam function

$$\mu \frac{d}{d\mu} B_i(t, x, \mu) = \int dt' \gamma_i(t - t', \mu) B_i(t', x, \mu) \quad (12.47)$$

Like the jet function  $B_i$  is independent of mass evolution. The RGE sums  $ln^2(t/\mu)$ , is independent of  $x$  and has no mixing.

## A More on the Zero-Bin

### A.1 0-bin subtractions with a 0-bin field Redefinition

### A.2 0-bin subtractions for phase space integrations

## B Feynman Rules with a mass

If we add a mass the collinear Lagrangian becomes

$$\mathcal{L}_{\xi\xi}^{(0)} = \bar{\xi}_n(x) \left[ in \cdot D + (i\not{D}_\perp - m) \frac{1}{i\bar{n} \cdot D^c} (i\not{D}_\perp + m) \right] \frac{\bar{\eta}}{2} \xi_n(x), \quad (B.1)$$

and the modified Feynman rules are shown in Fig. 12.

$$\begin{aligned}
 (\tilde{p}, p_r) &= i \frac{\not{n}}{2} \frac{\bar{n} \cdot p}{n \cdot p_r \bar{n} \cdot p + p_\perp^2 - m^2 + i\epsilon} \\
 &= ig T^A n_\mu \frac{\not{n}}{2} \\
 &= ig T^A \left[ n_\mu + \frac{\gamma_\mu^\perp (\not{p}_\perp + m)}{\bar{n} \cdot p} + \frac{(\not{p}'_\perp - m) \gamma_\mu^\perp}{\bar{n} \cdot p'} - \frac{(\not{p}'_\perp - m) (\not{p}_\perp + m) \bar{n}_\mu}{\bar{n} \cdot p \bar{n} \cdot p'} \right] \frac{\not{n}}{2} \\
 &= \frac{ig^2 T^A T^B}{\bar{n} \cdot (p-q)} \left[ \gamma_\mu^\perp \gamma_\nu^\perp - \frac{\gamma_\mu^\perp (\not{p}_\perp + m)}{\bar{n} \cdot p} \bar{n}_\nu - \frac{(\not{p}'_\perp - m) \gamma_\nu^\perp}{\bar{n} \cdot p'} \bar{n}_\mu + \frac{(\not{p}'_\perp - m) (\not{p}_\perp + m) \bar{n}_\mu \bar{n}_\nu}{\bar{n} \cdot p \bar{n} \cdot p'} \right] \frac{\not{n}}{2} \\
 &\quad + \frac{ig^2 T^B T^A}{\bar{n} \cdot (q+p')} \left[ \gamma_\nu^\perp \gamma_\mu^\perp - \frac{\gamma_\nu^\perp (\not{p}_\perp + m)}{\bar{n} \cdot p} \bar{n}_\mu - \frac{(\not{p}'_\perp - m) \gamma_\mu^\perp}{\bar{n} \cdot p'} \bar{n}_\nu + \frac{(\not{p}'_\perp - m) (\not{p}_\perp + m) \bar{n}_\mu \bar{n}_\nu}{\bar{n} \cdot p \bar{n} \cdot p'} \right] \frac{\not{n}}{2}
 \end{aligned}$$

 Figure 12: Order  $\lambda^0$  Feynman rules as in Fig. 6, but with a collinear quark mass.

## C Feynman Rules for the Wilson line $W$

Results for the Feynman rules for the expansion of the  $W$  Wilson line are also useful

$$\begin{aligned}
 W &= 1 - \frac{g T^A \bar{n} \cdot \varepsilon_n^A(q)}{\bar{n} \cdot q} + \dots, \\
 W^\dagger &= 1 + \frac{g T^A \bar{n} \cdot \varepsilon_n^A(q)}{\bar{n} \cdot q} + \dots,
 \end{aligned} \tag{C.1}$$

where here the momentum  $q$  is incoming and  $\varepsilon_n^A$  is the gluon-polarization vector.

## D Feynman Rules for Subleading Lagrangians

In this subsection Feynman rules are given for the subleading quark Lagrangians involving two collinear quarks

$$\begin{aligned}
 \mathcal{L}_{\xi\xi}^{(1)} &= (\bar{\xi}_n W) i \not{D}_{us}^\perp \frac{1}{\bar{n} \cdot \mathcal{P}} (W^\dagger i \not{D}_c^\perp \frac{\not{n}}{2} \xi_n) + (\bar{\xi}_n i \not{D}_c^\perp W) \frac{1}{\bar{n} \cdot \mathcal{P}} i \not{D}_{us}^\perp (W^\dagger \frac{\not{n}}{2} \xi_n) \\
 \mathcal{L}_{\xi\xi}^{(2)} &= (\bar{\xi}_n W) i \not{D}_{us}^\perp \frac{1}{\bar{n} \cdot \mathcal{P}} i \not{D}_{us}^\perp \frac{\not{n}}{2} (W^\dagger \xi_n) + (\bar{\xi}_n i \not{D}_c^\perp W) \frac{1}{\bar{n} \cdot \mathcal{P}^2} i \bar{n} \cdot D_{us} \frac{\not{n}}{2} (W^\dagger i \not{D}_c^\perp \xi_n),
 \end{aligned} \tag{D.1}$$

and for the mixed usoft-collinear Lagrangians from Eq. (??),

$$\begin{aligned}
 \mathcal{L}_{\xi q}^{(1)} &= \bar{\xi}_n \frac{1}{i\bar{n}\cdot D_c} ig\mathcal{B}_c^\perp W q_{us} + \text{h.c.} , \\
 \mathcal{L}_{\xi q}^{(2a)} &= \bar{\xi}_n \frac{1}{i\bar{n}\cdot D_c} igM W q_{us} + \text{h.c.} , \\
 \mathcal{L}_{\xi q}^{(2b)} &= \bar{\xi}_n \frac{\not{\eta}}{2} i\mathcal{D}_\perp^c \frac{1}{(i\bar{n}\cdot D_c)^2} ig\mathcal{B}_\perp^c W q_{us} + \text{h.c.} .
 \end{aligned} \tag{D.2}$$

All Feynman rules for  $\mathcal{L}_{\xi q}^{(i)}$  involve at least one collinear gluon. From  $\mathcal{L}_{\xi q}^{(1)}$  we obtain Feynman rules with zero or one  $A_n^\perp$  gluons and any number of  $\bar{n}\cdot A_n$  gluons. The one and two-gluon results are shown in Fig. 15. For  $\mathcal{L}_{\xi q}^{(2a)}$  we have Feynman rules with zero or one  $\{n\cdot A_n, A_{us}^\perp\}$  gluon and any number of  $\bar{n}\cdot A_n$  gluons. The one and two-gluon results are shown in Fig. 16. Finally, for  $\mathcal{L}_{\xi q}^{(2b)}$  one finds Feynman rules with zero, one, or two  $A_n^\perp$  gluons and any number of  $\bar{n}\cdot A_n$  gluons. In this case the one and two gluon Feynman rules are shown in Fig. 17.

Finally, for the subleading terms in the mixed usoft-collinear gluon action we find

$$\begin{aligned}
 \mathcal{L}_{cg}^{(1)} &= \frac{2}{g^2} \text{tr} \left\{ [iD_0^\mu, iD_c^{\perp\nu}] [iD_{0\mu}, WiD_{us\nu}^\perp W^\dagger] \right\} , \\
 \mathcal{L}_{cg}^{(2)} &= \frac{1}{g^2} \text{tr} \left\{ [iD_0^\mu, WiD_{us}^{\perp\nu} W^\dagger] [iD_{0\mu}, WiD_{us\nu}^\perp W^\dagger] \right\} \\
 &\quad + \frac{1}{g^2} \text{tr} \left\{ W [iD_{us}^{\perp\mu}, iD_{us}^{\perp\nu}] W^\dagger [iD_{c\mu}^\perp, iD_{c\nu}^\perp] \right\} + \frac{1}{g^2} \text{tr} \left\{ [iD_0^\mu, in\cdot D] [iD_{0\mu}, Wi\bar{n}\cdot D_{us} W^\dagger] \right\} \\
 &\quad + \frac{1}{g^2} \text{tr} \left\{ [WiD_{us}^{\perp\mu} W^\dagger, iD_c^{\perp\nu}] [iD_{c\mu}^\perp, WiD_{us\nu}^\perp W^\dagger] \right\} ,
 \end{aligned} \tag{D.3}$$

where  $iD_0^\mu = i\mathcal{D}^\mu + gA_n^\mu$ .

$$\begin{aligned}
 (\tilde{p}, p_r) \quad (1) \quad \text{---} \rightarrow \text{---} \times \text{---} \rightarrow \text{---} &= i \frac{\bar{\eta}}{2} \frac{2p^\perp \cdot p_r^\perp}{\bar{n} \cdot p} \\
 \begin{array}{c} \mu, A \\ \text{---} \uparrow \text{---} \\ \text{---} \rightarrow \text{---} \\ p \end{array} &= ig T^A \frac{\bar{\eta}}{2} \frac{2p^\mu}{\bar{n} \cdot p} \\
 \begin{array}{c} \mu, A \\ \text{---} \uparrow \text{---} \\ \text{---} \rightarrow \text{---} \rightarrow \text{---} \\ p \quad p' \end{array} &= ig T^A \frac{\bar{\eta}}{2} \left[ \frac{\gamma_\mu^\perp \not{p}_r^\perp}{\bar{n} \cdot p} + \frac{\not{p}'^\perp \gamma_\mu^\perp}{\bar{n} \cdot p'} + \frac{\bar{n}^\mu \not{p}_r^\perp \not{p}^\perp}{\bar{n} \cdot q \bar{n} \cdot p} - \frac{\bar{n}^\mu \not{p}'^\perp \not{p}_r^\perp}{\bar{n} \cdot q \bar{n} \cdot p'} - \frac{\bar{n}^\mu \not{p}_r^\perp \not{p}^\perp}{\bar{n} \cdot q \bar{n} \cdot p'} + \frac{\bar{n}^\mu \not{p}'^\perp \not{p}_r^\perp}{\bar{n} \cdot q \bar{n} \cdot p} \right] \\
 \begin{array}{c} \mu, A \quad \nu, B \\ \text{---} \uparrow \text{---} \uparrow \text{---} \\ \text{---} \rightarrow \text{---} \rightarrow \text{---} \\ p \quad p' \end{array} &= ig^2 T^A T^B \frac{\bar{\eta}}{2} \left[ \gamma_\mu^\perp \gamma_\nu^\perp \dots \right] \\
 &+ ig^2 T^B T^A \frac{\bar{\eta}}{2} \left[ \gamma_\nu^\perp \gamma_\mu^\perp \dots \right]
 \end{aligned}$$

 Figure 13: Order  $\lambda^1$  Feynman rules with two collinear quarks from  $\mathcal{L}_{\xi\xi}^{(1)}$ .

$$\begin{aligned}
(\tilde{p}, p_r) \quad (2) \\
\text{---} \rightarrow \text{---} \times \text{---} \rightarrow \text{---} &= i \frac{\bar{\eta}}{2} \frac{p_{r\perp}^2}{\bar{n}\cdot p} \\
\begin{array}{c} \mu, A \\ \text{---} \rightarrow \text{---} \\ \text{---} \uparrow \text{---} \\ \text{---} \rightarrow \text{---} \end{array} &= ig T^A \frac{\bar{\eta}}{2} \left[ \frac{2p_r^\perp{}^\mu}{\bar{n}\cdot p} - \frac{\bar{n}^\mu p_\perp^2}{(\bar{n}\cdot p)^2} \right] \\
\begin{array}{c} \mu, A \\ \text{---} \rightarrow \text{---} \\ \text{---} \uparrow \text{---} \\ \text{---} \rightarrow \text{---} \\ p \qquad p' \end{array} &= ig T^A \frac{\bar{\eta}}{2} \left[ \frac{\bar{n}^\mu p_{r\perp}^2}{\bar{n}\cdot p} - \frac{\bar{n}^\mu p'_{r\perp}{}^2}{\bar{n}\cdot p'} - \frac{\gamma_\mu^\perp \not{p}_\perp \bar{n}\cdot p_r}{(\bar{n}\cdot p)^2} - \frac{\not{p}'_\perp \gamma_\mu^\perp \bar{n}\cdot p_r}{(\bar{n}\cdot p')^2} - \frac{\bar{n}^\mu \not{p}'_\perp \not{p}_\perp \bar{n}\cdot p_r}{\bar{n}\cdot q (\bar{n}\cdot p)^2} + \frac{\bar{n}^\mu \not{p}'_\perp \not{p}_\perp \bar{n}\cdot p_r}{\bar{n}\cdot q (\bar{n}\cdot p')^2} \right] \\
\begin{array}{c} \mu, A \quad \nu, B \\ \text{---} \rightarrow \text{---} \\ \text{---} \uparrow \text{---} \downarrow \text{---} \\ \text{---} \rightarrow \text{---} \\ p \qquad p' \end{array} &= \frac{ig^2 T^A T^B}{2} \frac{\bar{\eta}}{2} \left[ \gamma_\mu^\perp \gamma_\nu^\perp \dots \right] \\
&+ \frac{ig^2 T^B T^A}{2} \frac{\bar{\eta}}{2} \left[ \gamma_\nu^\perp \gamma_\mu^\perp \dots \right]
\end{aligned}$$

Figure 14: Order  $\lambda^2$  Feynman rules with two collinear quarks from  $\mathcal{L}_{\xi\xi}^{(2)}$ .

$$\begin{aligned}
\begin{array}{c} \mu, a \\ \text{---} \rightarrow \text{---} \\ \text{---} \uparrow \text{---} \\ \text{---} \rightarrow \text{---} \\ (q, t) \qquad (p, k) \end{array} &= ig T^a \left[ \gamma_\mu^\perp - \bar{n}_\mu \frac{\not{q}_\perp}{\bar{n}\cdot q} \right] \\
\begin{array}{c} \mu, a \quad \nu, b \\ \text{---} \rightarrow \text{---} \\ \text{---} \uparrow \text{---} \downarrow \text{---} \\ \text{---} \rightarrow \text{---} \\ (q_1, t_1) \quad (q_2, t_2) \qquad (p, k) \end{array} &= ig^2 \frac{T^b T^a}{\bar{n}\cdot q_1} \left[ \frac{\bar{n}_\mu \bar{n}_\nu \not{q}_\perp}{\bar{n}\cdot p} - \gamma_\nu^\perp \bar{n}_\mu \right] \\
&+ ig^2 \frac{T^a T^b}{\bar{n}\cdot q_2} \left[ \frac{\bar{n}_\mu \bar{n}_\nu \not{q}_\perp}{\bar{n}\cdot p} - \gamma_\mu^\perp \bar{n}_\nu \right]
\end{aligned}$$

Figure 15: Feynman rules for the subleading usoft-collinear Lagrangian  $\mathcal{L}_{\xi q}^{(1)}$  with one and two collinear gluons (springs with lines through them). The solid lines are usoft quarks while dashed lines are collinear quarks. For the collinear particles we show their (label,residual) momenta. (The fermion spinors are suppressed.)

### D.1 Feynman rules for $J_{hl}$

Here we give Feynman rules for the  $\mathcal{O}(\lambda)$  heavy-to-light currents  $J^{(1a)}$  and  $J^{(1b)}$  in Eq. (??) which are valid in a frame where  $v_\perp = 0$  and  $v\cdot n = 1$ .

For the subleading currents the zero and one gluon Feynman rules for  $J^{(1a)}$  and  $J^{(1b)}$  are shown in Figs. 18 and 19 respectively. (From the results in the previous sections the Feynman rules for the currents

$$\begin{aligned}
& \text{Diagram 1: } \text{collinear quark } (p, k) \text{ and gluon } (q, t) \text{ with index } \mu, a \\
& \qquad = ig T^a \frac{\not{n}}{2} \left( n_\mu - \frac{\bar{n}_\mu n \cdot t}{\bar{n} \cdot q} \right) \\
& \text{Diagram 2: } \text{collinear quark } (p, k) \text{ and two gluons } (q, t) \text{ and } (v, b) \text{ with indices } \mu, a \text{ and } \nu, b \\
& \qquad = \frac{-g^2 f^{abc} T^c}{\bar{n} \cdot q} \frac{\not{n}}{2} \bar{n}_\mu n_\nu \\
& \text{Diagram 3: } \text{collinear quark } (p, k) \text{ and two gluons } (q_1, t_1) \text{ and } (q_2, t_2) \text{ with indices } \mu, a \text{ and } \nu, b \\
& \qquad = ig^2 \frac{T^a T^b}{\bar{n} \cdot q_2} \left[ -n_\mu \bar{n}_\nu + \bar{n}_\mu \bar{n}_\nu \frac{n \cdot (t_1 + t_2)}{\bar{n} \cdot p} \right] \frac{\not{n}}{2} \\
& \qquad \quad + ig^2 \frac{T^b T^a}{\bar{n} \cdot q_1} \left[ -n_\nu \bar{n}_\mu + \bar{n}_\mu \bar{n}_\nu \frac{n \cdot (t_1 + t_2)}{\bar{n} \cdot p} \right] \frac{\not{n}}{2}
\end{aligned}$$

Figure 16: Feynman rules for the  $O(\lambda^2)$  usoft-collinear Lagrangian  $\mathcal{L}_{\xi q}^{(2a)}$  with one and two gluons. The spring without a line through it is an usoft gluon. For the collinear particles we show their (label,residual) momenta, where label momenta are  $p, q, q_i \sim \lambda^{0,1}$  and residual momenta are  $k, t, t_i \sim \lambda^2$ . Note that the result is after the field redefinition made in Ref. [?].

$$\begin{aligned}
& \text{Diagram 1: } \text{collinear quark } (p, k) \text{ and gluon } (q, t) \text{ with index } \mu, a \\
& \qquad = ig \frac{T^a}{\bar{n} \cdot q} \frac{\not{n}}{2} \left[ \not{q}_\perp \gamma_\mu^\perp - \bar{n}_\mu \frac{q_\perp^2}{\bar{n} \cdot q} \right] \\
& \text{Diagram 2: } \text{collinear quark } (p, k) \text{ and two gluons } (q_1, t_1) \text{ and } (q_2, t_2) \text{ with indices } \mu, a \text{ and } \nu, b \\
& \qquad = ig^2 \frac{T^a T^b}{\bar{n} \cdot q_2} \frac{\not{n}}{2} \left[ \gamma_\mu^\perp \gamma_\nu^\perp - \frac{\not{p}_\perp}{\bar{n} \cdot p} (\gamma_\mu^\perp \bar{n}_\nu + \gamma_\nu^\perp \bar{n}_\mu) - \frac{\gamma_\mu^\perp \bar{n}_\nu \not{q}_{2\perp}}{\bar{n} \cdot q_2} \right. \\
& \qquad \quad \left. + \bar{n}_\mu \bar{n}_\nu \left( \frac{p_\perp^2}{(\bar{n} \cdot p)^2} + \frac{\not{p}_\perp \not{q}_{2\perp}}{\bar{n} \cdot p \bar{n} \cdot q_2} \right) \right] + [(a, \mu, q_1, t_1) \leftrightarrow (b, \nu, q_2, t_2)]
\end{aligned}$$

Figure 17: Feynman rules for the  $O(\lambda^2)$  usoft-collinear Lagrangian  $\mathcal{L}_{\xi q}^{(2b)}$  with one and two gluons. For the collinear particles we show their (label,residual) momenta, where label momenta are  $p, q, q_i \sim \lambda^{0,1}$  and residual momenta are  $k, t, t_i \sim \lambda^2$ .

with  $v_\perp \neq 0$  and  $v \cdot n \neq 1$  can also be easily derived.) For  $J^{(1a)}$  the Wilson coefficients depend only on the total  $\lambda^0$  collinear momentum, while for  $J^{(1a)}$  the coefficients depend on how the momentum is divided between the quark and gluons. The  $J^{(1a)}$  current has non-vanishing Feynman rules with zero or one  $A_n^\perp$  gluon and any number of  $\bar{n} \cdot A_n$  gluons. The possible gluons that appear in the  $J^{(1b)}$  currents are similar, but the current vanishes unless it has one or more collinear gluons present.

$$\begin{aligned}
\begin{array}{c} J^{(1a)} \\ \text{---} \otimes \text{---} \\ \text{---} \end{array} &= -i B_i^{(d)}(\bar{n} \cdot \hat{p}) \frac{p_\alpha^\perp \Upsilon_i^{(d)\alpha}}{\bar{n} \cdot p} \\
\begin{array}{c} J^{(1a)} \\ \text{---} \otimes \text{---} \\ \text{---} \end{array} &= -i B_i^{(d)}(\bar{n} \cdot (\hat{p} + \hat{q})) \frac{g T^a}{\bar{n} \cdot (p+q)} \left[ \Upsilon_i^{(d)\mu} + \frac{\bar{n}^\mu p_\alpha^\perp \Upsilon_i^{(d)\alpha}}{\bar{n} \cdot q} \right]
\end{aligned}$$

Figure 18: Feynman rules for the  $O(\lambda)$  currents  $J^{(1a)}$  in Eq. (??) with zero and one gluon (the fermion spinors are suppressed). For the collinear particles we show their (label,residual) momenta, where label momenta are  $p, q \sim \lambda^{0,1}$  and residual momenta are  $k, t \sim \lambda^2$ . Momenta with a hat are normalized to  $m_b$ ,  $\hat{p} = p/m_b$  etc.

$$\begin{aligned}
\begin{array}{c} J^{(1b)} \\ \text{---} \otimes \text{---} \\ \text{---} \end{array} &= 0 \\
\begin{array}{c} J^{(1b)} \\ \text{---} \otimes \text{---} \\ \text{---} \end{array} &= i B_i^{(d)}(\bar{n} \cdot \hat{p}, \bar{n} \cdot \hat{q}) \frac{g T^a}{m_b} \left[ \Theta_i^{(d)\mu} - \frac{\bar{n}^\mu q_\alpha^\perp \Theta_i^{(d)\alpha}}{\bar{n} \cdot q} \right]
\end{aligned}$$

Figure 19: Feynman rules for the  $O(\lambda)$  currents  $J^{(1b)}$  in Eq. (??) with zero and one gluon. For the collinear particles we show their (label,residual) momenta, where label momenta are  $p, q, q_i \sim \lambda^{0,1}$  and residual momenta are  $k, t \sim \lambda^2$ . Momenta with a hat are normalized to  $m_b$ ,  $\hat{p} = p/m_b$  etc.



## E Integral Tricks

Feynman parameter tricks:

$$\begin{aligned}
 a^{-1} b^{-1} &= \int_0^1 dx [a + (b-a)x]^{-2} & (E.1) \\
 a^{-n} b^{-m} &= \frac{\Gamma(n+m)}{\Gamma(n)\Gamma(m)} \int_0^1 dx \frac{x^{n-1}(1-x)^{m-1}}{[a + (b-a)x]^{n+m}} \\
 a^{-1} b^{-1} c^{-1} &= 2 \int_0^1 dx \int_0^{1-x} dy [c + (a-c)x + (b-c)y]^{-3} \\
 &= 2 \int_0^1 dx \int_0^1 dy x [a + (c-a)x + (b-c)xy]^{-3} \\
 a_1^{-1} \cdots a_n^{-1} &= (n-1)! \int_0^1 dx_1 \cdots dx_n \delta\left(\sum x_i - 1\right) \left(\sum x_i a_i\right)^{-n} \\
 (a_1^{m_1} \cdots a_n^{m_n})^{-1} &= \frac{\Gamma(\sum m_i)}{\Gamma(m_1) \cdots \Gamma(m_n)} \int_0^1 dx_1 \cdots dx_n \delta\left(\sum x_i - 1\right) \left(\sum x_i a_i\right)^{-n} \prod x_i^{m_i-1}
 \end{aligned}$$

To get the fourth line from the third we let  $x' = 1 - x$  and  $y' = y/x$ .

Georgi parameter tricks (when one or more propagators are linear in loop momenta):

$$\begin{aligned}
 a^{-1} b^{-1} &= \int_0^\infty d\lambda [a + b\lambda]^{-2} & (E.2) \\
 a^{-q} b^{-1} &= q \int_0^\infty d\lambda [a + b\lambda]^{-(q+1)} = 2q \int_0^\infty d\lambda [a + 2b\lambda]^{-(q+1)} \\
 a^{-q} b^{-p} &= \frac{2^p \Gamma(p+q)}{\Gamma(p)\Gamma(q)} \int_0^\infty d\lambda \lambda^{p-1} [a + 2b\lambda]^{-(p+q)} \\
 a^{-1} b^{-1} c^{-1} &= 2 \int_0^\infty d\lambda d\lambda' [c + a\lambda' + b\lambda]^{-3} = 8 \int_0^\infty d\lambda d\lambda' [c + 2a\lambda' + 2b\lambda]^{-3}
 \end{aligned}$$

## F QCD Summary

The  $SU(N_c)$  QCD Lagrangian without gauge fixing

$$\begin{aligned} \mathcal{L} &= \bar{\psi}(i\not{D} - m)\psi - \frac{1}{4}G_{\mu\nu}^A G^{\mu\nu A}, & G_{\mu\nu}^A &= \partial_\mu A_\nu^A - \partial_\nu A_\mu^A - gf^{ABC}A_\mu^B A_\nu^C \\ D_\mu &= \partial_\mu + igA_\mu^A T^A, & [D_\mu, D_\nu] &= igG_{\mu\nu}^A T^A. \end{aligned} \quad (\text{F.1})$$

The equations of motion and Bianchi

$$(i\not{D} - m)\psi = 0, \quad \partial^\mu G_{\mu\nu}^A = gf^{ABC}A^{B\mu}G_{\mu\nu}^C + g\bar{\psi}\gamma_\nu T^A\psi, \quad \epsilon^{\mu\nu\lambda\sigma}(D_\nu G_{\lambda\sigma})^A = 0. \quad (\text{F.2})$$

Color identities

$$\begin{aligned} [T^A, T^B] &= if^{ABC}T^C, & \text{Tr}[T^A T^B] &= T_F \delta^{AB}, & \bar{T}^A &= -T^{A*} = -(T^A)^T, \\ T^A T^A &= C_F \mathbf{1}, & f^{ACD}f^{BCD} &= C_A \delta^{AB}, & f^{ABC}T^B T^C &= \frac{i}{2}C_A T^A, \\ T^A T^B T^A &= \left(C_F - \frac{C_A}{2}\right)T^B, & d^{ABC}d^{ABC} &= \frac{40}{3}, & d^{ABC}d^{A'BC} &= \frac{5}{3}\delta^{AA'}, \end{aligned} \quad (\text{F.3})$$

where  $C_F = (N_c^2 - 1)/(2N_c)$ ,  $C_A = N_c$ ,  $T_F = 1/2$ , and  $C_F - C_A/2 = -1/(2N_c)$ . The color reduction formula and Fierz formula are

$$T^A T^B = \frac{\delta^{AB}}{2N_c} \mathbf{1} + \frac{1}{2}d^{ABC}T^C + \frac{i}{2}f^{ABC}T^C, \quad (T^A)_{ij}(T^A)_{kl} = \frac{1}{2}\delta_{il}\delta_{kj} - \frac{1}{2N_c}\delta_{ij}\delta_{kl}. \quad (\text{F.4})$$

Feynman gauge rules, fermion, gluon, ghost propagators, and Fermion-gluon vertex

$$\frac{i(\not{p} + m)}{p^2 - m^2 + i0}, \quad \frac{-ig^{\mu\nu}\delta^{AB}}{k^2 + i0}, \quad \frac{i}{k^2 + i0}, \quad -ig\gamma^\mu T^A. \quad (\text{F.5})$$

Triple gluon and Ghost Feynman rules in covariant gauge for  $\{A_\mu^A(k), A_\nu^B(p), A_\rho^C(q)\}$  all with incoming momenta, and  $\bar{c}^A(p)A_\mu^B c^C$  with outgoing momenta  $p$ :

$$-gf^{ABC}[g^{\mu\nu}(k-p)^\rho + g^{\nu\rho}(p-q)^\mu + g^{\rho\mu}(q-k)^\nu], \quad gf^{ABC}p^\mu. \quad (\text{F.6})$$

Triple gluon Feynman rule in bkgnd Field covariant gauge  $\mathcal{L}_{gf} = -(D_\mu^A Q_\mu^A)^2/(2\xi)$  for  $\{A_\mu^A(k), Q_\nu^B(p), Q_\rho^C(q)\}$  with  $A_\mu^A$  a bkgnd field:

$$-gf^{ABC}\left[g^{\mu\nu}\left(k-p-\frac{q}{\xi}\right)^\rho + g^{\nu\rho}(p-q)^\mu + g^{\rho\mu}\left(q-k+\frac{p}{\xi}\right)^\nu\right]. \quad (\text{F.7})$$

Lorentz gauge:

$$\mathcal{L} = -\frac{(\partial_\mu A^\mu)^2}{2\xi}, \quad D^{\mu\nu}(k) = \frac{-i}{k^2 + i0}\left(g^{\mu\nu} - (1-\xi)\frac{k^\mu k^\nu}{k^2}\right), \quad (\text{F.8})$$

where Landau gauge is  $\xi \rightarrow 0$ . Coulomb gauge:

$$\begin{aligned} \vec{\nabla} \cdot \vec{A} &= 0, & D^{\mu\nu}(k) &= \frac{-i}{k^2 + i0}\left(g^{\mu\nu} - \frac{[g^{\nu 0}k^0 k^\mu + g^{\mu 0}k^0 k^\nu - k^\mu k^\nu]}{\vec{k}^2}\right), \\ D^{00}(k) &= \frac{i}{\vec{k}^2 - i0}, & D^{ij}(k) &= \frac{i}{k^2 + i0}\left(\delta^{ij} - \frac{k^i k^j}{\vec{k}^2}\right). \end{aligned} \quad (\text{F.9})$$

Running coupling with  $\beta_0 = 11C_A/3 - 4T_F n_f/3 = 11 - 2n_f/3$ :

$$\alpha_s(\mu) = \frac{\alpha_s(\mu_0)}{1 + \frac{\beta_0}{2\pi}\alpha_s(\mu_0)\ln\frac{\mu}{\mu_0}} = \frac{2\pi}{\beta_0 \ln\frac{\mu}{\Lambda_{\text{QCD}}}}, \quad \frac{1}{\alpha_s(\mu)} = \frac{1}{\alpha_s(\mu_0)} + \frac{\beta_0}{2\pi}\ln\frac{\mu}{\mu_0}. \quad (\text{F.10})$$

## References

- [1] C. W. Bauer, S. Fleming, and M. E. Luke, *Phys. Rev. D* **63**, 014006 (2001), [hep-ph/0005275].
- [2] C. W. Bauer, S. Fleming, D. Pirjol, and I. W. Stewart, *Phys. Rev. D* **63**, 114020 (2001), [hep-ph/0011336].
- [3] C. W. Bauer, D. Pirjol, and I. W. Stewart, *Phys. Rev.* **D66**, 054005 (2002), [hep-ph/0205289].
- [4] C. W. Bauer and I. W. Stewart, *Phys. Lett. B* **516**, 134 (2001), [hep-ph/0107001].
- [5] A. V. Manohar and I. W. Stewart, *Phys. Rev.* **D76**, 074002 (2007), [hep-ph/0605001].
- [6] C. W. Bauer, D. Pirjol, and I. W. Stewart, *Phys. Rev. D* **65**, 054022 (2002), [hep-ph/0109045].
- [7] A. V. Manohar, T. Mehen, D. Pirjol, and I. W. Stewart, *Phys. Lett.* **B539**, 59 (2002), [hep-ph/0204229].
- [8] C. W. Bauer, S. Fleming, D. Pirjol, I. Z. Rothstein, and I. W. Stewart, *Phys. Rev. D* **66**, 014017 (2002), [hep-ph/0202088].
- [9] I. W. Stewart, F. J. Tackmann, and W. J. Waalewijn, *JHEP* **1009**, 005 (2010), [1002.2213].
- [10] C. W. Bauer, D. Pirjol, and I. W. Stewart, *Phys. Rev.* **D68**, 034021 (2003), [hep-ph/0303156].
- [11] J.-Y. Chiu, A. Jain, D. Neill, and I. Z. Rothstein, *JHEP* **1205**, 084 (2012), [1202.0814].
- [12] M. Beneke, A. P. Chapovsky, M. Diehl, and T. Feldmann, *Nucl. Phys.* **B643**, 431 (2002), [hep-ph/0206152].
- [13] C. W. Bauer, D. Pirjol, and I. W. Stewart, *Phys. Rev. D* **67**, 071502 (2003), [hep-ph/0211069].
- [14] C. Marcantonini and I. W. Stewart, *Phys.Rev.* **D79**, 065028 (2009), [0809.1093].